

QUANTITATIVE NUCLEAR FEATURE ANALYSIS IN THE PROGNOSIS OF  
BENIGN BREAST DISEASE AND DUCTAL CARCINOMA *IN SITU*

by

BARBARA SUSNIK

MD, University of Ljubljana, 1988

A THESIS SUBMITTED IN PARTIAL FULFILLMENT OF  
THE REQUIREMENTS FOR THE DEGREE OF  
DOCTOR OF PHILOSOPHY

in

THE FACULTY OF GRADUATE STUDIES

Department of Pathology

We accept this thesis as conforming  
to the required standard

THE UNIVERSITY OF BRITISH COLUMBIA

January 1994

© Barbara Susnik, 1993

In presenting this thesis in partial fulfilment of the requirements for an advanced degree at the University of British Columbia, I agree that the Library shall make it freely available for reference and study. I further agree that permission for extensive copying of this thesis for scholarly purposes may be granted by the head of my department or by his or her representatives. It is understood that copying or publication of this thesis for financial gain shall not be allowed without my written permission.

(Signature)

Department of PATHOLOGY

The University of British Columbia  
Vancouver, Canada

Date March 9<sup>th</sup> 1994

## ABSTRACT

Except of the diagnostic categories based on the morphology of cells and tissue there are currently no significant prognostic markers for patients with benign breast disease or ductal carcinoma *in situ* (DCIS). This thesis proposed that such prognostic information could be obtained based on quantitative nuclear feature analysis of diagnostic cells and/or normal appearing cells in breast tissue. Image cytometry (IC) measurements provide numerous quantitative nuclear features which reflect the DNA content, nuclear morphology and chromatin condensation patterns in stained nuclei. With the use of this technique it is possible to detect slight morphological nuclear changes which can not be observed by the human eye. Measurements on tissue sections were chosen for this study because in these specimens visualization of tissue histology and precise identification of affected glands is possible. The thesis involved testing of the following postulates:

1) *DNA ploidy can be evaluated by IC measurements of tissue sections*

DNA content measurements of archival breast specimens showed that the performance of manual IC measurements of nuclei on tissue sections was comparable to the results of flow cytometry and automated IC techniques.

2) *Quantitative nuclear features change in different histological patterns of breast diseases*

The analysis of normal tissue, non-proliferative breast disease, proliferative breast disease, carcinoma *in situ* and invasive cancer specimens demonstrated differences in nuclear features between different histopathological patterns. Compared to normal tissue characteristics, the deviations of features

related to the nuclear area, shape, DNA content and chromatin texture all increased with advancing morphological changes.

3) *Various histological types of DCIS can be characterized on the basis of the nuclear features*

The differences in quantitative nuclear features were defined for various histological types of DCIS. The nuclear DNA content, size, irregularity of shape and chromatin texture, all increased from the lowest values in cribriform type to the highest values in comedo type DCIS. Aneuploidy was demonstrated in about 60% of non-comedo DCIS and in about 95% of comedo DCIS.

4) *Differences in nuclear morphology, which may be related to the invasive potential of ductal carcinomas in situ (DCIS), exist between i) pure DCIS, and ii) DCIS with synchronous invasive carcinoma*

An important task of this thesis was to obtain a prognostic indicator for ductal carcinoma *in situ* (DCIS). Nuclear features of DCIS which were associated with the presence of invasive carcinoma in the surrounding breast tissue were identified. A classification system based on these nuclear features was then used to discriminate between cases with pure DCIS and cases of DCIS with invasive cancer in the surrounding tissue. This classification predicted accurately the presence of invasive carcinoma in about 80% of non-comedo DCIS and in about 100% of comedo DCIS cases.

5) *Subtle changes of nuclear morphology exist in epithelial cells of normal appearing breast tissue adjacent to invasive carcinoma (malignancy associated changes)*

The final goal was to test the hypothesis that small deviations in nuclear morphology, indicative of the malignancy in the surrounding tissue, can be detected through nuclear measurements of non-diagnostic, normal appearing

cells in the vicinity of DCIS or invasive carcinoma. This phenomenon has been previously studied in other tissues and has been described as a part of malignancy associated changes (MAC). The present study illustrated the existence of MAC in the normal appearing breast tissue adjacent to *in situ*, or invasive carcinoma. Patients with benign or malignant diseases could be distinguished solely on the basis of the measurements of epithelial nuclei from the normal appearing glands. With the analysis of MAC about 85% of cases were correctly classified as benign or malignant.

In conclusion: A) Differences in nuclear features which were demonstrated for various groups of breast diseases suggest that these features could be applied as an objective aid in the classification and diagnosis of breast diseases. B) The analysis of DCIS nuclei can provide useful prognostic information making it possible to suspect the presence of invasive carcinoma in the breast when only DCIS is present in the biopsy. Moreover, specific changes in nuclear morphology, which are characteristic of DCIS associated with invasive carcinoma in the surrounding breast might be associated with the progressive capacity of DCIS and may be helpful as a marker predictive of the subsequent behavior of DCIS tumors. C) Nuclear features, characteristic of MAC, are important as markers for occult malignancy in cases where only benign breast disease is found in a biopsy. In addition, a high frequency of "MAC" nuclei in a benign breast tissue may be suggestive of a higher progressive potential and of an increased risk for the development of invasive carcinoma from benign breast tissue which has a high frequency of "MAC" nuclei. In view of the clinical relevance of these findings it is very important to confirm and expand the results with further studies on larger number of patients.

## TABLE OF CONTENTS

	PAGE
ABSTRACT	ii
TABLE OF CONTENTS	v
LIST OF TABLES	ix
LIST OF FIGURES	xii
LIST OF ABBREVIATIONS	xvi
ACKNOWLEDGMENTS	xviii
1. INTRODUCTION	1
1.1 Background	1
1.1.A DNA content of breast carcinoma	1
1.1.B DNA measurements of invasive breast carcinoma performed on archival tissues by flow and image cytometry	5
1.1.C Analysis of DNA histograms obtained by image cytometry	6
1.1.D Various nuclear features employed by image cytometry	11
1.1.E Benign breast disease and premalignant changes	13
1.1.F Image cytometry of benign breast disease	16
1.1.G Malignancy associated changes (MAC)	18
1.1.H Ductal carcinoma <i>in situ</i>	19
1.1.I Image cytometry of ductal carcinoma <i>in situ</i>	25
1.2 Proposal	27
1.2.A Measurements of DNA content: Comparison of different cytometry techniques	27
1.2.B The relationship between the histological patterns of breast diseases and quantitative nuclear features	28

1.2.C	Nuclear features as a prognostic factor for DCIS	29
1.2.D	Malignancy associated changes	31
2.	OBJECTIVES	33
3.	MATERIALS AND METHODS	34
3.1	Tissues	34
3.1.A	Comparison of image and flow cytometry	34
3.1.B	Comparison of image cytometry measurements performed on smears, cytospins and sections	34
3.1.C	Correlation of quantitative features with advancing morphological changes	35
3.1.D	Heterogeneity of ductal carcinoma <i>in situ</i>	44
3.1.E	Differences between pure carcinoma <i>in situ</i> and carcinoma <i>in situ</i> associated with invasive carcinoma in the surrounding tissue	44
3.1.F	Malignancy associated changes	44
3.2	Staining	46
3.2.A	Flow cytometry	46
3.2.B	Image cytometry	48
3.3	Image cytometry measurements	49
3.3.A	Image cytometry of tissue sections	49
3.3.B	Comparison of measurements performed on tissue sections, cytospins and smears	52
3.4	Description of main nuclear features	54
3.5	Analysis of DNA histograms	58
3.5.A	Image cytometry	58
3.5.B	Flow cytometry	59

3.6	Statistics	61
4.	RESULTS	65
4.1	The distribution of values in the image cytometry DNA histograms of normal cells	65
4.2	Comparison of flow and image cytometry of tissue sections	67
4.3	Comparison of image cytometry measurements performed on smears, cytopins and sections	71
4.4	Correlation of quantitative features with advancing morphological changes	79
4.5	Heterogeneity of ductal carcinoma <i>in situ</i>	86
	4.5.A Comparison of comedo and non-comedo types	95
	4.5.B Quantitative nuclear features in different histological types of non-comedo DCIS	100
4.6	Differences between pure carcinoma <i>in situ</i> and carcinoma <i>in situ</i> associated with invasive carcinoma in the surrounding tissue	111
	4.6.A Non-comedo type	114
	4.6.B Comedo type	123
4.7	Malignancy associated changes	127
5.	DISCUSSION	140
5.1	Comparison of different cytometry techniques	140
	5.1.A Flow cytometry and image cytometry of tissue sections	142
	5.1.B Comparison of different image cytometry techniques	144
5.2	The correlation between quantitative nuclear features and advancing morphological changes	146
5.3	Heterogeneity of ductal carcinoma <i>in situ</i>	149

5.4	Differences between pure carcinoma <i>in situ</i> and carcinoma <i>in situ</i> associated with invasive carcinoma in surrounding tissue	151
5.5	Malignancy associated changes	155
6.	SUMMARY	158
7.	REFERENCES	161

## LIST OF TABLES

	PAGE
Table 1. Different approaches for the ploidy analysis.	7
Table 2. The number of cases analyzed in six groups of breast diseases.	36
Table 3. The number of pure DCIS and DCIS with adjacent invasive carcinoma included in the study.	45
Table 4. Cases involved in the analysis of malignancy associated changes.	47
Table 5. Histogram parameters obtained from DNA histograms of normal cells.	66
Table 6. Ploidy determined by image and flow cytometry.	70
Table 7. DI analysis of cases where FC and IC disagreed in ploidy.	72
Table 8. Heterogeneity of tumors.	73
Table 9. DNA histogram parameters of corresponding smears, cytospins and tissue sections.	80
Table 10. DNA histogram parameters in six diagnostic groups.	83
Table 11. The mean values of the representative features and their variances in six groups of breast diseases.	85
Table 12. Ploidy in comedo and non-comedo DCIS.	96
Table 13. DNA histogram parameters of different histological types of DCIS.	97
Table 14. Significant differences in nuclear features between non-comedo and comedo DCIS.	99
Table 15. Jackknifed classification of non-comedo and comedo DCIS nuclei.	102

Table 16. The mean values of the representative features, and their variances, in different histological types of DCIS.	103
Table 17. Ploidy of different histological types of non-comedo DCIS.	110
Table 18. Average values of DNA histogram parameters obtained from different histological types of DCIS (with or without associated invasive carcinoma in the surrounding tissue).	112
Table 19. Ploidy of pure DCIS and DCIS associated with invasive carcinoma in surrounding breast tissue.	113
Table 20. Significant differences in nuclear features between non-comedo DCIS without invasion and non-comedo DCIS with adjacent invasive carcinoma.	116
Table 21. Pure DCIS vs. DCIS with adjacent invasive carcinoma: non-comedo type.	118
Table 22. Jackknifed classification of non-comedo DCIS1 and non-comedo DCIS2 nuclei.	121
Table 23. Discrimination of non-comedo DCIS1 and non-comedo DCIS2 cases based on the proportion of DCIS2 nuclei on the slides.	122
Table 24. Significant differences in nuclear features between comedo DCIS without invasion and comedo DCIS with adjacent invasive carcinoma.	126
Table 25. Jackknifed classification of comedo DCIS1 and comedo DCIS2 nuclei.	130
Table 26. Discrimination of comedo DCIS1 and comedo DCIS2 cases based on the proportion of DCIS2 nuclei on the slides.	131

Table 27. Jackknifed classification of nuclei to normal nuclei and "MAC" nuclei (A).	135
Table 28. Classification of benign cases and invasive carcinoma cases according to the proportion of "MAC" nuclei.	136
Table 29. Jackknifed classification of nuclei to normal nuclei and "MAC" nuclei (B).	137
Table 30. Classification of benign and malignant cases (invasive carcinoma and DCIS) according to the proportion of "MAC" nuclei.	139

## LIST OF FIGURES

	PAGE
Figure 1. A variety of features can be measured by image cytometry.	3
Figure 2. Phases of the cell cycle and a DNA histogram of normal breast tissue.	9
Figure 3. Examples of diploid , tetraploid and aneuploid peaks in DNA histograms.	10
Figure 4. Breast diseases with an increased risk of subsequent invasive carcinoma.	15
Figure 5. Ductal carcinoma in situ without invasive component (DCIS-) and ductal carcinoma in situ with invasive component (DCIS+).	30
Figure 6. MAC:malignancy associated changes.	32
Figure 7. Normal breast lobule.	37
Figure 8. Non-proliferative breast disease: mild hyperplasia.	39
Figure 9. Proliferative breast disease (A).	40
Figure 10. Proliferative breast disease (B).	41
Figure 11. Ductal carcinoma <i>in situ</i> : comedo type.	42
Figure 12. Invasive ductal carcinoma.	43
Figure 13. Image cytometry device, which was used for the measurements on tissue sections.	50
Figure 14. An example of normalized histogram and histogram parameters.	60
Figure 15. Statistical analysis based on cell by cell discrimination was used for the classification of patients.	64

Figure 16. Examples of aneuploid and diploid IC and FC histograms of five carcinoma cases.	68
Figure 17. Comparison of flow and image cytometry on the basis of the DNA index.	69
Figure 18. DNA index of invasive carcinoma and ductal carcinoma <i>in situ</i> .	74
Figure 19. Nuclear area vs. IOD scatter plots of a smear and a corresponding cytopsin and tissue section.	75
Figure 20. Micrograph of nuclei from a smear and a tissue section.	76
Figure 21. DNA histograms of corresponding smears, cytopsin and tissue sections (A).	77
Figure 22. DNA histograms of corresponding smears, cytopsin and tissue sections (B).	78
Figure 23. Nuclear area vs. IOD scatter plot of various histological patterns present on the same slide.	82
Figure 24. Nuclear area vs. IOD scatter plots of six groups of breast diseases.	87
Figure 25. Variation of radius vs. variance of IOD scatter plots of six groups of breast diseases.	88
Figure 26. Cribriform DCIS.	89
Figure 27. Confluent DCIS.	90
Figure 28. Papillary DCIS.	91
Figure 29. Comedo DCIS.	92
Figure 30. Area vs. IOD scatter plots of various DCIS present on the same slide: case A.	93

Figure 31. Area vs. IOD scatter plots of various DCIS present on the same slide: case B.	94
Figure 32. Micrograph of comedo and non-comedo nuclei.	98
Figure 33. Comedo vs. non-comedo nuclei: the relationship between the number of employed features and the rate of correct classification.	101
Figure 34. Nuclear area in different DCIS types.	105
Figure 35. IOD in different DCIS types.	106
Figure 36. Variation of radius in different DCIS types.	107
Figure 37. Variation of optical density in different DCIS types.	108
Figure 38. Variance of IOD in different DCIS types.	109
Figure 39. Examples of DCIS1 and DCIS2 nuclei: non-comedo type.	115
Figure 40. Non-comedo DCIS1 vs. non-comedo DCIS2 nuclei: the relationship between the number of employed features and the rate of correct classification.	120
Figure 41. Classification of DCIS1 and DCIS2 cases: Noncomedo type.	124
Figure 42. Examples of DCIS1 and DCIS2 nuclei: comedo type.	125
Figure 43. Comedo DCIS1 vs. comedo DCIS2 nuclei: the relationship between the number of employed features and the rate of correct classification.	128
Figure 44. Classification of DCIS1 and DCIS2 cases: Comedo type.	129
Figure 45. Examples of normal nuclei from benign cases and normal nuclei from invasive carcinoma cases.	132

Figure 46. Normal vs. "MAC" nuclei: the relationship between the number of the employed features and the rate of correct classification.

134

Figure 47. Classification of malignant and benign cases.

138

## LIST OF ABBREVIATIONS

ADH:	disease: atypical ductal hyperplasia
ADH:	nuclear feature: average distance of the high density chromatin from the nuclear center
ADL:	average distance of the low density chromatin from the nuclear center
ADM:	average distance of the medium density chromatin from the nuclear center
BDY1:	coarse boundary variation
BDY2:	fine boundary variation
CIS:	carcinoma <i>in situ</i>
C-MASS	center of mass of the nucleus
C-MASSL	center of mass of the light density chromatin
CRH:	high density chromatin compactness ratio
CRL:	low density chromatin compactness ratio
DCIS:	ductal carcinoma <i>in situ</i>
DCIS1:	ductal carcinoma <i>in situ</i> without invasive carcinoma in the surrounding breast tissue
DCIS2:	ductal carcinoma <i>in situ</i> with synchronous invasive carcinoma in the surrounding breast tissue
DI:	DNA index
DNA:	deoxyribonucleic acid
FAREA1:	fractal area 1
FAREA2:	fractal area 2
FC:	flow cytometry

<b>HAER:</b>	<b>high average extinction ratio</b>
<b>IC:</b>	<b>image cytometry</b>
<b>IOD:</b>	<b>integrated optical density</b>
<b>MAC:</b>	<b>malignancy associated changes</b>
<b>MAER:</b>	<b>medium density chromatin average extinction ratio</b>
<b>MHAER:</b>	<b>medium/high density chromatin average extinction ratio</b>
<b>NH:</b>	<b>number of high density chromatin clusters</b>
<b>NL:</b>	<b>number of low density chromatin clusters</b>
<b>NM:</b>	<b>number of medium density chromatin clusters</b>
<b>OD MAX:</b>	<b>optical density maximum</b>
<b>OD SKEW:</b>	<b>skewness of the optical density distribution</b>
<b>OD VAR:</b>	<b>variation of optical density</b>
<b>TARH:</b>	<b>total area ratio for the high density chromatin</b>
<b>TARL:</b>	<b>total area ratio for the low density chromatin</b>
<b>TARM:</b>	<b>total area ratio for the medium density chromatin</b>
<b>TERH:</b>	<b>total extinction ratio for the high density chromatin</b>
<b>TERL:</b>	<b>total extinction ratio for the low density chromatin</b>
<b>TERM:</b>	<b>total extinction ratio for the medium density chromatin</b>
<b>VAR RAD:</b>	<b>variation of radius</b>
<b>V AREA:</b>	<b>variance of area</b>
<b>V IOD:</b>	<b>variance of integrated optical density</b>
<b>V NM:</b>	<b>variance of the number of medium density chromatin clusters</b>

## **ACKNOWLEDGMENTS**

I am very grateful to my supervisors Branko Palcic and Jean LeRiche for all their support and for making my work possible. I would like to express my gratitude to Ann Worth who reviewed all the slides and helped me to better understand breast pathology. I would also like to thank to many others who helped me during the past four years: Alan Harrison, Yvonne Zheng, Calum MacAulay, Jasenka Maticic, Jagoda Korbelik, Paul Lam, David Garner, and Neal Poulin.

## **1. INTRODUCTION**

### **1.1 BACKGROUND**

#### **1.1.A DNA content of breast carcinoma**

Breast cancer is one of the most frequently diagnosed cancers in European and North American women. At present more women die from this disease than from any other malignancy with the exception of lung cancer. Breast cancer accounts for about 30% of newly diagnosed cancer cases and for 20% of cancer deaths in women (Annual report, BCCA, 1990/1991). Nearly every ninth woman gets breast cancer once in her lifetime and almost half of the affected persons die from this disease.

At present, various factors are used to divide the heterogeneous group of breast carcinomas into distinctive prognostic subgroups (McGuire 1990, Elledge 1992). Established prognostic factors for breast carcinoma are tumor stage (defined by its size, lymph node involvement, and the presence or absence of metastasis), histological type, tumor grade, and the presence of estrogen and progesterone receptors. It is believed that other factors, such as tumor ploidy and proliferation markers, are important in breast cancer prognosis, but their role is not entirely clear. In addition, there is a variety of new potential prognostic markers, such as proteases, growth factors or the expression of various oncogenes, and these are at present the subject of numerous studies.

Ploidy of the tissue is related to quantitative chromosome changes which can be demonstrated by cytogenetic analysis. The DNA ploidy of breast carcinoma reflects the DNA amount in the nuclei. Two techniques that are

commonly used for the quantitative assessment of the nuclear amount of DNA are flow cytometry (FC) and image cytometry (IC).

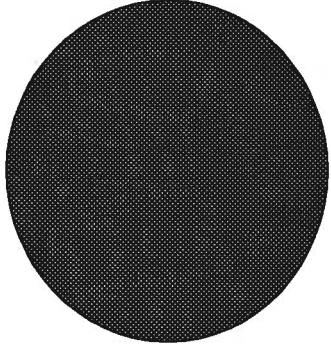
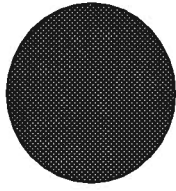
The basic principle of FC is that the suspension of nuclei is labeled with a specific fluorescent DNA dye which stains the DNA in a stoichiometric way. The cell suspension then flows in a stream, so that single nuclei pass a laser beam at the observation point. The laser induces fluorescence of the dye, which can be measured. The fluorescence signal is proportional to the total DNA amount in the nucleus. The size of nuclei can also be measured and is determined by the light scattering from the nuclear surface.

IC DNA measurements are based on measurements of optical density (or emitted fluorescence) of nuclei in cytological or histological specimens which are deposited on microscope slides and stained with a stoichiometric stain. In addition to the DNA content measurements, IC makes it possible to measure many other nuclear features related to nuclear size, shape, roughness of the nuclear boundary, and most importantly, a variety of texture features describing the DNA distribution in the nucleus (Figure 1).

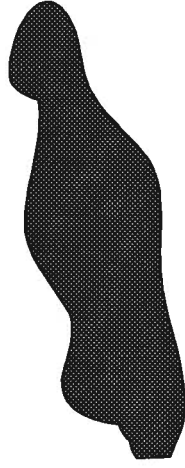
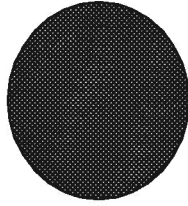
The advantage of FC is in the fast analysis of large populations of cells. This provides good resolution of the DNA content histograms with low coefficients of variation and assures statistical reliability. The disadvantage of FC is that the morphologic identification of different cell classes is not possible without additional labeling. The cells of interest are diluted with non-tumor cell populations (inflammatory cells, stromal cells, or normal cells from the surroundings of the tumor) and the extent of this dilution can not always be recognized.

MEASUREMENTS OF NUCLEAR FEATURES MAY BE PREDICTIVE OF THE PROGNOSIS OF BREAST DISEASES.

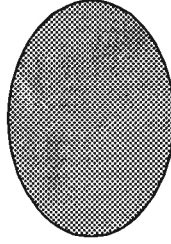
**SIZE**



**SHAPE**



**DNA AMOUNT**



**DNA DISTRIBUTION**

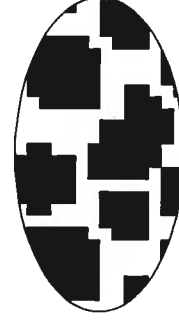


Figure 1. A VARIETY OF NUCLEAR FEATURES CAN BE ANALYZED BY IMAGE CYTOMETRY.

Image analysis on the other hand, allows visualization and morphologic identification of the cells. A trained operator can selectively collect cells of interest, or can interact later in the procedure by classifying the cells on the automatically collected images. With the use of IC it is therefore possible to discover small cell populations with abnormal DNA content, which would remain unnoticed when analyzed by FC. The disadvantage of IC is in the labor intensive nature of the analysis and in the relatively small number of cells that can be analyzed in a given time frame. This results in histograms with generally much lower resolution when compared to FC histograms.

The two techniques have been previously compared with an attempt to relate the DNA index or the DNA ploidy, acquired with IC or FC analysis of fresh tissue. A correlation has been demonstrated in about 90% of cases (Bauer 1990, Elsheikh 1992). The results of both techniques have also been found to correlate well in studies using isolated nuclei from fresh or frozen breast tissue or from breast aspirates (Auer 1985, Cornelisse 1984, Cornelisse 1985, Stal 1986, Fallenius 1987, Wilbur 1990, Falkmer 1990, Baldetorp 1992, Ghali 1992).

Various cytometry studies have been carried out on breast cancer tissue with an attempt to understand the significance of DNA content in prognosis. In these studies FC (Ewers 1984, Cornelisse 1987, Kallionemi 1987, Dressler 1988, Clark 1989, Beerman 1991, Fisher 1991) or IC was employed (Auer 1984, Fallenius 1988, Böcking 1989, Uterlinde 1988, von Rosen 1989, Troncosco 1989, Haroske 1991, Theissig 1991). Most, but not all, authors reported a correlation between aneuploidy and bad prognosis. However, the significance of DNA content in the prognosis of breast cancer is not yet fully understood. It seems that additional investigations will be necessary before the DNA content of

breast cancer will be commonly accepted as a prognostic factor in clinical practice.

#### 1.1.B DNA measurements of invasive breast carcinoma performed on archival tissues by flow and image cytometry techniques

The analysis of archival tissues is very convenient for retrospective studies of prognostic markers where a long follow-up and a large number of patients are essential. Retrospective analysis is the method of choice in evaluating the DNA content in prognosis of various cancers and breast cancer in particular.

IC of embedded tissue can be performed on isolated nuclei or on tissue sections. Studies comparing FC and IC of nuclei isolated from embedded tissues use a similar disaggregation procedure for both techniques (Hedley 1983). Nevertheless, aneuploid populations, undetected by FC, could often be detected by IC where representative cells were selectively chosen for the measurements (Rodenburg 1987, Bose 1989). Rare comparative studies demonstrate disagreements between the results of FC and IC performed on disaggregated nuclei from embedded breast tissue (Carpenter 1988, Ellis 1989, Roos 1989).

Larger discrepancies can be expected when FC is compared to IC performed on tissue sections because the tissue preparation methods are completely different. A limited number of studies have used IC of tissue sections in comparison to FC of embedded tissue from breast (Uyterlinde 1989) or from other tissues (Kreicbergs 1981, Bauer 1986, Cope 1991). The authors found

relatively large discrepancies and reported difficulties with the interpretation of tissue section histograms. Moreover, it has been suggested that histological sections of embedded breast cancer tissue are associated with large methodological problems and are not suitable for DNA measurements (Berryman 1984).

#### 1.1.C Analysis of integrated optical density histograms obtained by image cytometry

Among nuclear features measured by IC, the most widely used feature is integrated optical density (IOD). Optical density (OD) is proportional to the amount of light which is absorbed by a stained object and is proportional to the density of the stain. With the use of the DNA stoichiometric stain, the OD of a pixel is a function of the amount of the DNA in the pixel. IOD is the sum of the OD values of all pixels in a nucleus and is therefore proportional to the nuclear DNA content.

Aneuploid nuclear DNA content, as measured by cytometric techniques, is thought to be associated with poor prognosis in various tumors (Auer 1989, Atkin 1991). DNA ploidy measured by cytometry techniques is related to the ploidy determined by the cytogenetic analysis (Table 1). With FC measurements, as well as with IC measurements of smears or disaggregated tissue, the whole nuclei are analyzed. The DNA content of the nuclei can be obtained with these techniques. IC of tissue sections measures the DNA content of sectioned nuclei. The total DNA content of whole nuclei is reflected in the

**Table 1. DIFFERENT APPROACHES FOR THE PLOIDY ANALYSIS**

<b>TECHNIQUE</b>	<b>WHAT IS ANALYZED?</b>
<b>CYTOGENETICS</b>	<b>NUMBER AND TYPE OF CHROMOSOMES IN NUCLEI</b>
<b>FC</b>	<b>DNA AMOUNT IN NUCLEI</b>
<b>IC</b>	<b>DNA AMOUNT IN NUCLEI</b>
<b>IC OF TISSUE SECTIONS</b>	<b>DNA AMOUNT IN SECTIONS OF NUCLEI</b>

The nuclear DNA content (DNA ploidy) can be obtained with cytometry measurements of whole nuclei in smears or cytopins. With the measurements of tissue sections the amount of DNA of cut nuclei is analyzed.

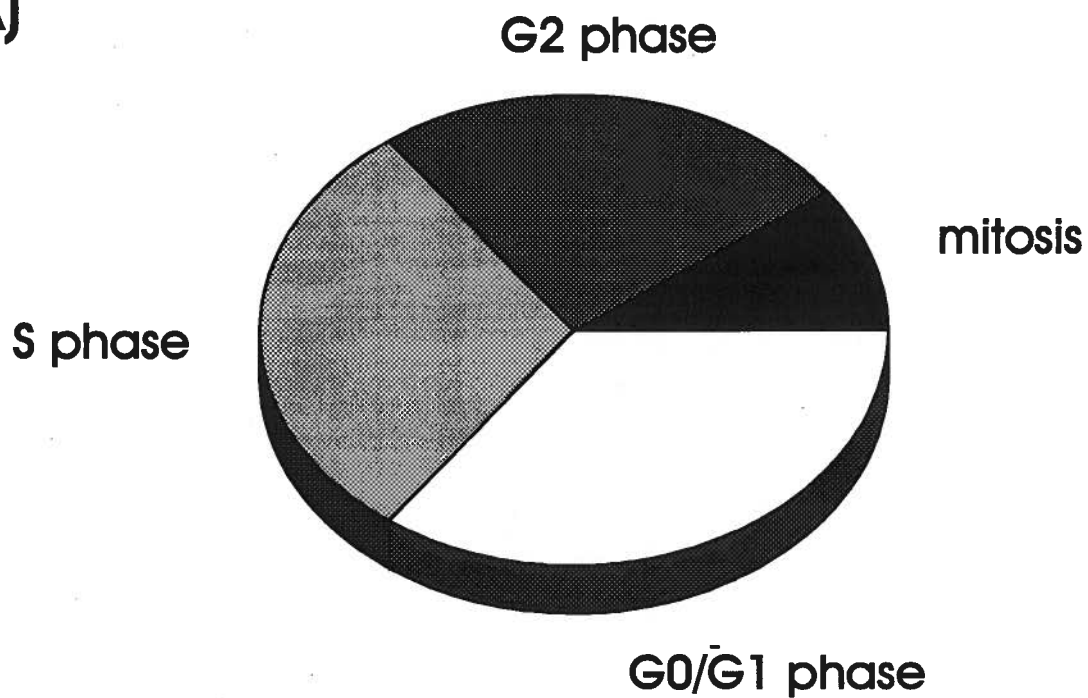
DNA content of sectioned nuclei. This depends on the section thickness and the nuclear size.

Generally, nuclei in normal tissues contain a double set of chromosomes ( $2c, n=1$ ) and are said to be in the diploid range. In normal tissues there is usually a certain proportion of cells which proliferate in order to replace the dying cells. The proliferating cells follow the events of the cell-cycle which is divided into four phases: i)  $G_1$ -phase, where cell performs its usual function, ii) S-phase, with the DNA synthesis, iii)  $G_2$ -phase, where the additional preparation for the cell division takes place, and iv) M (mitotic) phase with the division of nuclear material and cytoplasm to two daughter cells (Figure 2A). Non-cycling cells rest in the  $G_0$ -phase and have a diploid ( $2c, n=1$ ) DNA amount and so do the cells in the  $G_1$ -phase of the cycle. In the S-phase the cells double their DNA amount and during the  $G_2$ -phase and mitosis the cells contain a duplicated amount of DNA with four sets of chromosomes ( $4c, n=2$ ).

The events of the cell cycle are manifested in the IOD histograms (Figure 2B). The DNA distribution can be analyzed in the IOD histograms by determining boundaries for diploid, tetraploid and aneuploid peaks or in a more objective fashion by defining histogram statistics (Fallenius 1988, Opfermann 1987, Böcking 1989, Stenkvist 1990).

One way to define the DNA ploidy from the IOD histogram is with the use of the DNA index which corresponds to the modal value of the histogram peak (Figure 3). In a DNA diploid pattern histogram, which resembles normal tissue, the  $G_0/G_1$  peak is found in the peridiploid area ( $2c, n=1$ ) with some cells in the S-phase and some cells in the  $G_2M$ -phase ( $4c, n=2$ ). In tetraploid histograms the major cell population is in the tetraploid region ( $4c$ ). Histograms with peaks

A)



B)

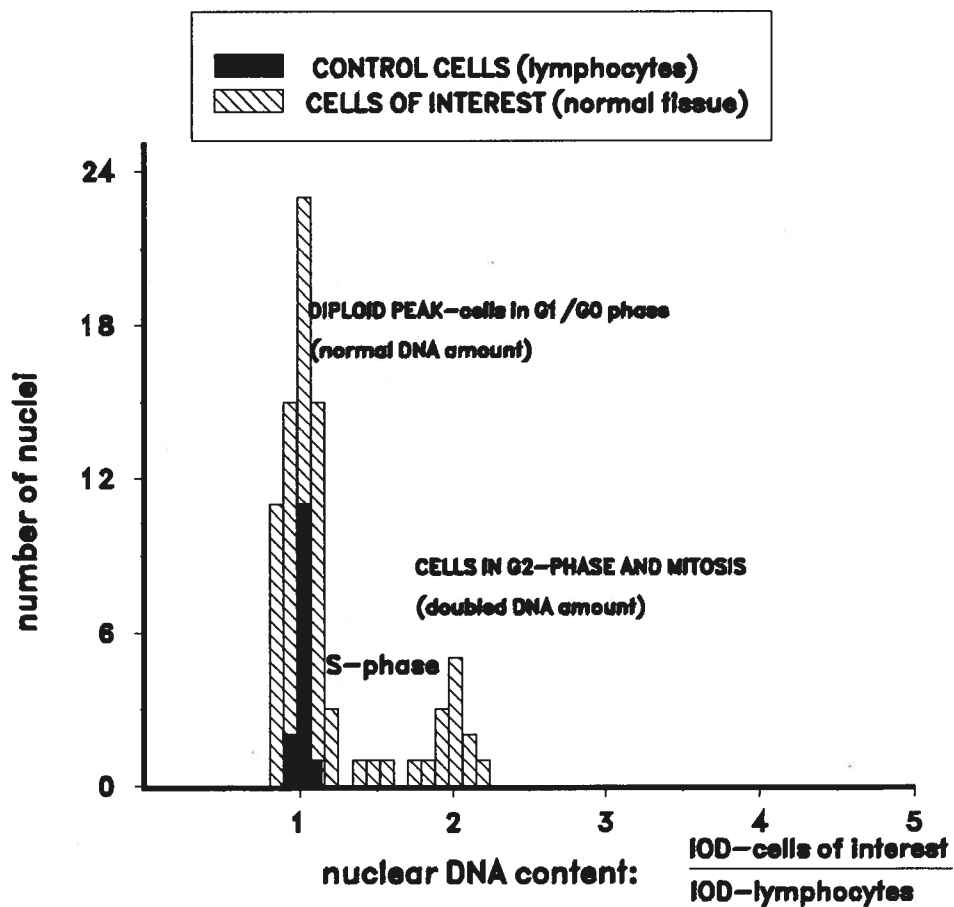


Figure 2a and 2b. PHASES OF THE CELL CYCLE (a) and DNA HISTOGRAM OF NORMAL BREAST TISSUE (b).

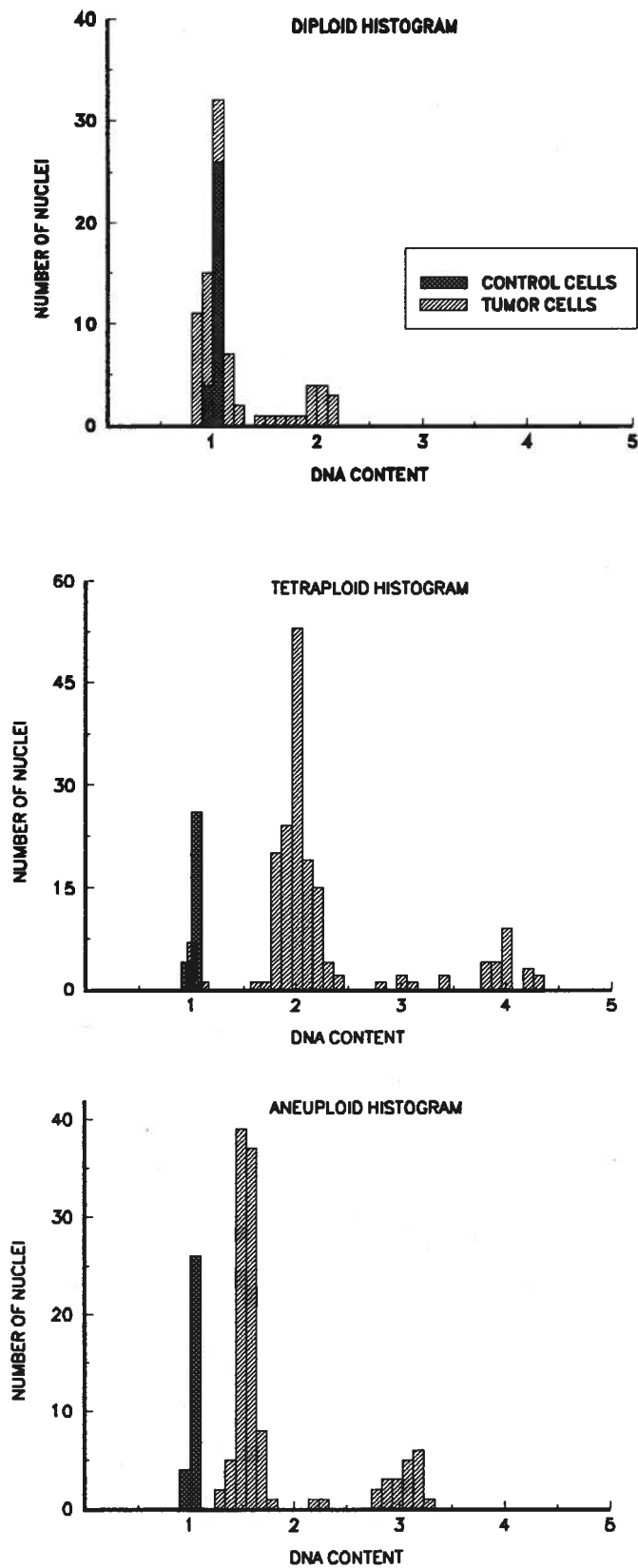


Figure 3. EXAMPLES OF DIPLOID , TETRAPLOID AND ANEUPLOID PEAKS IN DNA HISTOGRAMS.

outside the diploid or tetraploid area are considered aneuploid. Based on the DNA ploidy profile the histograms can be classified into four types I-IV (Auer 1980).

There are other approaches to the evaluation of IC-DNA histograms of breast cancer in an objective way. Quantitative histogram descriptors, which might have a prognostic value for breast carcinoma, are: Mean IOD (equals the average nuclear DNA content of the measured cell population), 2 $\sigma$ -deviation index, DNA-malignancy grade, percentage of cells exceeding various levels of DNA content, entropy of the histogram, and ploidy balance (Opfermann 1987, Fallenius 1988, Böcking 1989, Stenkvis 1990).

#### 1.1.D Various nuclear features employed by image cytometry

The morphological characteristics of nuclei as seen by the pathologist in cytological or histological specimens are among the most important criteria in the evaluation of tumors. Genetic alterations have an important role in the development and progression of malignant tumors (Feinberg 1982, Nowell 1989). Structural DNA changes are associated with changes in the chromatin pattern and alterations in nuclear morphology (Pienta 1989).

One of the advantages of IC is, that in addition to DNA content, several other nuclear features expressing morphologic nuclear characteristics in a quantitative way can be measured. Nuclear features can be categorized as: i) morphometric features, describing the nuclear size and shape, and ii) texture features, which describe the distribution of DNA in the nucleus. Examples of

morphometric features are nuclear area, and various shape features, such as compactness, variation of nuclear radius, and elongation.

In the past years several new features have been developed with the emphasis on the textural features (Komitowski 1985, MacAulay 1989). The alterations in the nuclear chromatin structure in fixed cells or tissues reflect the state of chromatin organization at the time of fixation and can be measured and reported in the form of texture features. Texture features can be divided into continuous and discrete texture features. Examples of continuous texture features are the variance of optical density and contrast. Discrete texture features are related to the DNA condensation and the distribution of heterochromatin and euchromatin in the nucleus. Discrete features are based on the separation of chromatin into low, medium and high density chromatin with the use of thresholds. Examples of this type of texture features are: Number of high density chromatin pixels, total area of medium density chromatin pixels, and average distance of low density chromatin pixels from the object center.

The use of various types of nuclear features for diagnostic or prognostic purposes in tumor pathology may offer superior results, as compared to DNA content alone. The value of using multiple nuclear features (DNA ploidy, texture and morphometric features) in grading of breast cancer was recognized in many studies (Stenkvist 1978, Larsimont 1989a, Baak 1985, Umbricht 1989, Dawson 1991, Komitowski 1990, Theissig 1991). It has been shown that nuclear grade of breast carcinoma correlated better with other prognostic factors when it was aided by image analysis of nuclear morphology and chromatin pattern (Komitowski 1990). Quantitative grading seemed to be more reproducible and gave better predictive values (Theissig 1991). Estrogen receptor positive and

negative tumors could be distinguished on the basis of different nuclear features such as area, DNA content and certain texture features (Larsimont 1989b). In addition to the prognostic implications, this finding is interesting, because it shows the ability of IC to detect morphologic nuclear changes which are related to the altered biology of the cell.

#### 1.1.E Benign breast disease and premalignant changes

The term benign breast disease encompasses a wide spectrum of benign conditions. Current understanding of these diseases has been described in detail (Harris 1991, Page 1987). It is suspected that some benign breast diseases are associated with an increased risk of subsequent breast carcinoma. The relationship between benign breast diseases and subsequent breast cancer has been the subject of numerous studies. However, it has not yet been demonstrated if they are the precursors of invasive cancer, or just the markers of increased risk of developing invasive carcinoma at another site.

A continuum of morphologic changes between normal lobules and ductal carcinoma in situ (DCIS) has been described by Wellings (Wellings 1975). These changes have been characterized by hyperplasia and varying degrees of atypia. In the above study, breasts with invasive cancer and breasts contralateral to cancerous breasts were obtained by mastectomy. Tissues were thoroughly examined by a subgross sampling technique, and compared to breasts without invasive carcinoma, which were obtained from autopsies. Their results showed that DCIS and atypical proliferative changes were much more frequently present in cancerous and contralateral breasts than in breasts without

carcinoma. Also, the number of such lesions in cancer-affected breast was much higher than in breasts without carcinoma. A similar study performed on a larger sample, reported additional foci of DCIS (unrelated to invasive cancer) in 52% of breasts with carcinoma, 48% of contralateral breasts and in only 6% of breasts from random autopsies (Alpers 1985). Moreover, proliferative lesions with severe atypia showed a similar tendency to appear in cancerous breasts. These findings support the association between i) proliferative changes with severe atypia and invasive carcinoma, and ii) between DCIS and invasive carcinoma.

Retrospective studies of women with benign breast biopsies indicate that subgroups of women with benign breast disease have an increased relative risk of getting breast cancer as compared to a general population matched for age (Black 1971, Dupont 1985, Page 1985, Page 1986, Jensen 1989, Tavassoli 1990, Palli 1991, London 1992, Dupont 1993). These epidemiological studies support the division of benign breast diseases according to their increased cancer risk to three groups: i) non-proliferative breast disease with no increase in the risk, ii) proliferative breast disease with 2 times increased risk, and iii) atypical hyperplasias with 4-5 times increased relative risk of subsequent invasive carcinoma (Figure 4).

Non-proliferative breast disease includes mild hyperplasia, cysts, calcifications, fibroadenomas and papillary apocrine change. Proliferative breast disease without atypia consists of moderate and severe epithelial hyperplasia, papillomas and sclerosing adenosis. Proliferative changes with atypia consist of atypical epithelial hyperplasias. Cellular and architectural features of epithelial hyperplasia classified by this approach have been

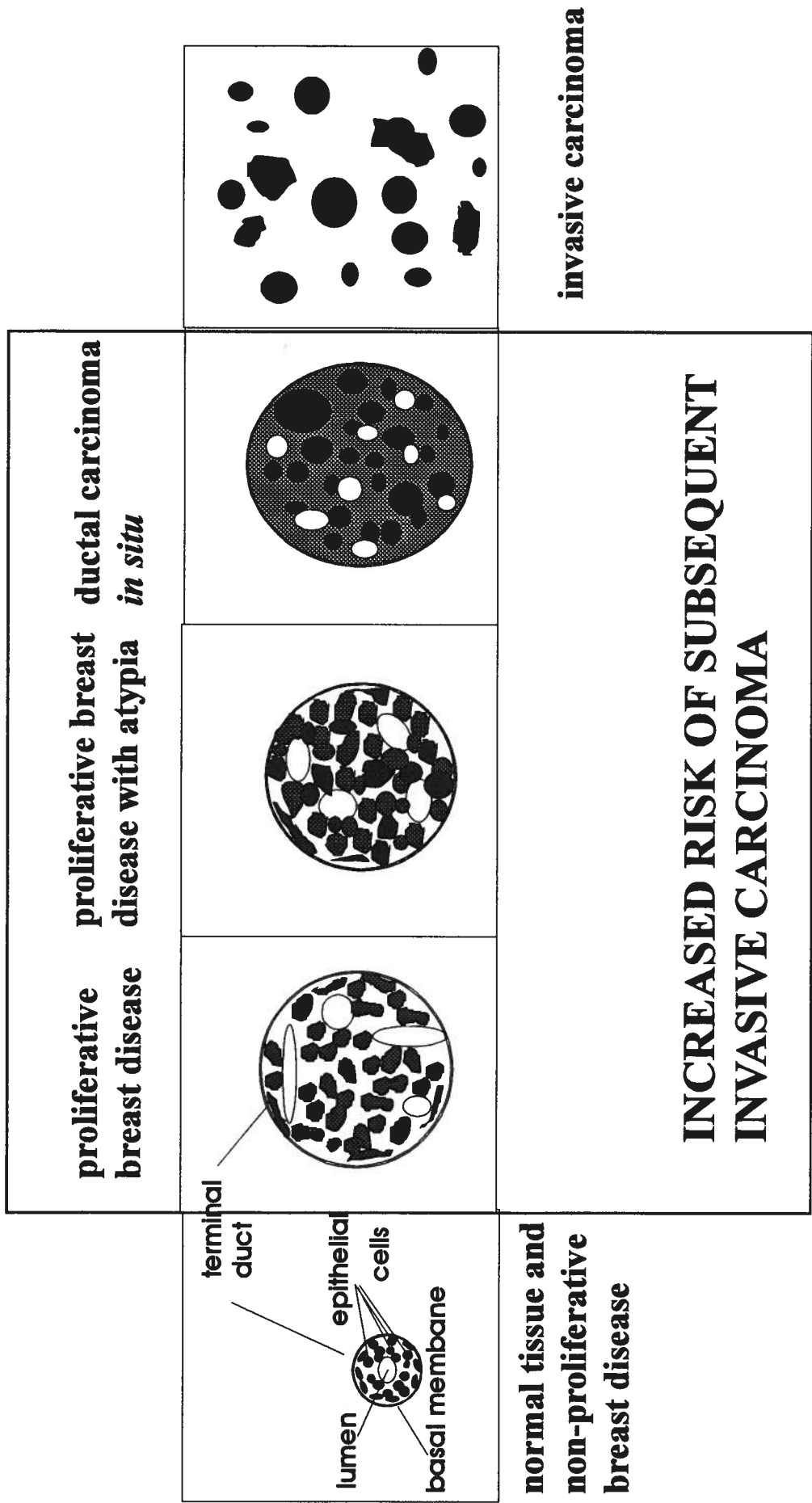


Figure 4. BREAST DISEASES WITH AN INCREASED RISK OF SUBSEQUENT DEVELOPMENT OF INVASIVE CARCINOMA.

described in detail by Page (Page 1987). This approach supports the continuum between hyperplasia, atypical hyperplasia and CIS in terms of morphology and in terms of the risk of subsequent invasive cancer. Unfortunately, variations in diagnosis in this area of pathology are frequent (Temple 1989) and the inter-observer variability of the diagnoses is high even when tested among pathologists highly experienced in breast pathology (Rosai 1991, Schnitt 1992).

It is obvious that the assessment of risk associated with a particular diagnosis is unreliable if the diagnosis itself is uncertain. Nuclear features may be useful as an aid in the evaluation of premalignant breast changes to increase the objectivity and the reproducibility of the diagnosis.

#### 1.1.F Image cytometry of benign breast disease

The process of malignant transformation of breast tissue is thought to be a sequence of molecular events which are associated with the alterations in tissue morphology of normal tissue to proliferative/hyperplastic changes, DCIS and finally to invasive ductal cancer. It should be possible to follow the sequence of these changes by the analysis of quantitative nuclear features, which reflect the changes in the DNA amount, nuclear size and shape, and chromatin structure. Similar progressive changes in nuclear size, nuclear shape, chromatin texture and/or in the DNA content have been demonstrated by IC in other tissues, such as cervix, colon, thyroid, and prostate (Bibbo 1989, Mulder 1992, Petein 1991, Salmon 1992, Wang 1992).

Analysis of nuclear features has not been performed on breast premalignant changes and DCIS as widely as on invasive cancer. King et al.

(1988) demonstrated the ability of IC to discriminate between normal, premalignant, CIS and invasive cancer cells on breast fine needle aspirates according to the diagnoses from the subsequent surgical biopsies. Moreover, with an appropriate statistical model, they have been able to classify premalignant lesions which could not be identified by routine cytology. With IC classification, which was based not only on the DNA content but on various nuclear features, the changes were clustered into a clinically insignificant group (mild and moderate hyperplasia) and into a clinically significant group (atypical hyperplasia, CIS and invasive cancer). Their results support the theory that like CIS, atypical hyperplasia is also a precursor of invasive carcinoma.

In another study, where IC was employed on breast tissue sections, a comparison of DNA content of preneoplastic (atypical hyperplasia) and neoplastic lesions demonstrated that the DNA ploidy acquired from tissue sections with preneoplastic changes was identical to the DNA ploidy of synchronous carcinoma (Teplitz 1990). In another study, nuclear area, nuclear perimeter and DNA content were measured for usual hyperplasia, ADH and DCIS (Norris 1988). These features were not found useful in differentiating between the histological groups. (It is possible that positive results could be obtained by the incorporation of chromatin distribution features in this study). Only DCIS with high grade nuclei could be separated from the other groups by using these two features. To the contrary, Crissman et al. (1990) found aneuploidy more often in DCIS (71%, n=25) than in ADH (36%, n=35). However such difference in a single feature can not be sufficient for a successful classification.

It was also shown that epithelial cells in the proliferative areas of fibrocystic disease are sometimes aneuploid (Izuo 1971). Proliferative changes of patients with fibrocystic disease who later developed invasive cancer were found to be aneuploid more often than proliferative changes of patients without subsequent invasive cancer. The results of the above study support the association of aneuploidy and the progressive potential of benign breast disease.

Another study demonstrated that hyperplastic changes associated with ductal carcinoma *in situ* exhibited higher mitotic counts than hyperplastic lesions in benign proliferative disease (DePotter 1987). This finding indicates that a higher proliferative activity might be predictive of the ductal malignancy in the surrounding tissue.

#### 1.1.G Malignancy associated changes (MAC)

Malignancy associated changes (MAC) are defined as subtle morphological nuclear changes in normal appearing tissues adjacent or distant to malignant tumors. The first reports on MAC began in the late sixties as qualitative observations. The characteristics of chromatin structural changes, which were first defined as MAC, were first described by Nieburgs (1968). He claimed that malignant tumors are associated with systemic cellular changes which can be recognized under high magnification of the light microscope by an experienced observer. MAC have been reported on nuclei of peripheral blood cells, buccal smears, sputum, bone marrow, uterus, pancreas, liver and skin

epithelia from patients with adjacent or distant malignancies (Nieburgs 1967, Nieburgs 1968, Finch 1971, van Oppen Toth 1975).

With the development of image cytometry devices, MAC studies became more objective and reproducible. Normal appearing nuclei originating from tissue adjacent to malignancy were analyzed and compared to normal nuclei from the same type of tissue of patients without cancer. Most of these studies were performed on material from cervix (Weid 1984, Montag 1989, Haroske 1990, Bibbo 1989, Zahniser 1991, Hutchinson 1992), colon epithelium (Bibbo 1990, Montag 1991), lung (Swank 1989), and thyroid (Bibbo 1986, Lerma-Puertas 1989). Majority of these studies described the changes of nuclear shape and chromatin distribution in normal appearing nuclei from the tissue adjacent to carcinoma. One of the authors used flow cytometry, and reported the presence of higher proliferation rate and even aneuploidy in nuclei of normal colon tissue, as far as 10 cm away from carcinoma (Ngoi 1990).

However, there have been no similar observations reported on breast tissue, except that higher proliferative activity has been demonstrated on nuclei from benign hyperplastic changes in the neighborhood of carcinoma *in situ* (DePotter 1987).

#### 1.1.H Ductal carcinoma *in situ* (DCIS)

Breast carcinoma *in situ* (CIS) consists of a heterogeneous group of lesions (Harris 1991, Schnitt 1988). Based on the cytological appearance and the pattern of growth, CIS is classified to two major types: Lobular and ductal CIS. Ductal carcinoma *in situ* (DCIS) is characterized by proliferation of

malignant cells in the ducts without evidence of invasion across the basement membrane. DCIS constitutes the majority of *in situ* breast cancer, about 80%.

There is a variety of histological types of DCIS with different growth patterns. Often different histologic types are found in the same biopsy. The most common histological types are cribriform, solid, micropapillary, papillary and comedo (Page 1987, Schnitt 1991). Various types of DCIS differ not only in their morphology but also in their clinical appearance, biological characteristics and malignant potential.

DCIS can be detected clinically as palpable lumps, with mammography as calcifications or a mass and incidentally when the breast is examined for other diseases. The detection of early stage cancers ensures better prognosis and facilitates the breast preserving approach in therapy. The frequency of DCIS in women who had breast malignancy detected by mammography is four times higher than the frequency of DCIS in women who present with palpable breast carcinoma (Stacey-Clear 1992). Since mammography screening has become a routine the detection of carcinoma *in situ* without associated invasive carcinoma has increased from less than 5% to 15-22% of cancers found in breast biopsies (Anderson 1991, McKinna 1992). One study reported that clinically occult DCIS were found in autopsies of middle aged women in 15% of cases (Nielsen 1987). This study indicates that some DCIS cases are not detected in a woman's life time and that the true incidence of DCIS is even higher than detected by the mammography screening.

The natural history of DCIS is not well understood because it is usually removed after the diagnosis. This situation is similar to carcinoma *in situ* changes in other tissues, with the best example in cervical CIS (Koss 1963, Koss

1989). It has become clear that not every DCIS is a life threatening disease and that a proportion of these lesions persist unchanged for long periods of time or even regress.

At present it is known that the risk for the development of subsequent invasive cancer from small DCIS, detected incidentally, is substantially elevated when compared to the general population matched for age. Two retrospective studies evaluated the prognosis of small DCIS which were missed in the initial diagnosis and were therefore treated only with biopsy. Both have shown an increased risk of subsequent invasive carcinoma in these patients. The first study presented the follow-up results of 15 such lesions (Rosen 1980). In the average time of 9.7 years, 10 women (66%) developed cancer in the same breast. Recurrent carcinomas were ductal in origin and invasive in 8 cases. This group of patients had 20% mortality from breast cancer (3 patients). The second study followed 25 cases of DCIS treated only by biopsy for average of 16 years. Seven women (28%) presented with invasive cancer in the same breast three to ten years after the initial biopsy (Page 1982).

In the prospective study of Lagios, small DCIS was treated only with excision and a relatively small recurrence rate (3/20) was found. However, the follow-up period in this study was only 44 months (Lagios 1982). On a larger sample of 79 patients with DCIS detected by mammography and treated only with biopsy, 10% recurrence has been described with an average follow-up time of 4 years (Lagios 1989). One half of the recurrent cases were DCIS and the other half were invasive carcinomas. The recurrence was associated with the high nuclear grade of DCIS and mostly occurred with comedo DCIS. Another

prospective study reported 23% (5/22) recurrence of DCIS treated only by lumpectomy with the average of 39 months follow-up after surgery (Fisher 1986).

The above studies point to the heterogeneity of DCIS and indicate that DCIS are common but not necessarily dangerous changes and do not need to be treated aggressively in every case. However, there is a lack of prognostic factors which would predict the destiny of individual patients. In the past, mastectomy used to be the treatment of the choice for DCIS. Mastectomy can be justified by i) frequent occult invasion; ii) frequent DCIS multicentricity which is not identified clinically or with mammography, iii) possible malignant transformation of the remaining normal tissue (Ashikari 1977, Schnitt 1988, Lagios 1982). Mastectomy provides nearly 100% cure for DCIS, but at the same time it represents overtreatment for many patients. It is clear that a better understanding of the biology and natural history of DCIS is required in order to improve the appropriateness of treatment.

Studies that have used a breast conserving approach for the treatment of DCIS included a relatively small number of patients and provided different conclusions. Some authors found conservative surgery for DCIS with or without additional radiotherapy acceptable with the rationale that recurrence could be successfully treated with more radical treatment, while others reported an unacceptable recurrence rate following a local excision (Fischer 1986, Kinne 1989, Arnesson 1989, Carpenter 1989, Price 1990, Bornstein 1991). Local excision appears to be an adequate treatment for incidentally detected DCIS and for the non-comedo subset of mammographically detected DCIS. Comedo DCIS was very seldom discovered incidentally and was often associated with the recurrence after conservative treatment (Schwartz 1992).

Two characteristics of DCIS present a risk to breast conserving therapy: multicentricity and occult invasion. Many studies demonstrated that DCIS is a multifocal disease with the increasing size of the lesion being predictive of multicentricity as well as occult invasion. Multicentricity has been detected in 30 - 68% of breasts removed because of a biopsy diagnosis of DCIS (Ashikari 1977, Rosen 1980, Lagios 1982, Silverstein 1987, Patchefsky 1989). In contrast to these findings, a study by Holland reported that DCIS typically did not have a multicentric pattern but showed a continuous growth (Holland 1990A).

After the diagnosis of DCIS in a biopsy, the subsequent mastectomy specimens show coexistent invasive carcinoma in 6% - 42% of cases depending on the precision of the method (Rosen 1980, Carter 1977, Lagios 1982, Patchefsky 1989). DCIS detected incidentally in a biopsy performed for other disease are usually not associated with invasive foci in the remaining breast. The rate of microinvasion depends on the histological type of DCIS (Patchefsky 1989). Microinvasion is often found with comedo type, even with the small DCIS. In contrast, cribriform, solid and papillary types are rarely associated with microinvasion. The micropapillary type has an intermediate frequency of microinvasion.

At present the factors which determine the progressive potential of DCIS are not understood. Therefore, it is not possible to predict the high risk of recurrence or progression to invasive cancer for individual patients. It is known that the histological type of DCIS has an effect on prognosis. Other factors, which are also thought to have the effect on prognosis of DCIS, are i) size, ii) grade, iii) proliferation rate, iv) aneuploidy, v) hormone receptors, vi) c-erbB-2 overexpression, vii) altered expression of p53 gene, and others (Meyer 1986,

van de Vijver 1988, Locker 1990, Bartkova 1990, Killeen 1991, Bur 1992, Pallis 1992, Schimmelpenning 1992, Poller 1993).

Most of these potential prognostic markers for DCIS are related to a histological type of DCIS. The aggressive nature of comedo DCIS is well known (Lagios 1989, Schwartz 1992). This type of DCIS is most often aneuploid (Locker 1990, Killeen 1991, Schimmelpenning 1992, Pallis 1992). Compared to non-comedo DCIS, the comedo type much more often exhibits an increased expression of c-erbB-2 oncogene, which has been associated with bad prognosis in invasive breast carcinoma (van de Vijver 1988, Bartkova 1990). Immunostaining of estrogen receptors is much more often negative in the comedo type than in other, better differentiated DCIS types (Bur 1992). The expression of mutant p53 protein, which is associated with genetic instability and tumor progression, is also much more often present in comedo type than in non-comedo types (Poller 1993).

Comedo tumors have a higher growth rate than other types of DCIS. Proliferation rate can be analyzed by the thymidine labeling technique, which identifies cells in the S-phase. Different proliferation rates of DCIS with different histological characteristics were detected with this method (Meyer 1986): Cribriform/micropapillary types are slowly proliferating, the solid type is an intermediate entity, and the comedo type has high proliferative rates. The histologic type of DCIS is predictive not only of proliferative rate of DCIS itself, but also of the proliferative rate of the associated invasive carcinoma. The thymidine labeling index of an associated invasive component is similar to the index of DCIS in about 90% of cases.

Moreover, the expression of nm23, a metastasis suppressor gene, is often negative in comedo DCIS, while other types show positive staining (Royds 1993). Microinvasion is commonly found in association with the comedo type (Patchefsky 1989) and is often multifocal.

It has been demonstrated that the comedo type of DCIS have a higher capacity to recur or to progress into invasive cancer than other types of DCIS (Lagios 1989, Schwartz 1992). Therefore, the biological characteristics associated with comedo DCIS might be linked to the aggressive behavior of DCIS.

#### 1.1.1 Image cytometry of ductal carcinoma *in situ*

Aneuploid DNA profile was more commonly found in DCIS which lacks the cytological or architectural differentiation (Crissman 1990) and was related to the overexpression of c-erbB-2 oncogene, a putative prognostic factor for breast cancer (Visscher 1991). The findings of Schimmelpenning, who found aneuploidy in 61% of DCIS, were similar. Aneuploidy was most common in comedo type (90%) and was related to the high nuclear grade and to the c-erbB-2 overexpression.

Other authors, who used flow cytometry (FC), also reported significant correlation between aneuploidy and high nuclear grade of DCIS (Killen 1991). FC of embedded tissue was used in another study and the relationship between histological type of DCIS, DNA content and S-phase fraction was analyzed (Locker 1990). In this study the cribriform type appeared to be rarely aneuploid,

had a low proliferative rate and was usually low grade in contrast to comedo, solid, micropapillary or mixed types of DCIS.

Differences in the DNA ploidy between different histological types have also been reported by other authors: The proportion of aneuploid tumors estimated on small samples with mostly 17 cases included in a single group was 38-50% in cribriform type, 52-71% in micropapillary type, 70-80% in solid type and 82-91% in comedo type DCIS (Crissman 1990, Fisher 1992, Schimmelpenning 1992, Pallis 1992). The overall frequency of aneuploid DCIS cases appears to be between 60% and 70%, but is clearly much higher in comedo type than in the other types.

Since aneuploidy in tumors most often marks a worse prognosis, it is likely that the same could be true for carcinoma *in situ*. With the use of the image analysis of Feulgen-stained nuclei, aneuploidy was detected much more often in DCIS accompanied with microinvasion than in DCIS without any invasive foci (Carpenter 1987a). Moreover, an association has been indicated between aneuploidy of DCIS and the recurrence after excision biopsy. Similarly, aneuploidy has been more frequently found in DCIS associated with invasion than in DCIS alone in a study performed on tissue sections (Carpenter 1987b). In contrast to these results, no differences in the DNA ploidy were found between pure DCIS and DCIS with an invasive component in the study performed by Fisher (Fisher 1992). In the above study no differences in the DNA ploidy could be demonstrated between comedo and non-comedo types. The reason for this surprising result might be that the comedo type was diagnosed only on the basis of intraluminal necrosis, while the grade of nuclei was not taken into account.

## 1.2. PROPOSAL

### 1.2.A Measurements of DNA content: Comparison of different cytometry techniques

Different cytometry techniques were compared in order to establish the value of the DNA content measurements performed with image cytometry on tissue sections. The purpose was to examine if the nuclear DNA content obtained by measurements on tissue sections can be applied to diagnosis and/or prognosis of breast diseases in addition to other nuclear features.

Measurements of tissue sections have not been as widely used and accepted for the purpose of DNA content measurements as other cytometric techniques. However, image cytometry (IC) of tissue sections was chosen to test the hypothesis that nuclear features can offer a useful prognostic information in various breast diseases. With the use of IC it is possible to obtain information covering a wide spectrum of morphological characteristics of nuclei. With IC measurements performed on sections it is possible to visualize tissue histology, to precisely localize the affected epithelium, and to selectively collect the images of nuclei. With IC of tissue sections a lesion limited to a single duct can be analyzed. This is important for the analysis of benign breast diseases and DCIS where areas of affected tissue are often small or scattered throughout the section with a variety of disease patterns being present on the same section.

The performance of different cytometric techniques was compared in the DNA measurements on archival specimens of invasive breast carcinoma. The first question was, how do the FC measurements of the DNA content relate to the IC DNA measurements performed on tissue sections from the same tissue

blocks. DI and ploidy acquired by FC and IC from the adjacent tissue sections were compared.

The effect of different preparative and sampling methods on the DNA content measurements of breast carcinoma was also studied. IC measurements were performed on: i) archival smears of breast aspirates, ii) tissue sections from embedded tissue blocks, and iii) disaggregated nuclei from corresponding tissue blocks. The DNA ploidy and DNA histogram parameters, obtained by the three techniques were then analyzed.

#### 1.2.B            The relationship between the histological patterns of breast diseases and quantitative nuclear features

Quantitative nuclear features reflect morphologic nuclear changes. It may be expected that changes in quantitative features correspond to increasing structural and functional DNA abnormalities, which are associated with the development of malignant tumors. Nuclear features of various categories of breast diseases were studied in order to demonstrate how nuclear features correspond to human classification of breast diseases. Quantitative features could be possibly used as an aid for a more objective diagnosis of these diseases.

The aim was to characterize nuclear morphology of various breast diseases in a quantitative way with the use of nuclear features measured by image cytometry. Nuclear features were analyzed in the following groups of breast diseases: Normal breast tissue, non-proliferative breast disease, proliferative breast disease, DCIS, and invasive carcinoma. It was expected that

certain features, such as nuclear area or shape, would change progressively in relation with advancing histological changes and with an increasing degree of proliferation and atypia.

### 1.2.C Nuclear features as a prognostic factor for DCIS

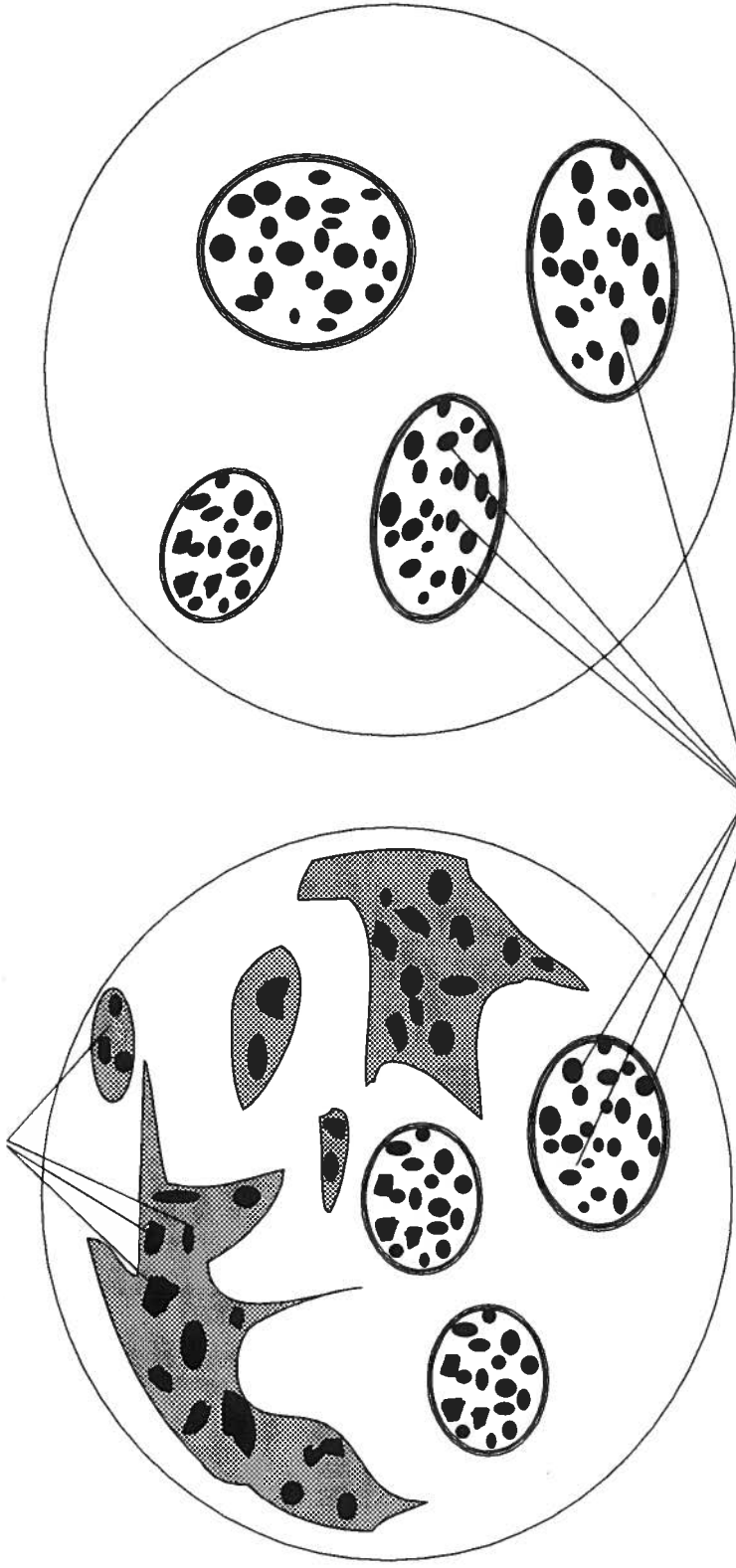
Prior to the study of the prognostic value of nuclear features for DCIS, the main histological types of DCIS were characterized on the basis of their nuclear features. The differences between main types were analyzed for the DNA ploidy, nuclear size, shape and chromatin distribution. The purpose of this analysis was to avoid any effects that these differences might have on the study of the prognostic value of nuclear features.

The importance of prognostic factors for DCIS is difficult to study because the lesion is usually completely removed in order to be successfully treated. Indirectly it might be possible to evaluate some prognostic factors with a comparison of i) DCIS without invasive cancer (DCIS1) and ii) DCIS with synchronous invasive cancer in the same breast (DCIS2).

One of the objectives in the present study was to test the hypothesis that nuclear features of DCIS2 differ from nuclear features of DCIS1. The hypothesis assumed that some nuclear features, related to the DNA amount in the nucleus, nuclear size, shape, contour, chromatin texture or proliferation rate of cells, may be more irregular when measured on DCIS with invasive cancer present in the same breast. We proposed that DCIS1 and DCIS2 could be distinguished on the basis of their nuclear features measured by image cytometry (Figure 5).

The demonstration of differences between DCIS1 and DCIS2 would have

**INVASIVE CARCINOMA NUCLEI**



**CARCINOMA IN SITU NUCLEI:  
DIFFERENCES IN NUCLEAR MORPHOLOGY BETWEEN DCIS1 AND DCIS2 CAN BE  
DEMONSTRATED WITH QUANTITATIVE ANALYSIS OF NUCLEAR FEATURES.**

**CARCINOMA IN SITU WITH  
ASSOCIATED INVASIVE  
COMPONENT (DCIS2)**

**CARCINOMA IN SITU  
WITHOUT INVASIVE  
COMPONENT (DCIS1)**

**Figure 5. DUCTAL CARCINOMA IN SITU WITHOUT INVASIVE COMPONENT (DCIS1) AND DUCTAL CARCINOMA IN SITU WITH INVASIVE COMPONENT (DCIS2).**

an important, clinically relevant implication: Nuclear features may be predictive of the invasive potential of DCIS and may be possibly applied as markers predictive of the subsequent behavior of DCIS tumors.

#### 1.2.D Malignancy associated changes

The hypothesis proposed that nuclear features of normal tissue in breasts with carcinoma differ from the nuclear features of normal tissue obtained from breasts without a malignancy. Similar observations have been reported previously as malignancy associated changes (MAC), but have not been yet demonstrated in breast tissue.

One of the objectives of this thesis was to demonstrate the existence of MAC in breast tissue with the analysis of quantitative nuclear features of nuclei from normal appearing lobules in the vicinity of carcinoma. The comparison of nuclear features of normal appearing tissues obtained from cancerous and non-cancerous breast could provide useful prognostic information. If differences could be demonstrated, then the combination of selected quantitative features could be used as a marker to indicate the presence of malignancy in the breast.

The demonstration of MAC on breast tissue could aid in the cases where malignancy is present in the breast but not found in the biopsy because of the inadequate sampling. The implications of such finding would also be important for studying the prognosis of benign breast disease: The presence of MAC in a benign breast biopsy may be indicative of progressive potential of the benign tissue and might be associated with an increased risk of the subsequent invasive carcinoma (Figure 6).

# MALIGNANCY ASSOCIATED CHANGES (MAC)

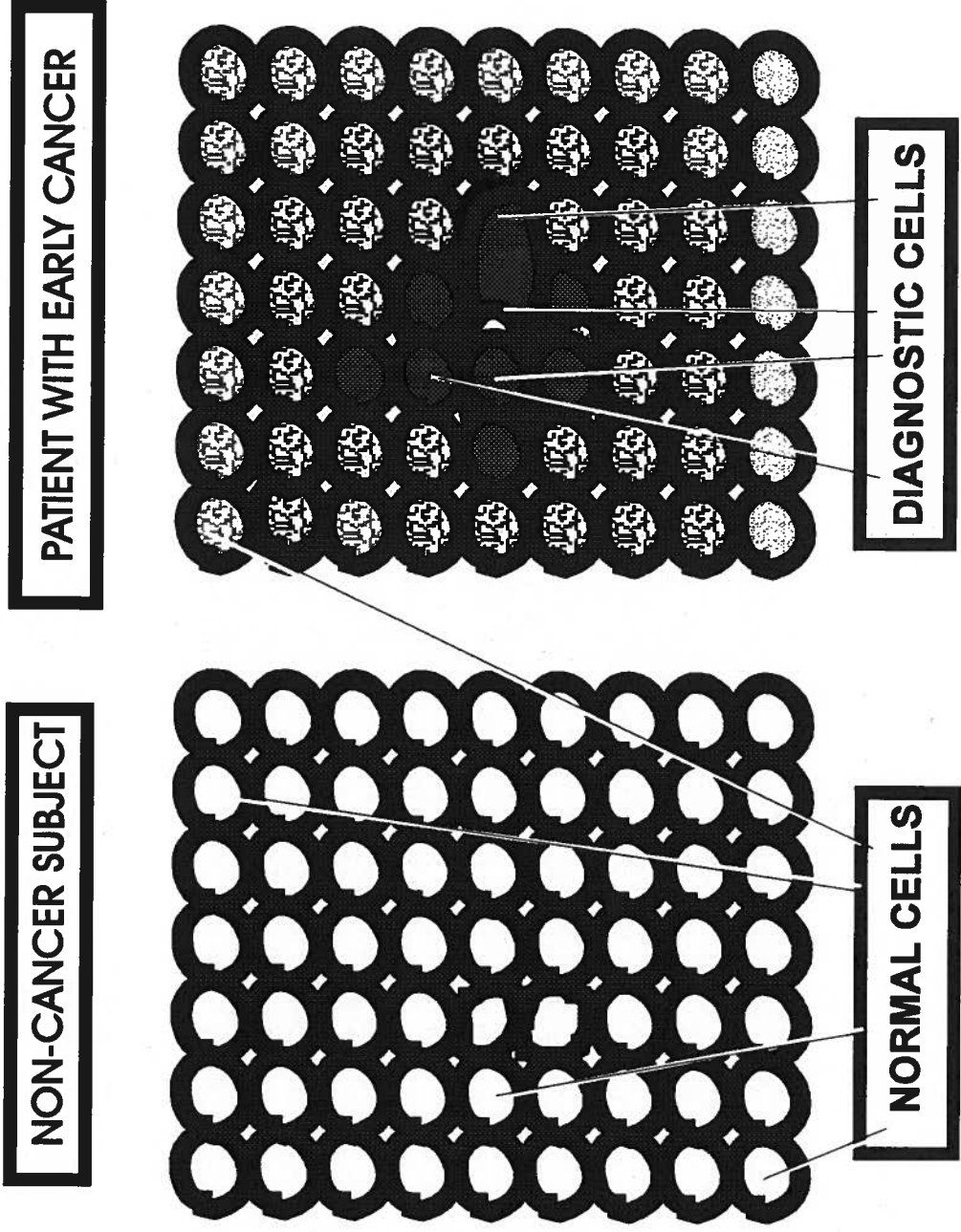


Figure 6. MAC: MALIGNANCY ASSOCIATED CHANGES.

Normal cells in the proximity of malignancy (and a pre-malignant lesion?) have slightly different nuclear texture features than the cells from a non-cancer subject.

## **2. OBJECTIVES**

THE OBJECTIVE OF THIS THESIS WAS TO INVESTIGATE THE HYPOTHESIS THAT QUANTITATIVE NUCLEAR FEATURES CAN PROVIDE PROGNOSTIC INFORMATION FOR BENIGN BREAST DISEASE AND DUCTAL CARCINOMA IN SITU. THE FOLLOWING ISSUES WERE STUDIED:

1. THE VALUE OF DNA MEASUREMENTS PERFORMED BY IMAGE CYTOMETRY ON TISSUE SECTIONS IN RELATION TO THE DNA MEASUREMENTS PERFORMED BY FLOW CYTOMETRY OR AUTOMATED IMAGE CYTOMETRY TECHNIQUES;
2. THE RELATIONSHIP BETWEEN QUANTITATIVE NUCLEAR FEATURES AND ADVANCING MORPHOLOGICAL CHANGES OF BREAST TISSUE;
3. QUANTITATIVE NUCLEAR FEATURES OF VARIOUS HISTOLOGICAL TYPES OF DCIS;
4. DIFFERENCES IN NUCLEAR MORPHOLOGY BETWEEN PURE DCIS AND DCIS ASSOCIATED WITH SYNCHRONOUS INVASIVE CARCINOMA;
5. MALIGNANCY ASSOCIATED CHANGES: SUBTLE CHANGES OF NUCLEAR MORPHOLOGY IN THE EPITHELIAL CELLS OF NORMAL LOBULES IN THE VICINITY OF INVASIVE CARCINOMA.

### **3. MATERIALS AND METHODS**

#### **3.1 TISSUES**

One pathologist (dr. Ann Worth) reviewed the diagnoses of all the slides and of all the selected areas on each slide.

##### **3.1.A Comparison of image and flow cytometry**

Forty-eight formaldehyde fixed paraffin embedded tissue blocks were available for the study. The blocks were one to ten years old. The presence of tumor was confirmed on haematoxylin-eosin (HE) stained sections. After the first HE section, two 50 $\mu$ m sections were cut for FC, followed by two serial 4  $\mu$ m tissue sections for IC and for another HE slide. The majority of cases were diagnosed as invasive ductal cancers and many had a coexisting ductal carcinoma *in situ* (DCIS). One case was diagnosed as colloid carcinoma and another case as medullary carcinoma. In six cases only DCIS was present in the tissue block.

##### **3.1.B Comparison of image cytometry measurements performed on smears, cytopins and sections**

Archival smears from breast aspirates, and formaldehyde-fixed, paraffin-embedded tissue blocks from subsequent biopsy or mastectomy, were available for seven patients with invasive breast carcinoma. Three adjacent tissue

sections were cut from each tissue block. The first 4 $\mu$ m section was stained with the routine haematoxylin-eosin stain in order to confirm the diagnosis. The second 4 $\mu$ m section was used for the image cytometry measurements, and the third section, 50 $\mu$ m thick, was used to prepare the cytopsin of the nuclear suspension for the image cytometry measurements. All of the patients had invasive breast carcinoma. The diagnosis of smears was in agreement with the histological diagnosis in all cases except one, where the smear was negative for malignancy due to the lack of the diagnostic cells.

### 3.1.C Correlation of quantitative features with advancing morphological changes

The paraffin embedded tissues used for image analysis originated from fine wire biopsies taken as a result of positive mammography screening or from mastectomy material. Tissues of patients with the diagnosis of benign breast disease, DCIS or invasive carcinoma were analyzed. The number of cases which were analyzed is shown in Table 2.

Measurements were performed on following tissues: i) areas of normal tissue from breasts with a variety of diseases, ii) non-proliferative disease, iii) proliferative breast disease, iv) non-comedo DCIS, v) comedo DCIS, and vi) invasive ductal carcinoma.

Images of normal nuclei were collected from normal breast lobules of patients with benign or malignant breast disease. Normal breast lobule is shown in Figure 7.

Table 2. THE NUMBER OF CASES ANALYZED IN SIX GROUPS OF BREAST DISEASES.

<b>DIAGNOSIS OF THE ANALYZED AREA</b>	<b>NUMBER OF CASES</b>
<b>NORMAL TISSUE</b>	<b>53</b>
<b>NON-PROLIFERATIVE DISEASE</b>	<b>8</b>
<b>PROLIFERATIVE DISEASE</b>	<b>18</b>
<b>NON-COMEDO DCIS</b>	<b>60</b>
<b>COMEDO DCIS</b>	<b>21</b>
<b>INVASIVE DUCTAL CARCINOMA</b>	<b>37</b>

Proliferative diseases included moderate or severe ductal hyperplasia, sclerosing adenosis and papilloma. Non-proliferative disease group consisted of mild ductal hyperplasia. Mild hyperplasia is truly a proliferative disorder. However, in the classification of breast diseases mild hyperplasia is included in the group of non-proliferative diseases.

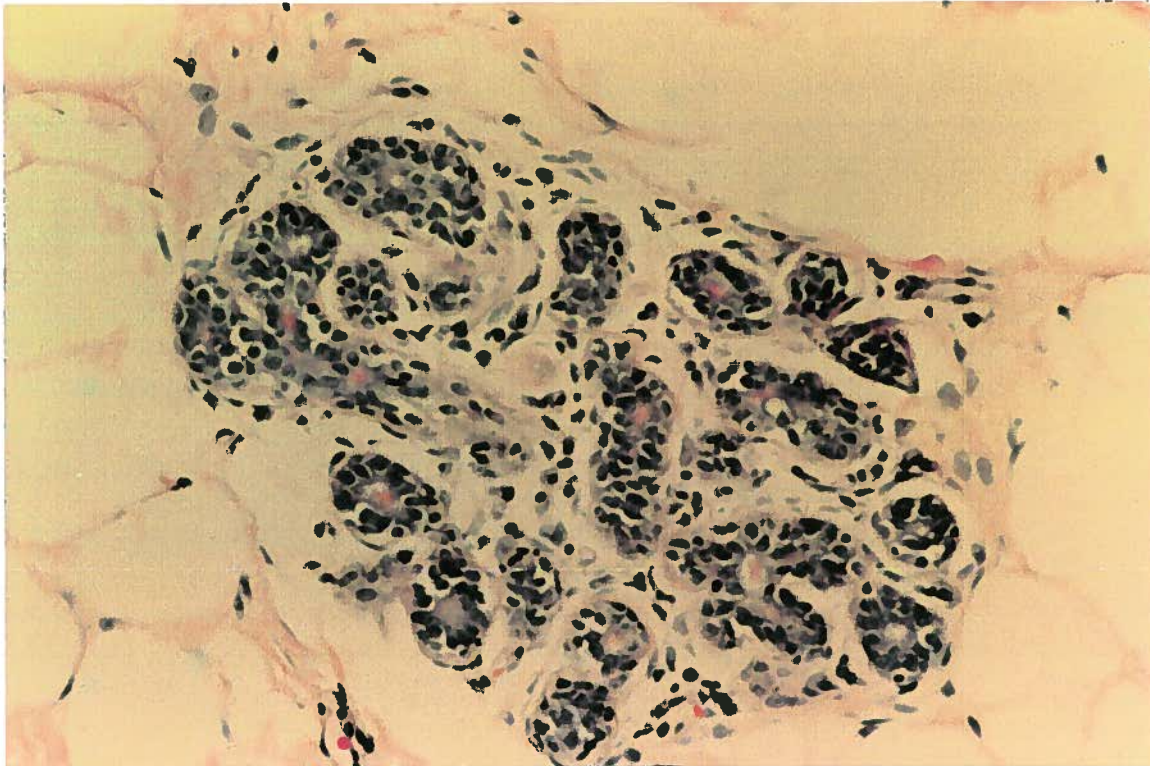


**Figure 7. NORMAL BREAST LOBULE.**

Haematoxylin-eosin stain. Magnification on the print is approximately 172:1:  
(objective 16 X wide-field system factor 0.63 X optovar factor 1.25 X projective  
3.2 X magnification of the print 4.3 = 172)

For the cases included in the non-proliferative disease group, measurements were performed only on areas with mild hyperplastic changes (Figure 8). Mild hyperplasia is truly a proliferative disorder. However, in the classification of breast diseases mild hyperplasia is included in the group of non-proliferative diseases because it is not associated with an increased risk of subsequent carcinoma as are the other entities in the group of proliferative breast disease.

Changes analyzed in proliferative disease group included moderate and severe ductal hyperplasia, sclerosing adenosis and papilloma. Proliferative lesions showed various degrees of nuclear and/or architectural atypia. However, due to a small number of analyzed cases in this group, they were not further divided according to the degree of atypia. Figure 9 and 10 show examples of proliferative breast disease.

DCIS consisted of 21 comedo and 60 non-comedo cases. For the purpose of this study, criteria for the diagnosis of comedo type consisted of: i) ducts distended by a confluent proliferation of CIS cells, ii) intraluminal necrosis, iii) and a high nuclear grade with the majority of cells having grade 3 nuclei. Periductal fibrosis and inflammation were found in most comedo cases included in this study. Figure 11 shows an example of comedo DCIS.

Invasive carcinoma group consisted of 37 cases of invasive ductal carcinoma (Figure 12).

One pathologist reviewed the diagnosis of the slides, as well as all selected areas on each slide.



**Figure 8. NON-PROLIFERATIVE BREAST DISEASE: MILD HYPERPLASIA.**

Haematoxylin-eosin stain. Magnification on the print is approximately 172:1.

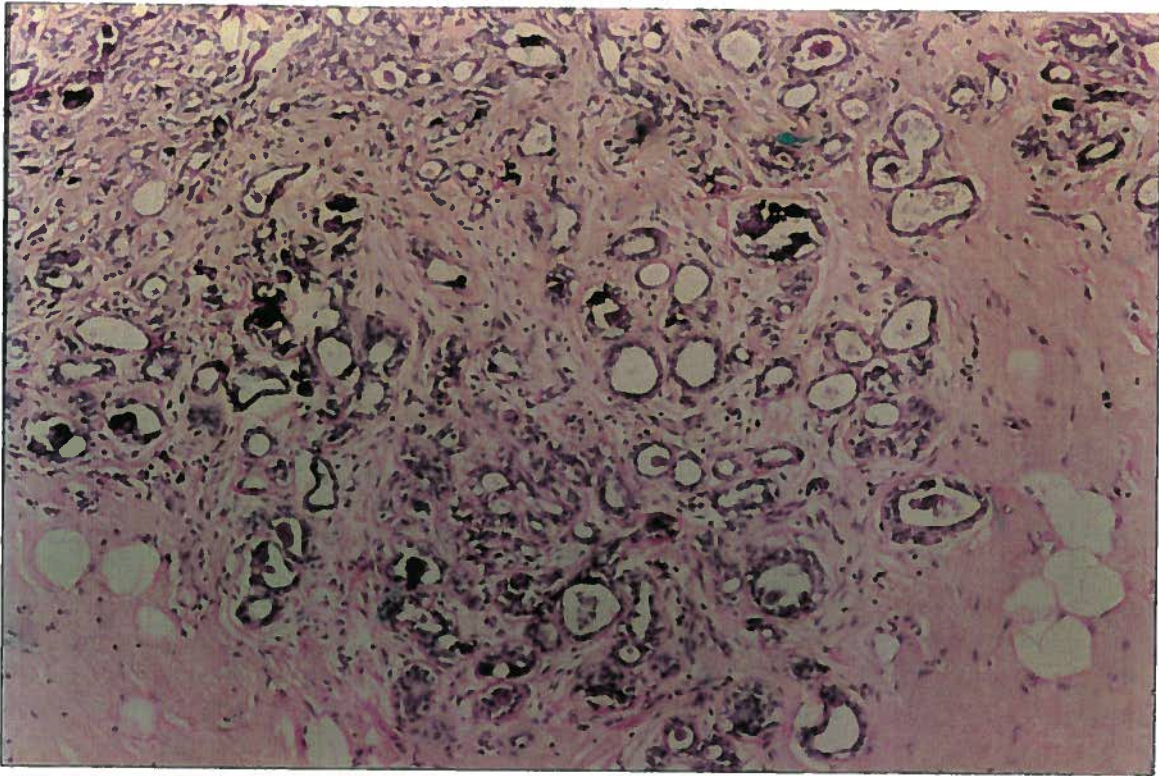


**Figure 9. PROLIFERATIVE BREAST DISEASE (A): SCLEROSING ADENOSIS.**

**Haematoxylin-eosin stain. Magnification on the print is approximately 69:1.**



**Figure 10. PROLIFERATIVE BREAST DISEASE (B): MODERATE DUCTAL HYPERPLASIA.**

**Haematoxylin-eosin stain. Magnification on the print is approximately 107:1.**

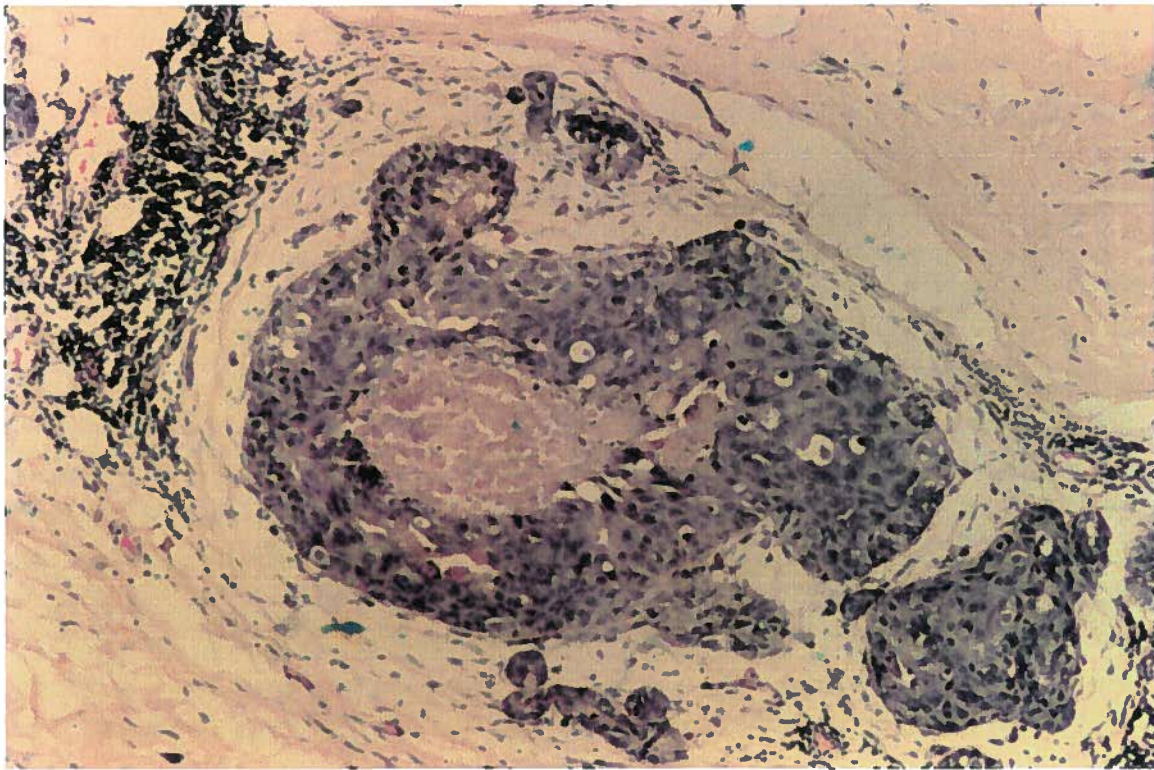


Figure 11. DUCTAL CARCINOMA IN SITU: COMEDO TYPE.

Haematoxylin-eosin stain. Magnification on the print is approximately 107:1.

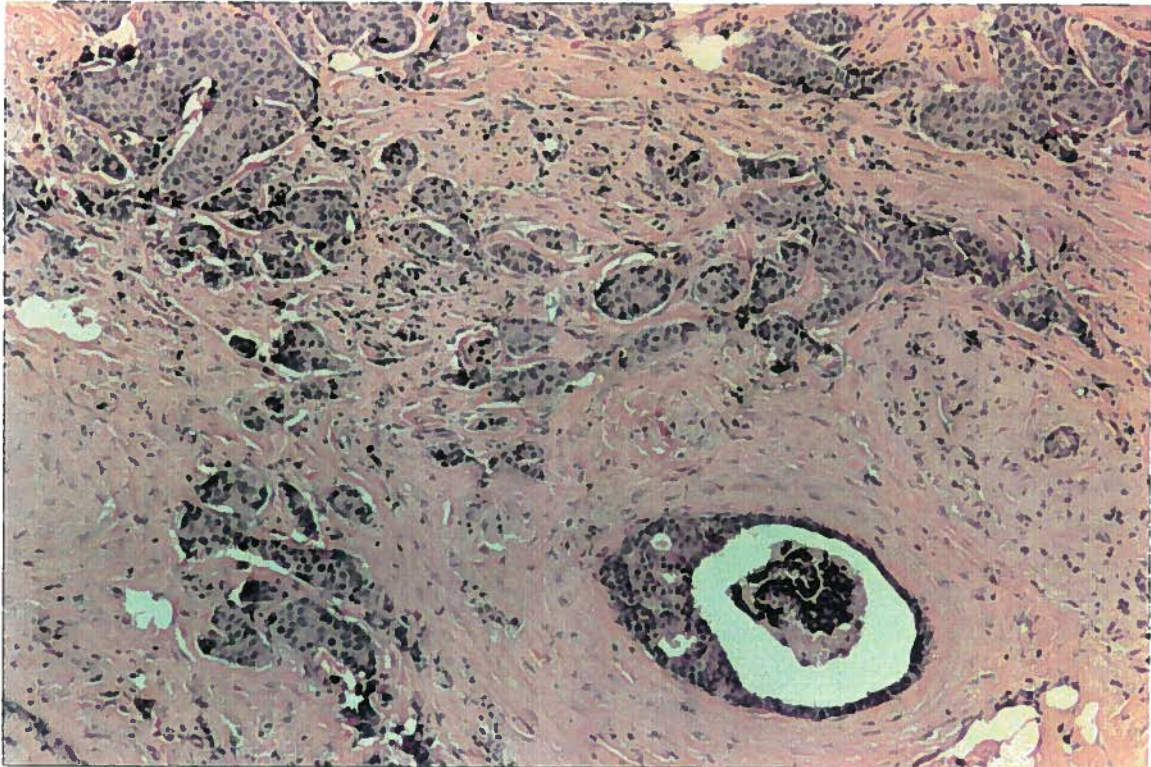


Figure 12. INVASIVE DUCTAL CARCINOMA.

Haematoxylin-eosin stain. Magnification on the print is approximately 69:1.

### 3.1.D Heterogeneity of DCIS

Differences in quantitative nuclear features were studied between comedo DCIS (21 cases) and non-comedo DCIS (60 cases). Also, comparison of nuclear features was made between various histological types of non-comedo DCIS. The analysis included cribriform (11 cases), papillary (5 cases), confluent/acinar (24 cases), mixed (13 cases), and non-specific types (7 cases). In mixed type the combinations of two or more non-comedo types were present. Non-specific type consisted of non-comedo DCIS with architectural patterns that did not fit to any of above categories.

### 3.1.E Differences between pure ductal carcinoma *in situ* and ductal carcinoma *in situ* associated with invasive carcinoma in the surrounding tissue

To test for differences in quantitative nuclear features between pure ductal carcinoma *in situ* (DCIS) and DCIS with synchronous invasive carcinoma, specimens containing DCIS were obtained from patients with or without invasive carcinoma of the breast. Comedo and non-comedo types of DCIS were studied separately. The numbers of cases involved are shown in Table 3.

### 3.1.F Malignancy associated changes

The aim was to compare normal breast epithelial nuclei originating from patients with benign breast disease and normal epithelial nuclei from breast

**Table 3. THE NUMBER OF PURE DCIS AND DCIS WITH ADJACENT INVASIVE CARCINOMA INCLUDED IN THE STUDY.**

<b>HISTOLOGICAL TYPE</b>	<b>DCIS WITHOUT ASSOCIATED INVASIVE CARCINOMA</b>	<b>DCIS WITH ASSOCIATED INVASIVE CARCINOMA</b>
<b>CRIBRIFORM</b>	<b>6</b>	<b>5</b>
<b>PAPILLARY</b>	<b>2</b>	<b>3</b>
<b>CONFLUENT / ACINAR</b>	<b>12</b>	<b>12</b>
<b>MIXED</b>	<b>7</b>	<b>6</b>
<b>NON-SPECIFIC</b>	<b>4</b>	<b>3</b>
<b>NON-COMEDO</b>	<b>31</b>	<b>29</b>
<b>COMEDO</b>	<b>6</b>	<b>15</b>

Cases included in the study of the differences in nuclear features between pure DCIS and DCIS associated with invasive carcinoma of the breast. Comedo and non-comedo type were studied separately. Different histological types of noncomedo DCIS were similarly distributed in both groups (DCIS without associated invasive carcinoma and DCIS with associated invasive carcinoma). The majority of noncomedo cases had nuclear grade I or II. Three cases of noncomedo DCIS had a high nuclear grade (III): two of them were associated with invasive carcinoma in the surrounding breast.

carcinoma patients to see if malignancy associated changes could be detected. In all cases only nuclei designated as normal were selected for the study from normal lobules without any apparent changes (an example of normal lobule is in Figure 7).

The benign group included 18 cases of non-proliferative disease with the diagnosis of mild fibrocystic disease, which included mild hyperplastic changes, cysts, fibrosis and duct ectasia. An additional 2 cases with proliferative disease were diagnosed as sclerosing adenosis and as mild to moderate hyperplasia.

The malignant group included 23 cases of invasive carcinoma and 11 cases of DCIS. Normal nuclei were selected from normal lobules from the neighborhood of carcinoma or DCIS. In most of the malignant cases normal nuclei were collected from the slides on which carcinoma was also present. However, in some cases the sections with carcinoma did not contain any normal lobules and thus cells from the adjacent sections where no carcinoma was present were analyzed. Table 4 shows the numbers of cases and nuclei analyzed to detect MAC.

## 3.2 STAINING

### 3.2.A Flow cytometry

From a 50 $\mu$ m section an area with invasive carcinoma was selected. The tissue was cut out, dewaxed in xylol and rehydrated using a series of alcohols. The tissue was mechanically disaggregated and centrifuged at 400 rpm for 10 minutes at 4°C. The pellet was resuspended in 0.5% pepsin in 0.9% sodium chloride with the addition of 3% PEG 6000 at pH of 1.5. The disaggregated

**Table 4. CASES INVOLVED IN THE ANALYSIS OF MALIGNANCY ASSOCIATED CHANGES.**

<b>DIAGNOSIS</b>	<b>NUMBER OF CASES (NUCLEI)</b>
<b>BENIGN</b>	<b>20 (1931)</b>
<b>DCIS</b>	<b>11 (577)</b>
<b>INVASIVE CARCINOMA</b>	<b>23 (1188)</b>

Table shows the diagnosis and number of cases, where normal nuclei were collected from normal areas of tissue for the purpose of MAC analysis. Benign group included 18 cases with a diagnosis of nonproliferative disease, and 2 cases with a diagnosis of proliferative disease.

tissue was then incubated in a water bath at 37°C for 30 minutes and vortexed at 5-minute intervals. Samples were treated with Pepstatin A to arrest enzymatic activity. The suspension was filtered through a 60µm mesh and nuclei were centrifuged at 400 rpm for 10 minutes at 4°C. The pellet was resuspended in Hanks/Hepes solution at 4°C. Nuclei were treated with 0.1% TritonX100 in PBS for 3 minutes at 4°C and incubated with RNA-ase for 20 minutes at 37°C. The samples were stained at 4°C with Propidium iodide (50µg/ml in PBS) and stored at 4°C until the measurements were carried out. The measurements were performed using a Coulter Epics-C flow cytometer within 12 hours after staining. FC staining and measurements were performed by the Analytical Cytology Laboratory of the Pathology Department in the B.C. Cancer Agency.

### 3.2.B Image cytometry

Alcohol fixed smears stained with the Papanicolaou method were deposited in xylol for 48 hours and then the coverslips were removed. Slides were washed in 100% ethanol, destained in acid alcohol (70 ml of 100% ethanol + 30 ml of distilled water + 1 ml of concentrated HCl) for 30 minutes. To prepare the cytopins 50µm sections were cut from formaldehyde fixed, paraffin embedded tissue blocks. Sections were treated with the same disaggregation procedure which was used in the preparation of nuclear suspensions for flow cytometry measurements (3.2.A). Nuclear suspensions (0.75 ml) were centrifuged onto the slides with the Shandon cytopsin centrifuge (900 rpm, 5 minutes) and air-dried. Tissue sections, 4µm thick, were incubated in an oven for 10 minutes (50-60°C) and dewaxed in xylol (2X10 minutes).

The following staining procedure was the same for tissue sections, smears and cytopins. Slides were rehydrated in series of alcohols (5 minutes in 100% ethanol, 2X1 minute in 75% methanol, 2X1 minute in 50% ethanol and 2X1 minute in water). Slides were post-fixed in Bohm-Sprenger fixative (640 ml methanol + 120 ml formaldehyde + 40 ml glacial acetic acid) for 45 minutes, washed in water, and incubated in 5N HCl for 30 minutes. After hydrolysis the slides were washed in running water for 5 minutes, stained with Thionin-SO<sub>2</sub> and washed again in running water for 5 minutes. This procedure provides stoichiometric staining of DNA and can therefore be used for quantitative DNA nuclear measurements (Mikel 1991, Tezcan 1994). The slides were then counterstained with Orange G which binds cationic groups on the proteins (0.5g of Orange G in 100ml of 50% ethanol) for 30 seconds (Oud 1984). Orange G stains connective tissue and makes it easier to visualize histological features. DNA measurements are not appreciably affected by the use of this counterstain, since the absorption spectra of Thionin and Orange G are minimally overlapped. Sections were then washed in 100% alcohol, dehydrated in xylol for 5 minutes and mounted with Paramount.

### **3.3 IMAGE CYTOMETRY MEASUREMENTS**

#### **3.3.A Image cytometry of tissue sections**

The image analysis device consisted of a Nikon Optiphot microscope with a 1X video projection lens, 100W halogen light with a stabilized power supply, 3-chip CCD video camera (Sony, DXC-3000), MVP-AT Matrox image processing board and IBM compatible personal computer (Figure 13). The photometric

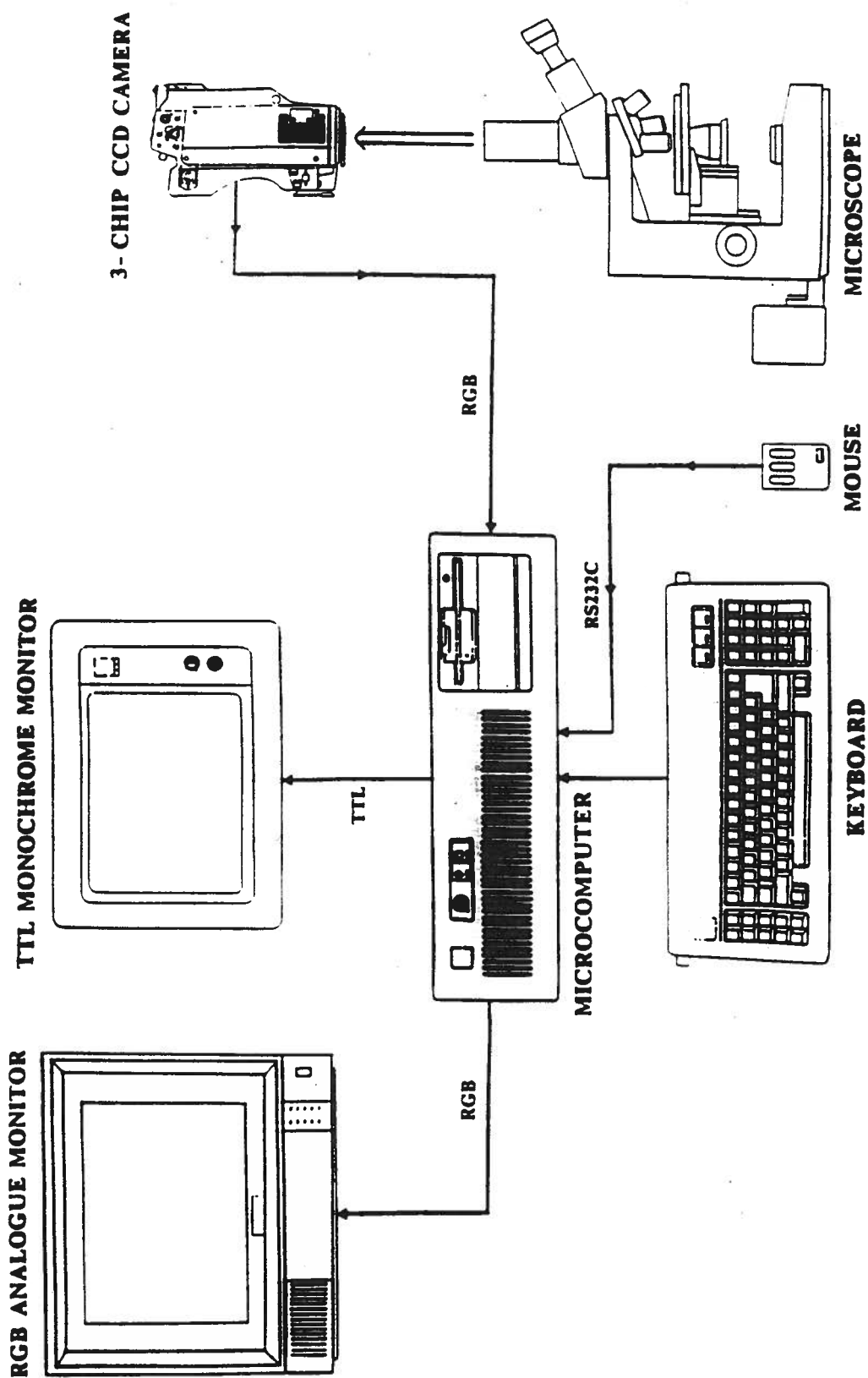


Figure 13. IMAGE CYTOMETRY DEVICE.

The diagram shows major components of the image cytometry system, which was used for the measurements performed on tissue sections.

resolution was 256 gray levels. Measurements were performed with Plan Apo 60X objective (60/1.40, Oil) (Zbieranowski 1992). The pixel size of the camera was 13X13 $\mu\text{m}$ . This resulted in a pixel spacing on the specimen plane of 0.23  $\mu\text{m}$ . Camera non-linear response was corrected for by calibrating measured intensities against a known optical density reference. Non-uniformity of the field illumination was corrected for by subtraction of the image of a blank field. These corrections have been described previously (Jaggi 1988, Mac Aulay 1989).

From each section 50 lymphocytes and 50-200 epithelial nuclei were selected for each diagnostic category. Their nuclear images were acquired into separate classes in the image file. Up to five different classes of cells could be selected from the same slide. On a section with invasive carcinoma for example, the nuclei of DCIS, nuclei of proliferative disease, normal nuclei and lymphocytes could be collected in addition to invasive cancer cells. Cells from areas with different histological patterns were always collected as distinct classes in the image file. Different histological types of DCIS were also collected as different classes in image file, whenever a sufficient number of nuclei was available. Comedo and non-comedo nuclei were distinguished in every case where they were present in the same section. The number of selected cells depended on how many were present on the analyzed slide; at least 50 and up to 200 nuclei were collected for each cell class. Multiple fields were scanned across the slide. Approximately ten nuclei were selected from each field. Only non-overlapping nuclei, that appeared to be in focus, were selected.

Nuclei were automatically segmented on the basis of the selected threshold and their images were stored in the computer memory (Mac Aulay

1989). The process of segmentation refers to the separation of nuclei from the background. To delineate nuclei from the background, an appropriate optical intensity threshold was chosen for different cell types by the observer. This threshold separated nuclei from the lighter background. Nuclei with more condensed chromatin, such as lymphocytes, needed a lower threshold to be delineated from the surroundings. Manual correction of the nuclear contour was applied in the instances of touching, but not overlapping, nuclei.

### 3.3.B Comparison of measurements performed on tissue sections, cytopins and smears

A different IC device was used for this part of the study than for the rest of the IC measurements because of its advantage that measurements can be performed in both ways, automatically or manually. This system has been recently developed in our department for the purpose of automated cervical screening (Garner 1992), but it is currently also applied for measurements on various other tissues. The device consists of Microimager 1400 digital camera, automated stage and IBM-compatible computer. This system is optimized for quantitative measurements, and provides much higher spatial resolution than the conventional system (Jaggi 1990, Jaggi 1991, Palcic 1990).

The measurements were performed at 25X magnification. The width of a single pixel of this system is  $6.8\mu\text{m}$ , corresponding to a spatial resolution of  $0.27\mu\text{m}$  ( $6.8/25=0.27$ ) at the specimen plane. Pixel refers to a picture element and is defined as the area on the image which is covered by one sensing element of the detector.

From tissue sections 150-200 carcinoma nuclei and 50 lymphocyte nuclei were selected and their images collected manually. On average, 15 nuclei were collected from each microscopic field and 10-20 fields were scanned across the whole section.

Smears were scanned in an automated way. The focusing and segmentation was entirely automated. The upper limit of the number of collected cells was 1000. In smears with sparse cells all microscopic fields were scanned in an attempt to collect all cells on the slide. Cellular smears were scanned in a zigzag pattern at regular spacings over the surface of the entire microscope slide. Cytospins were also scanned in an automated way.

The machine was instructed to scan as many microscope fields as necessary to collect 1000 cells. Images were reviewed on the screen and unacceptable images were discarded. Images were considered unacceptable if the nuclei were not in focus, if they contained more than one nucleus, or if they contained non-nuclear objects, such as cellular debris. The selection of unacceptable images was performed in a semi-automated way. For example, a few images representative of poorly focused cells were selected by the observer, and then all similar images were classified with the use of thresholds of selected features. Lymphocytes and granulocytes were classified into separate classes in a similar manner, and their mean value of integrated optical density (IOD) was used to normalize the IOD of other nuclei. In two smears and in one cytopsin no cell could be recognized as normal (lymphocytes, granulocytes, fibroblasts, myoepithelial cells) and the histogram was normalized against the mean value of the first peak.

### 3.4. DESCRIPTION OF MAIN NUCLEAR FEATURES

Sixty-three features were calculated for each nucleus and stored in the form of feature files. The algorithms of the features have been defined previously (Mac Aulay 1989). Here the main nuclear features are described. The following features are representative of the feature classes and were found to be more important than other features for the purpose of this study.

#### *Photometric features*

- 1) IOD (integrated optical density): Optical density is proportional to the amount of light which is absorbed by a stained object and hence the density of stain. Integrated optical density is the sum of the optical density values of all object pixels and is proportional to the amount of stain in the object. If the stain is a stoichiometric DNA stain, then IOD is proportional to the DNA amount in the nucleus.
- 2) OD VAR (variation of optical density) represents the variation of the optical density distribution over the pixels of an object. It is equal to the variance of optical density values in the object, normalized by the square of the mean optical density of this object.
- 3) OD MAX (optical density maximum) is the largest optical density value detected inside the object.

#### *Area and shape features*

- 4) AREA (nuclear area) is defined as the number of pixels which compose the object image.

- 5) **MEAN RADIUS** is the mean distance from the center to the edge of the object.
- 6) **VAR RAD** (variation of radius) is calculated as a variance of the distances from the object center to the object edge.
- 7) **COMPACTNESS** expresses the ratio between the perimeter and area of the object. It is an indicator of the shape irregularity.
- 8) **ELONGATION** represents the ratio between the major to the minor axis of the object.
- 9) **BDY1** (coarse boundary variation), and **BDY2** (fine boundary variation) are the measure of the smoothness of the object's contour.

*Continuous texture features*

- 10) **C-MASS** (center of mass) corresponds to the distance between the geometrical center of the nucleus and the center of the mass of optical densities of all the pixels in a nucleus..
- 11) **C-MASSL** (center of mass of the low density chromatin): the same as C-MASS but calculated only for the low density chromatin.
- 12) **ENERGY** is related to the regularity of chromatin distribution. A large energy value indicates a high degree of organization in spatial or gray scale distribution of optical density values in the nucleus.
- 13) **ENTROPY** is related to the irregularity of chromatin distribution. A large entropy value indicates a low degree of organization in spatial or gray scale distribution of optical density values in the nucleus.
- 14) **CONTRAST** is related to the number of neighboring pixels with diverse optical density values. A nucleus with a large contrast has large gray

scale variations at high spatial frequencies.

- 15) **HOMOGENEITY:** a large value indicates a gray level variation that is spatially smooth (it occurs at low spatial frequency).
- 16) **CLUSTER SHADE:** a large value of this feature indicates that distinct clumps exist in the nucleus, with a large contrast between clumps and the rest of the nucleus. A positive value indicates bright clumps on the dark background, and a negative value indicates dark clumps on the light background.
- 17) **FAREA1 (fractal area 1) and FAREA2 (fractal area 2):** for the calculation of these two features, the optical density values are taken as the height of the pixels in three dimensional space. The area of the obtained surface is measured for both features but at different scales.

#### *Discrete texture features*

- 18) **TARL (total area ratio for the low density chromatin)** is the area occupied with the low density chromatin divided by the area of nucleus.
- 19) **TARM (total area ratio for the medium density chromatin)**
- 20) **TARH (total area ratio for the high density chromatin)**
- 21) **TERL (total extinction ratio for the low density chromatin)** is the integrated optical density of the low chromatin area divided by the integrated optical density of the nucleus.
- 22) **TERM (total extinction ratio for the medium density chromatin)**
- 23) **TERH (total extinction ratio for the high density chromatin)**
- 24) **ADL (average distance of the low density chromatin from the nuclear center)** is the average distance between individual light pixels and center

of the nucleus, normalized by the mean radius.

- 25) **ADM** (average distance of the medium density chromatin from the nuclear center)
- 26) **ADH** (average distance of the high density chromatin from the nuclear center)
- 27) **MAER** (medium average extinction ratio) is the ratio of mean optical density of medium density chromatin and the mean optical density of the low density chromatin.
- 28) **MHAER** (high average extinction ratio) is the ratio of mean optical density of medium/high density chromatin and the mean optical density of the low density chromatin.
- 29) **NL** (number of low density chromatin clusters) is the number of distinct groups of low density chromatin pixels in the nucleus.
- 30) **NM** (number of medium density chromatin clusters)
- 31) **NH** (number of high density chromatin clusters)
- 32) **CRL** (low density chromatin compactness ratio) is the ratio of compactness of the low density chromatin areas to the compactness of high and medium density areas.
- 33) **CRH** (high density chromatin compactness ratio) is the ratio of compactness of the high density chromatin areas to the compactness of low and medium density areas.

### 3.5 ANALYSIS OF DNA HISTOGRAMS

#### 3.5.A Image cytometry

Features could be displayed in the form of histograms, separately for each class of nuclei in the image file. The IOD of nuclei was normalized against the mean IOD of lymphocytes from the same slide (cells with normal DNA content). IOD histograms were plotted with 64 bins to span the region on the X axis from  $n=0$  to  $n=5$ . Normalized IOD histograms were then analyzed by the determination of the following conventionally accepted parameters: DNA index (DI) of the peaks, coefficient of variation of the peaks, entropy of the DNA histogram, 1.25 exceeding rate (percentage of cells with IOD higher than  $n=1.25$ ), and 2.5 exceeding rate (percentage of cells with IOD higher than  $n=2.5$ ). These limits for exceeding rates were used previously because they are related to the proliferation of tissue and to the proportion of aneuploid cells: Cells with DNA content higher than 1.25 could be aneuploid cells or proliferating diploid cells, and cells with DNA content higher than 2.5 are aneuploid cells (Fallenius 1988). Entropy of the DNA histogram was calculated as previously described (Stenkvist 1990). The DI refers to the modal value of the representative peak (or peaks) in the histogram. Separate peaks with more than 20% of cells were recognized as representative peaks. Peaks were identified as aneuploid if their DI was higher than 1.2. This limit covered the range of two standard deviations of the normal epithelial cells distribution. In some instances the mode of a peak was less than 1.2, but the distribution of a peak was very wide and the majority of values was spread beyond 1.2. These peaks were also identified as aneuploid. (Because of the relatively low resolution of the IC

histograms no tetraploid peaks were defined in this study). An example of a DNA histogram with histogram parameters is shown in Figure 14. Whenever the histograms showed a single diploid peak the tissue was designated to be diploid. Diploid cells by definition should have normal DNA content - however, it is obvious that slight deviations from euploidy cannot be detected with the precision of IC techniques. In most of the malignant tissues, assigned as diploid in this study, the DNA changes were probably too small to be detected by IC, but could be demonstrated with other techniques such as molecular genetics.

### 3.5.B Flow cytometry

To obtain comparable plots for the comparison of image cytometry (IC) and flow cytometry (FC) measurements, the raw features obtained by both techniques were plotted to histograms with the use of the same program. FC histograms had 200 channels, and IC histograms had 50 channels to span from 0 to 5, where the value 1 was equivalent to the diploid DNA content. IC histograms were analyzed as described in the previous paragraph.

Flow histograms were normalized against the modal value of the first peak in the histogram, assuming that this peak contained diploid cells. The DNA index (DI) was determined from the normalized histograms as the mode of representative peaks. A peak in FC histograms had to contain more than 10 % of nuclei in order to be recognized as a representative peak. The DNA ploidy was determined for the histograms according to the presence of aneuploid peaks. For the classification of peaks the limits were set on the DI value. In the

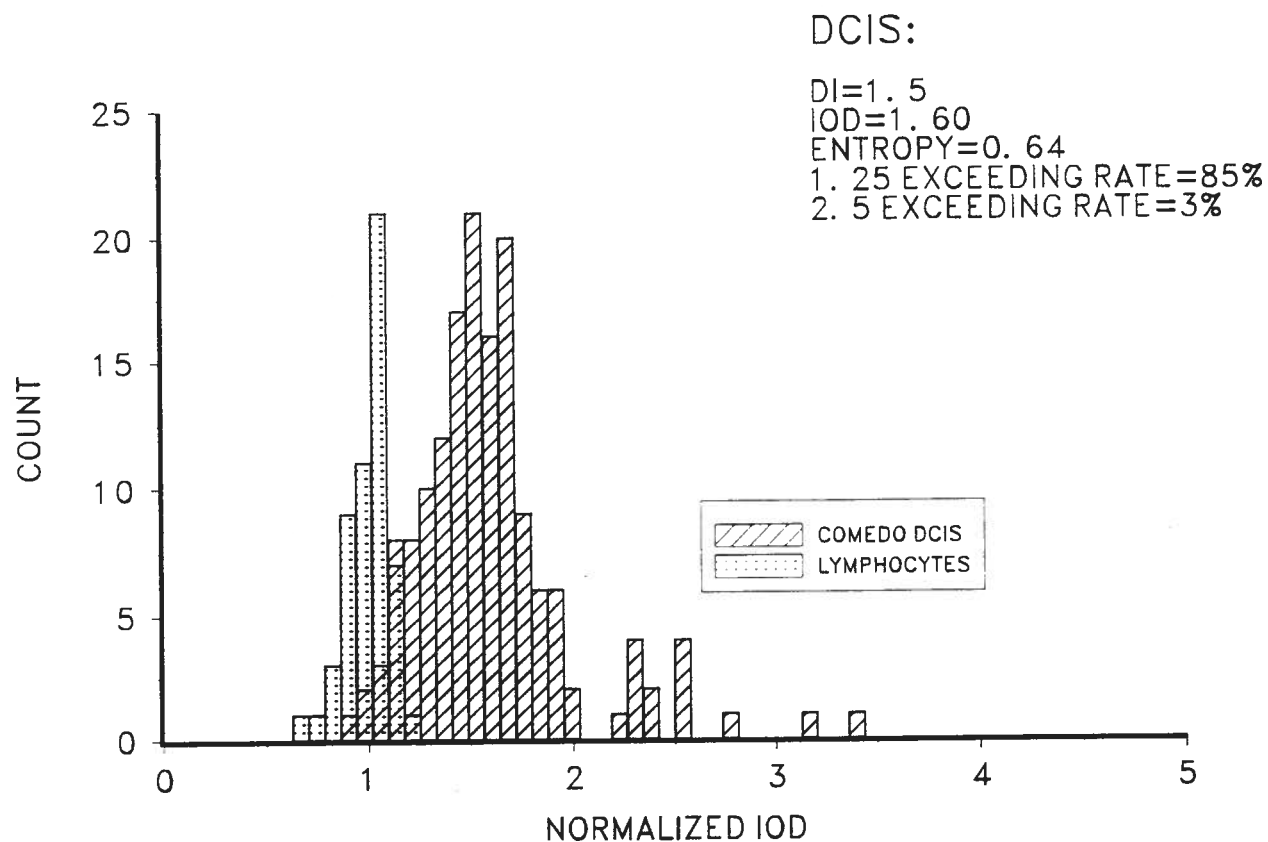


Figure 14. AN EXAMPLE OF NORMALIZED HISTOGRAM AND HISTOGRAM PARAMETERS.

Histograms of integrated optical density (IOD) are shown for comedo carcinoma *in situ* and for lymphocytes (internal control cells). DNA index of DCIS was determined as the mode of the peak. IOD was normalized by dividing the IOD of cells of interest with the IOD of control cells (lymphocytes). Mean IOD was calculated by dividing the sum of the integrated optical densities of all nuclei with the number of analyzed nuclei. Two exceeding rates were calculated as the percentage of nuclei with their IOD higher than the chosen limit (1.25- and 2.5-exceeding rates).

FC histograms a single peak was always classified as diploid. The second peak was recognized as aneuploid if its DI was higher than 1.1. Tetraploid peaks were not defined but were assigned as aneuploid for the purpose of this study.

### 3.6 STATISTICS

The statistical analysis procedures involved non-parametric tests and T-tests (to test the differences between the means of two populations and determine if the differences are statistically significant) and the discriminant function analysis (to produce a classification of patients based on nuclear features analysis). The analysis was carried out with the BMDP statistical package (BMDP, 1988). The analysis of cervical tissues has shown previously, that the distribution of the majority of the nuclear features is not normal (Mac Aulay 1989). This has been confirmed on our preliminary data set when the normality of feature distributions was tested. T-tests are valuable only when variables are normally distributed. Since non-parametric tests can be used for variables with the distribution other than normal, both types of tests were used together. Two variables were considered different when T-test and non-parametric (Mann-Whitney) test showed a significant difference ( $p < 0.05$ ). The p-value of the non-parametric test is shown in all the tables.

The 7M program of the BMDP statistical package was used for the linear discriminant function analysis with stepwise variable selection. This multivariate statistical method is used to develop a classification rule (based on observations made on known groups of objects) that will assign a new object into one of the possible groups on the basis of measurements made on the object. When a

large number of features is involved in the analysis, usually only the most discriminating features are selected. With the selection of features we can investigate the causes of the differences between the groups. In addition, the classification can sometimes be improved when irrelevant features are removed. The features are selected on the basis of their ability to discriminate between groups, which is determined by the F-value calculated for each feature. One of the methods that can be used for the selection of features is a stepwise forward procedure. With this method, a single most discriminating feature (with the highest F-value) is initially found. Then the second feature is selected which paired with the previous feature offers the best discrimination. In the same way the third variable, most discriminating in the combination with the previous two variables, is chosen. This continues until a chosen n number of features is selected. The size of the selected feature set in the analysis is usually limited to the number, above which adding new features to the discriminant function does not improve the classification in an important way. Possible bias and instabilities of the discriminant function analysis can be revealed using a jackknifed procedure to generate classification matrices. The jackknife classification matrix is produced in the following way: One object is left out of the analysis and then the calculated discriminant function coefficients are applied on the features of this object to classify it to one or the other group. This is then repeated for every object. The classification matrix, obtained in this manner, indicates how well the discriminant function would perform on a new data set.

Two approaches were used in the discriminant function analysis: Discrimination on a slide by slide basis, and discrimination on a cell by cell basis. Discrimination on a slide by slide basis provides classification of cases

(patients), based on the mean values and variances of features of nuclei from an individual slide.

With the second approach, all nuclei from all cases are gathered into the diagnostic groups and the feature values of individual nuclei are analyzed with the discriminant function. This results in a classification of individual nuclei to one of the diagnostic groups. The coefficients of discriminant function performed on a cell by cell basis can be then applied to the feature files of individual cases to classify the same nuclei. In this way, we can obtain the proportion of correctly classified nuclei in each case (slide). The proportion of correctly classified nuclei on slides can be then used to classify the slides (Figure 15).

**STATISTICS:**

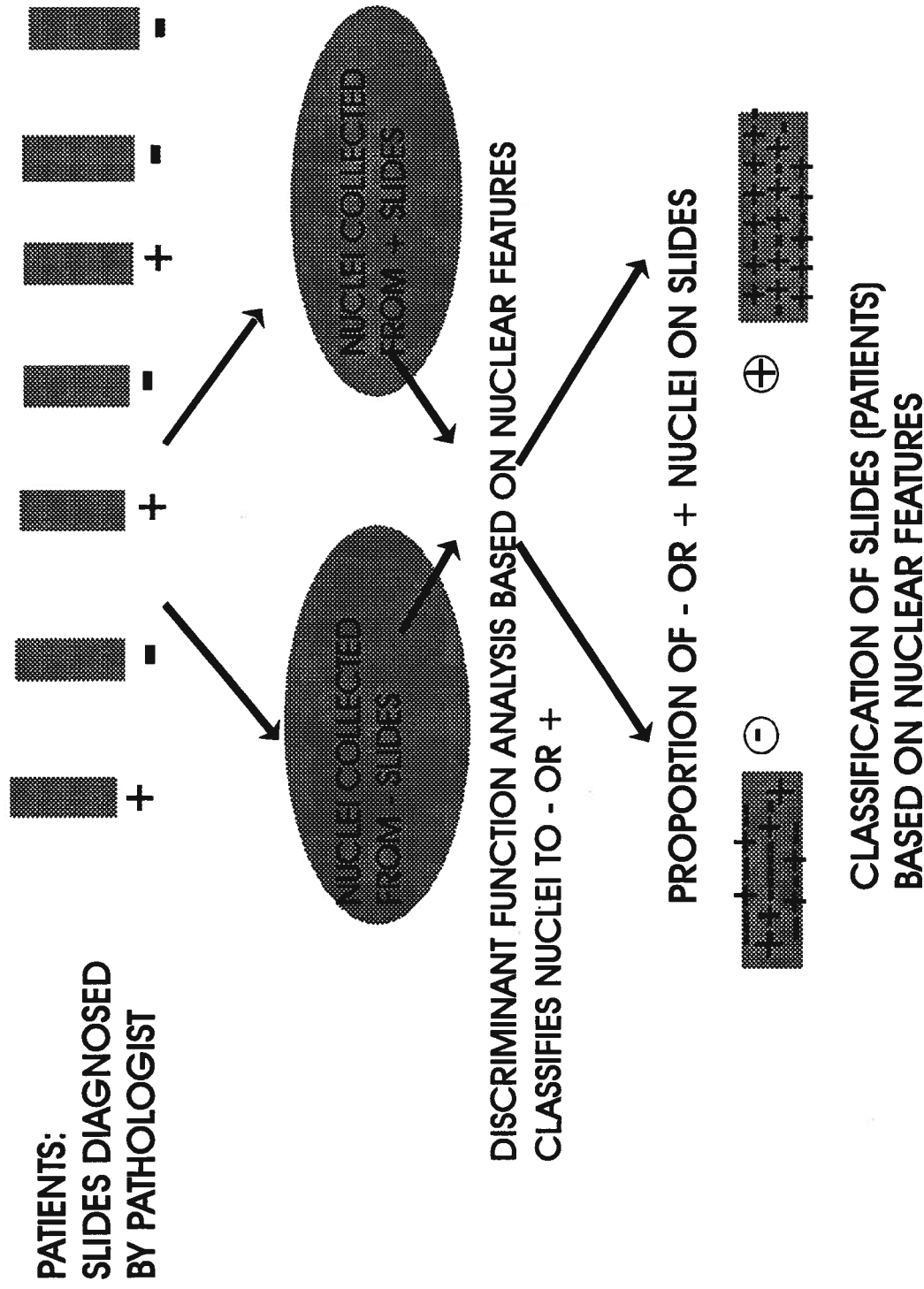


Figure 15. STATISTICAL ANALYSIS BASED ON CELL BY CELL DISCRIMINATION WAS USED FOR THE CLASIFICATION OF PATIENTS.

## 4. RESULTS

### 4.1 THE DISTRIBUTION OF VALUES IN IMAGE CYTOMETRY DNA HISTOGRAMS OF NORMAL CELLS

Normal epithelial cells or lymphocytes can be used as internal control cells with the DNA content in the diploid range. Lymphocytes were chosen as the internal control cells in our case, because they were always present in sufficient numbers (at least 30) on the tissue sections. On the contrary, normal epithelial cells were absent in many cases. The cells of interest were normalized by dividing their integrated optical density (IOD) by the IOD of lymphocytes. IOD equals the integrated optical density of a nucleus and corresponds to the nuclear DNA content.

Table 5 shows the DNA index (DI) in histograms of normal cells. DI is defined as the ratio between the modal value of the peak and IOD of lymphocytes. Even if discrepancies caused by differential staining of various cell types might exist, they do not show an effect in histograms with a low resolution, such as those obtained by the measurements of tissue sections.

In addition to the DI, Table 5 shows the IOD, the coefficient of variation of the peak (CV), the entropy of the histogram, and the 1.25-exceeding rate for 20 histograms of normal cells. These histogram parameters were calculated to demonstrate the limits of "normal" in the DNA histograms. The limits which were used to distinguish diploid and aneuploid peaks were determined from the distribution of DI values obtained from histograms of normal cells ( $1.0 \pm 0.2$ ).

Table 5. HISTOGRAM PARAMETERS, OBTAINED FROM THE DNA HISTOGRAMS OF NORMAL EPITHELIAL CELLS.

IOD	DNA INDEX	CV (%)	ENTROPY	%>1.25
1.08	1.1	12	0.49	10
1.03	1.0	10	0.44	-
0.90	0.8	15	0.49	3
1.05	0.9	12	0.43	0
1.22	1.1	12	0.52	32
1.26	1.15	10	0.43	32
0.93	0.9	12	0.44	2
0.98	1.0	13	0.40	2
0.99	1.0	13	0.47	3
0.90	0.95	9	0.37	0
1.02	0.95	13	0.53	11
1.00	1.0	10	0.43	3
1.21	1.15	9	0.43	25
1.24	1.2	10	0.50	23
1.14	1.15	13	0.52	24
1.08	1.0	12	0.46	8
1.33	1.15	9	0.53	44
0.97	0.95	13	0.43	2
1.24	1.1	10	0.50	27
1.14	1.1	10	0.49	15
<b>mean</b>				
<b>(standard deviation)</b>	<b>1.08 (0.13)</b>	<b>11 (1.7)</b>	<b>0.46 (0.04)</b>	<b>14 (13)</b>

Integrated optical density (IOD), DNA index (the modal value of the peak), coefficient of variation of the peak, entropy, and 1.25 exceeding rate are presented.

#### 4.2 COMPARISON OF FLOW CYTOMETRY (FC) AND IMAGE CYTOMETRY OF TISSUE SECTIONS (IC)

Examples of some IC and FC aneuploid and diploid histograms are presented in Figure 16. The average coefficient of variation (CV) of diploid FC peaks was 5%, while the average CV of the IC lymphocyte control peaks was 10%. The average CV of normal epithelial cells in IC histograms was 11%. All IC diploid peaks and some of the aneuploid tumor peaks were well confined and easy to interpret. However, some of the tumor peaks which were clearly aneuploid had a wide distribution of values resulting in a large CV.

Figure 17 shows the relationship between DI as determined by FC and IC on the fifty-one tissue blocks. When more than one DI was obtained by a single method the more irregular DI was used in the graph. When both invasive and *in situ* cancer had aneuploid peaks in the IC histograms, then DI of the invasive cancer was plotted. In about two thirds of the cases the IC values roughly corresponded to the FC values. Most IC values were lower than corresponding FC values. In the remaining cases IC and FC completely disagreed on the DI. Correlation between flow and image DNA index of cases which agreed on the ploidy pattern was relatively low ( $r = 0.69$ ).

Agreement between the two techniques in ploidy determination was reached in 79% (40/51) of all tissue blocks (Table 6) and/or 77% (36/47) of tumors. Both techniques confirmed aneuploidy in 62% of tumors (29/47) and diploidy in 15% of tumors (7/47). If FC was considered to be a standard, IC

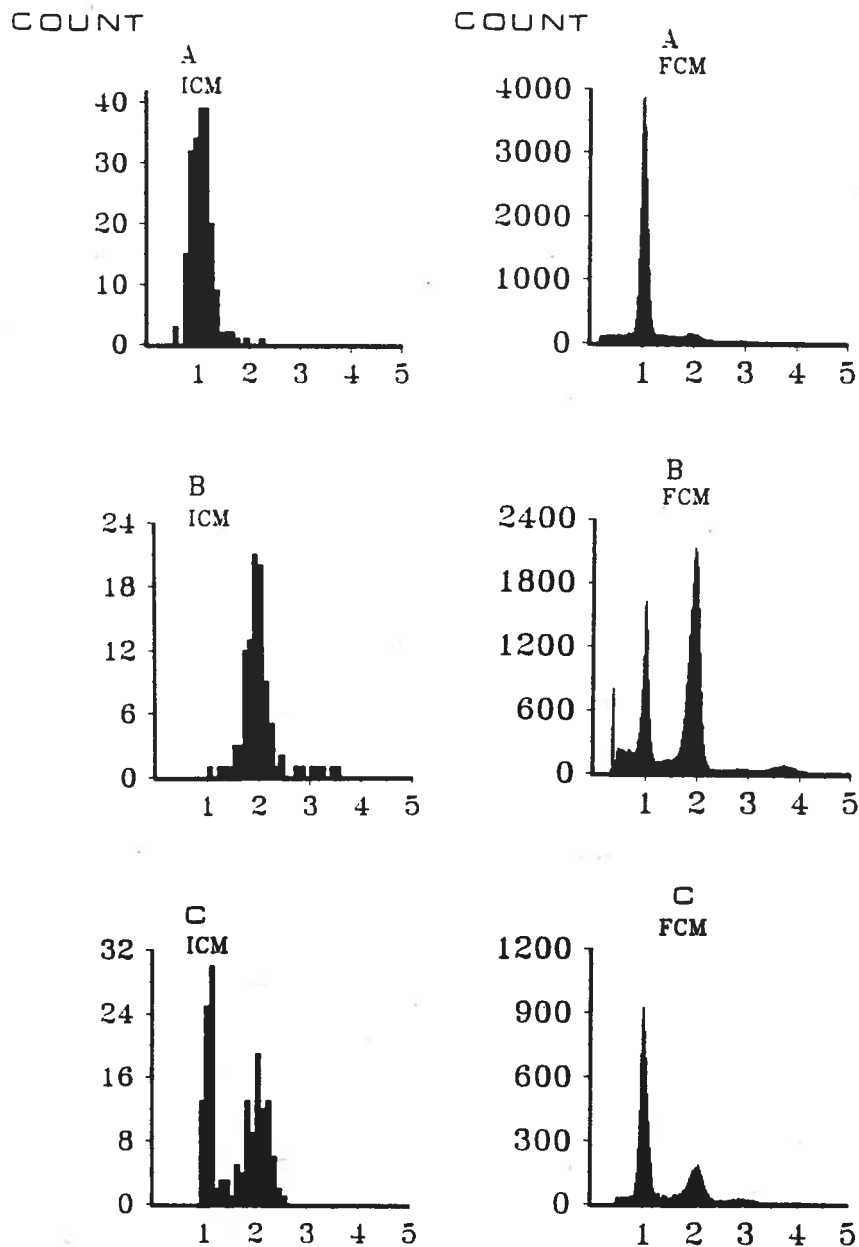
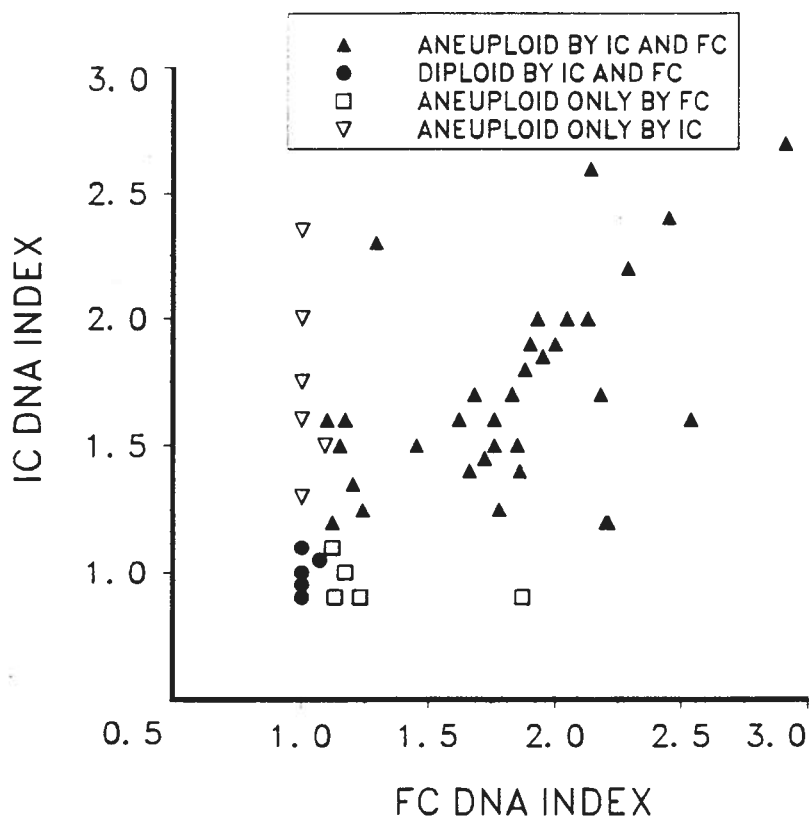


Figure 16 a, b, c, d, and e. EXAMPLES OF DIPLOID AND ANEUPLOID IC AND FC HISTOGRAMS OF THREE CARCINOMA CASES.

(A) IC and FC histograms have peaks in the diploid range, (B) both histograms are aneuploid, (C) both histograms are aneuploid, but IC demonstrates an additional population of cancer cells with a peak in the diploid range, while the proportion of carcinoma cells in the FC diploid peak is not known.



**Figure 17. COMPARISON OF FLOW AND IMAGE CYTOMETRY ON THE BASIS OF THE DNA INDEX.**

Measurements were performed on 51 tissue blocks from 47 tumors. Roughly, in two thirds of tissue blocks, the DNA indices obtained with image cytometry measurements corresponded to the DNA indices obtained with flow cytometry measurements.

Table 6. DNA ploidy as determined by IC and FC of 51 tissue blocks.

		FLOW CYTOMETRY		
		Diploid	Aneuploid	total
IMAGE CYTOMETRY	Diploid	7	5	12
	Aneuploid	6	33	35
	total	13	38	51

There was an agreement in 79% (40/51) of cases: 87% (33/38) of FC aneuploid cases were also aneuploid by IC, while only about one half (7/13) of FC diploid cases were also found diploid by IC. The agreement was low in diploid cases.

agreed with FC on almost 90% of aneuploid cases, but on only about 50% of diploid cases.

Six tumors were recognized as aneuploid only by IC. In five cases aneuploidy was detected only by FC. Table 7 shows the DI of the eleven cases where FC and IC did not agree in ploidy. Three of these cases (shown in the last three rows in Table 2) had a diploid IC histogram and a FC histogram with DI values just slightly above the artificially set limit of 1.1. They were therefore classified as aneuploid by FC.

For three tumors more than one tissue block was analyzed (Table 8). In all tumors there was an agreement in the ploidy between the two methods. Both methods demonstrated a tumor heterogeneity in different tissue blocks. In addition, IC showed differences between invasive cancer and DCIS.

Figure 18 presents the relationship between FC and IC DNA indices of invasive cancer and DCIS. In many of these cases DCIS nuclei seemed to belong to a different population than invasive cancer cells. In some FC histograms invasive cancer was masked by the abundant DCIS. Overall, aneuploid histograms were observed in 71% (22/31) of DCIS analyzed by IC.

#### **4.3 COMPARISON OF IMAGE CYTOMETRY MEASUREMENTS PERFORMED ON SMEARS, CYTOSPINS, AND SECTIONS**

Figure 19 shows scatter plots (area versus IOD) of a smear and a corresponding cytospin, and a tissue section originating from the same tumor. Nuclei of a smear and a tissue section are shown in Figure 20. Figures 21-22 show DNA histograms of 6 other carcinoma cases where a smear, a cytospin

Table 7. DI analysis of cases where FC and IC disagreed in ploidy.

FC		IC	
DI	Ploidy	DI	Ploidy
1.00	D	2.0/2.3*	A
1.00	D	2.0	A
1.00	D	1.7	A
1.00	D	0.8/1.6*	A
1.09	D	1.5/1.6*	A
1.00	D	1.3	A
1.87	A	0.9	D
1.23	A	0.9/0.9*	D
1.17	A	1.0	D
1.13	A	0.9	D
1.12	A	1.1/1.0*	D

Values indicated by \*denote the DI values of DCIS. The cases in the last three rows had DI found by FC in the near-diploid area, just exceeding the artificially set limit of 1.1. They were therefore classified as aneuploid by FC. In the remaining cases with the discordant DNA ploidy outcome clear differences in DI were obvious: FC failed to detect 6 and IC failed to detect 2 aneuploid cases.

Table 8. HETEROGENEITY OF TUMORS.

(DI analysis of seven tissue blocks derived from three tumors.)

PATIENT	TISSUE BLOCK	FLOW CYTOMETRY	IMAGE CYTOMETRY	
			INVASIVE	DCIS
1	A	2.00	-	1.0 / 1.9
1	B	2.05	-	2.0
1	C	1.93	2.0	1.1 / 2.0
2	A	2.13	1.1	1.1 / 2.0
2	B	1.17 / 1.29	-	1.1 / 2.3
3	A	2.20	1.2	1.1
3	B	1.88	-	1.0 / 1.8

DNA indices of seven tissue blocks derived from three tumors with image and flow cytometry measurements. In four tissue blocks only DCIS was present. Often two populations (two peaks) were present in DCIS. The differences between different tissue blocks of the same tumor are shown by both methods. In addition, image cytometry demonstrates the differences between invasive and *in situ* carcinoma.

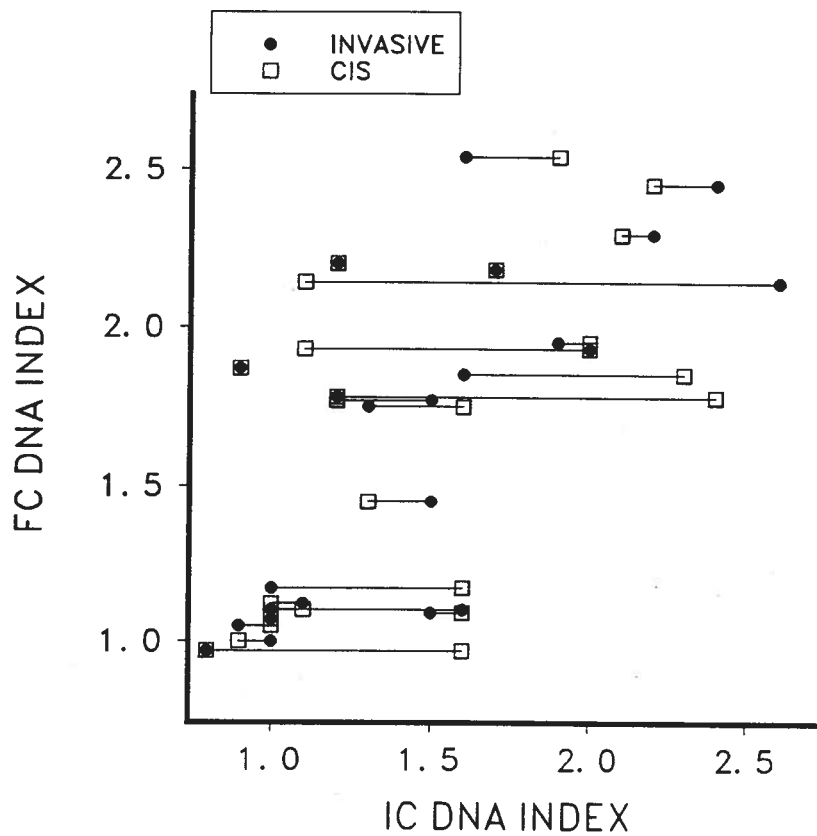
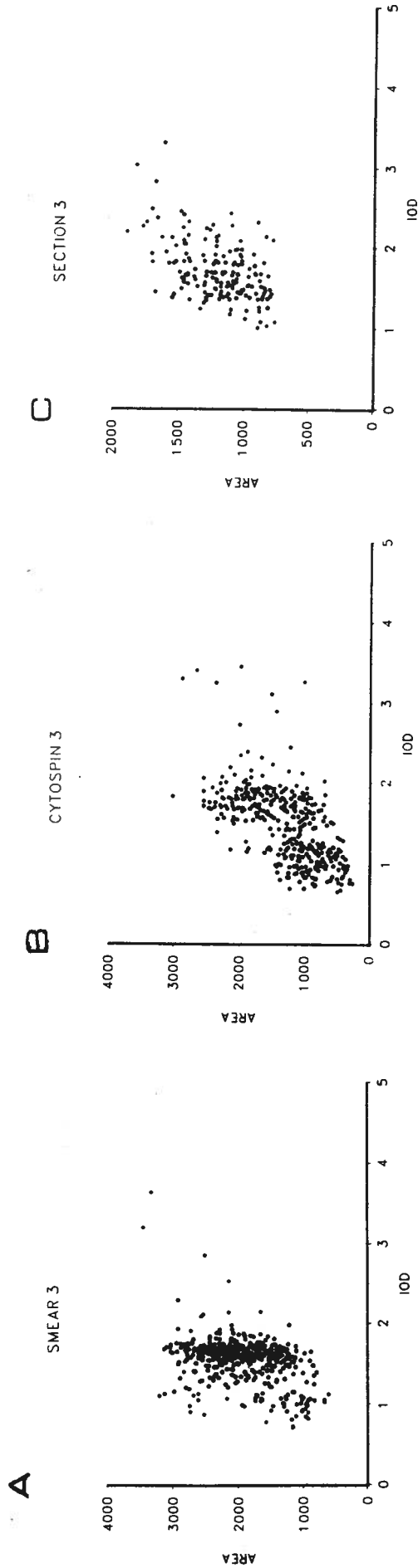


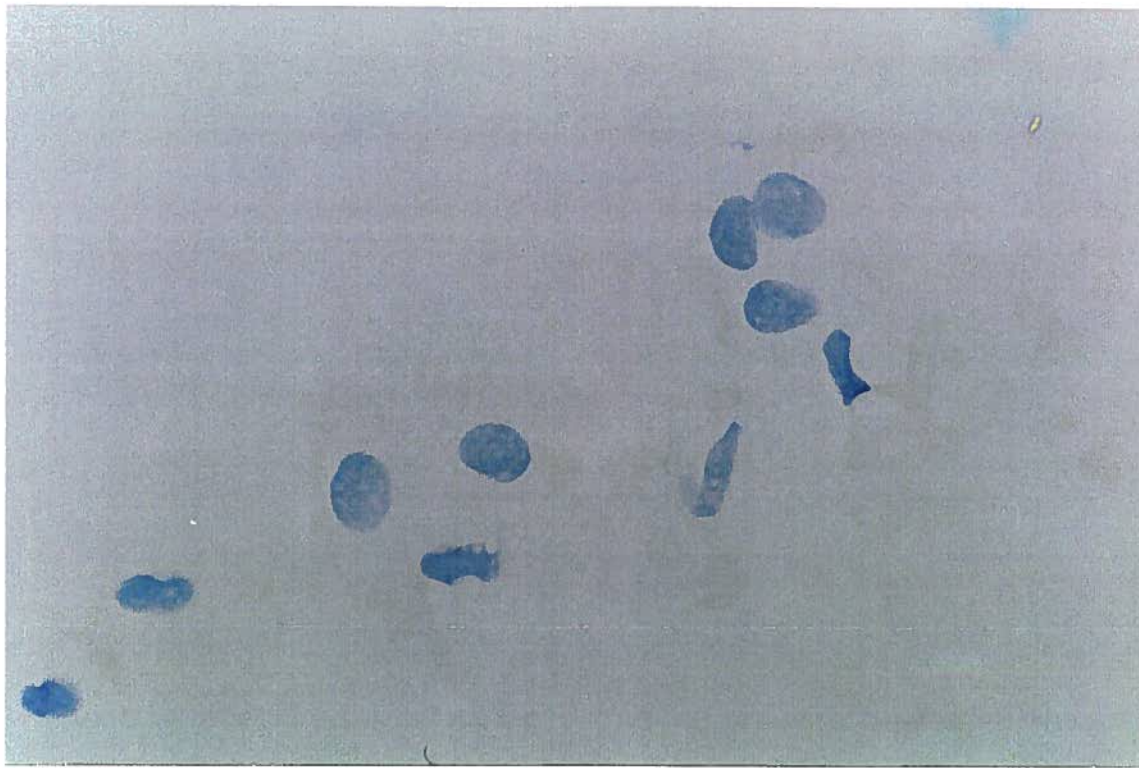
Figure 18. DNA INDEX OF INVASIVE CARCINOMA AND DUCTAL CARCINOMA *IN SITU*.

In tissues, where ductal carcinoma in situ was present in addition to invasive carcinoma, these were analyzed separately by image cytometry. Figure shows DNA indices of invasive and *in situ* carcinoma, measured by image cytometry, compared to a single DNA index measured by flow cytometry.

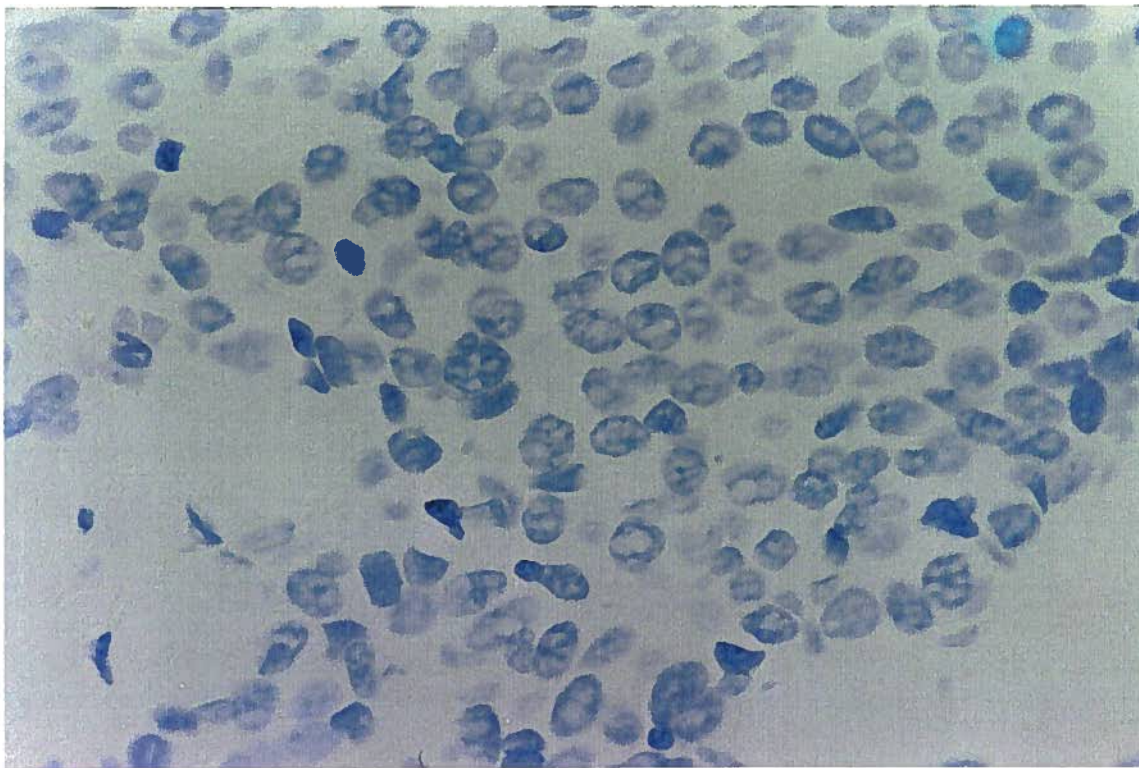


**Figure 19. NUCLEAR AREA VS. IOD SCATTER PLOTS OF A SMEAR, AND A CORRESPONDING CYTOSPIN AND TISSUE SECTION.**

Plots show the relationship between normalized IOD and nuclear area acquired by image cytometry of a breast aspirate, cytospin of disaggregated nuclei and tissue section, all obtained from the same breast carcinoma. Differences in sampling are represented by the varying proportion of aneuploid cells (only tumor cell images were collected from tissue section). The differences in the nuclear size of aneuploid populations from smear, cytospin and section may be the result of the disaggregation procedure and different fixatives.



A



B

Figure 20. MICROGRAPH OF NUCLEI ON A SMEAR AND ON A TISSUE SECTION.

Figure shows a photograph of the Feulgen stained nuclei on a smear (A), and on a tissue section (B). Haematoxylin-eosin stain. Magnification on the print is approximately 430:1.

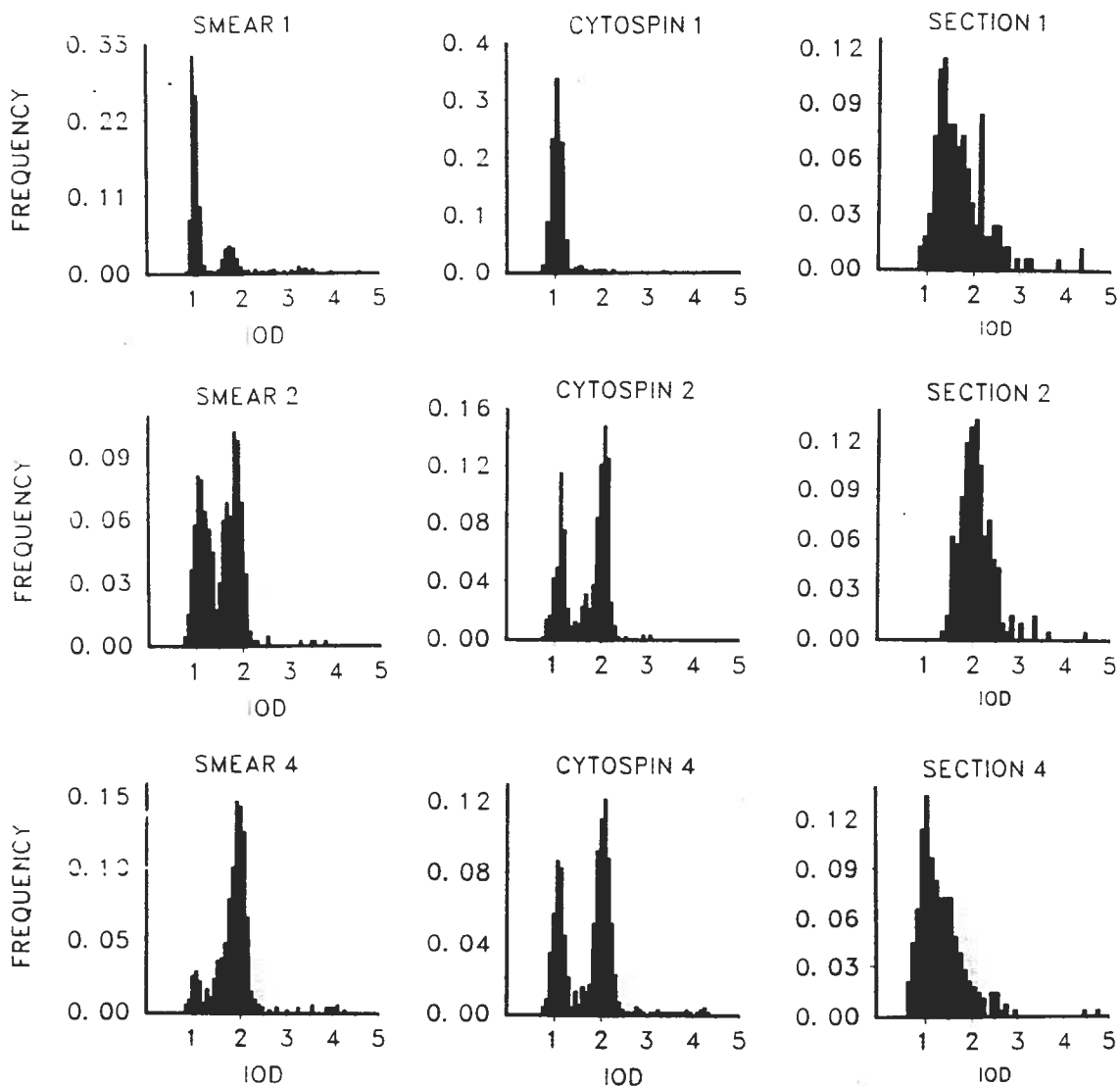


Figure 21. DNA HISTOGRAMS OF CORRESPONDING SMEARS, CYTOSPINS AND TISSUE SECTIONS (A).

DNA histograms obtained by automated collection of images from smears and cytospins of disaggregated nuclei correspond to the DNA histograms obtained by manual collection of nuclear images from tissue sections. The figure shows histograms of carcinoma cases 1, 2, and 4.

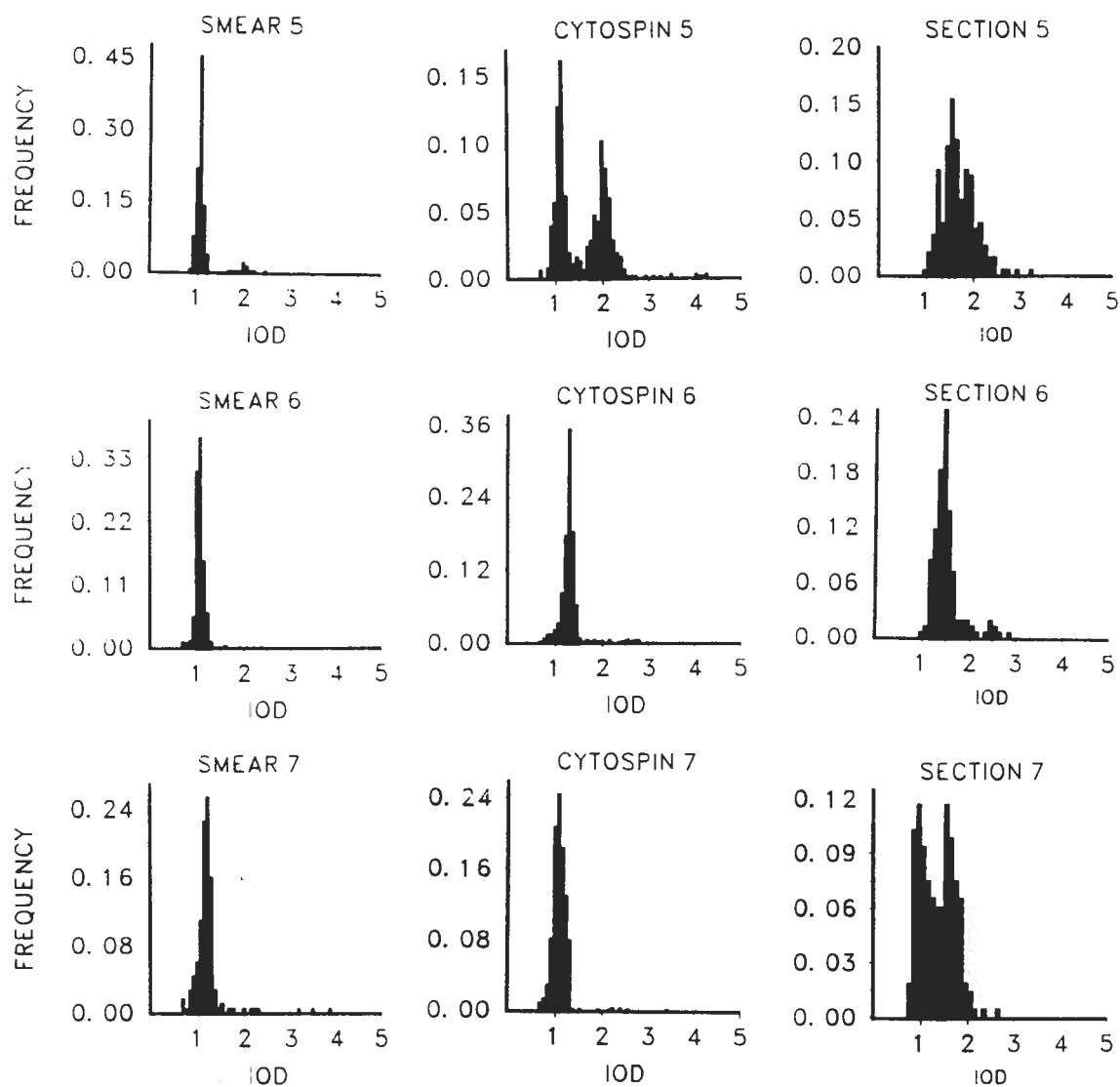


Figure 22. DNA HISTOGRAMS OF CORRESPONDING SMEARS, CYTOSPINS AND TISSUE SECTIONS (B).

DNA histograms obtained by automated collection of images from smears and cytopspins of disaggregated nuclei correspond to the DNA histograms obtained by manual collection of nuclear images from tissue sections. The figure shows histograms of carcinoma cases 5, 6, and 7.

and a tissue section were measured for each case. All collected nuclei are included in the histograms of the cytopins and smears while only carcinoma nuclei are plotted in the histograms of sections. Only in three cases (2, 3, and 4) do all three methods demonstrate aneuploidy, although in case 4 the peaks have different positions. In the case 1, the cytopsin failed to show an aneuploid peak (possibly because it contained a large number of inflammatory and necrotic cells) and the smear and section disagreed in the position of the aneuploid peak. The histograms of the smears failed to show an aneuploid peak in the case 5 and 6 (smear 6 was diagnosed as negative for malignancy). In these two cases the cytopsin and the section measurements disagreed in the position of the aneuploid peak. Case 7 is the only one where the histogram of the tissue section contradicts both other methods by showing an aneuploid peak in addition to a diploid peak.

Table 9 compares the DNA histogram parameters of corresponding smears, cytopins and tissue sections. Discrepancies are present in every case. The parameters of individual DNA histogram are in agreement with each other. When one of the parameters has a low value, the rest of them also have low values. It appears that if IOD and DI are known, entropy and exceeding rates do not add further information.

#### 4.4 CORRELATION OF QUANTITATIVE NUCLEAR FEATURES WITH ADVANCING HISTOLOGICAL CHANGES

In many cases, areas with various histological changes were present in the same tissue block or even on the same tissue section. By measuring nuclei

Table 9. DNA HISTOGRAM PARAMETERS OF CORRESPONDING SMEARS, CYTOSPINS AND TISSUE SECTIONS.

CASE	IOD	DNA index	CV (%)	ENTROPY	%>1.25	%>2.5
SMEAR 1	1.28	1.0/1.7	7/7	0.53	24	5
CYTOSPIN 1	1.07	1.0	10	0.47	5	0
SECTION 1	1.71	1.3/2.2	-	0.74	80	8
SMEAR 2	1.53	1.0/1.8	14/10	0.68	66	1
CYTOSPIN 2	1.78	1.1/2.0	10/9	0.62	68	0
SECTION 2	2.07	2.0	13	0.68	100	10
SMEAR 3	1.56	1.0/1.65	12/8	0.56	87	0
CYTOSPIN 3	1.47	1.1/1.65	16/10	0.71	59	2
SECTION 3	1.70	1.5	16	0.67	92	1
SMEAR 4	1.86	1.0/1.85	8/10	0.65	90	3
CYTOSPIN 4	1.75	1.0/2.0	11/8	0.70	70	4
SECTION 4	1.34	1.0/1.45	-	0.72	47	3
SMEAR 5	1.10	1.0	7	0.39	6	0
CYTOSPIN 5	1.58	1.05/1.95	10/9	0.68	54	2
SECTION 5	1.69	1.5	-	0.72	70	1
SMEAR 6	1.04	1.0	9	0.39	2	0
CYTOSPIN 6	1.3	1.25	7	0.48	65	1
SECTION 6	1.49	1.4	11	0.58	85	2
SMEAR 7	1.24	1.15	9	0.48	27	1
CYTOSPIN 7	1.09	1.0	11	0.47	9	0
SECTION 7	1.35	0.9/1.6	11/15	0.67	58	0

Table shows the discrepancies in histogram parameters between corresponding smears, cytopins and tissue sections of 7 invasive breast carcinoma cases: integrated optical density (IOD), DNA index, coefficient of variation of peaks (CV), entropy of the histogram, and exceeding rates (%>1.25 and %> 2.5).

of specific morphological changes, it was possible to observe the differences in nuclear features of different breast diseases in the same patient. With the use of only two features in a scatter plot, it was possible to demonstrate the variation of different diseases occurring in the same patient.

It has been claimed that various histological patterns represent steps in the progression to invasive carcinoma. An example of an area vs. IOD scatter plot shows how the irregularities of nuclear size, DNA content or texture increase with the advancing morphological changes in an individual patient (Figure 23).

The means of features and the standard deviations of the means were calculated for all cases in six groups of breast diseases in order to analyze the relationships between quantitative nuclear features and advancing morphological changes. A case here refers to a feature file, or feature files that belong to an individual patient and fit into one of the following six categories: Normal, non-proliferative disease, proliferative disease, non-comedo DCIS, comedo DCIS, or invasive carcinoma. (Each feature file carried the feature information for the nuclei collected from the areas of the slide with a specific diagnosis. Hence, some individual patients included in this part of the study were represented in more than one category, if their sections contained various conditions). The number of cases included in different groups of diseases was shown in Table 2.

DNA histograms were analyzed to detect the differences in histogram parameters between six categories of breast diseases. Average values of entropy and exceeding rates of all six groups are listed in Table 10. The increase in the entropy, 1.25-exceeding rate, and 2.5-exceeding rate can be

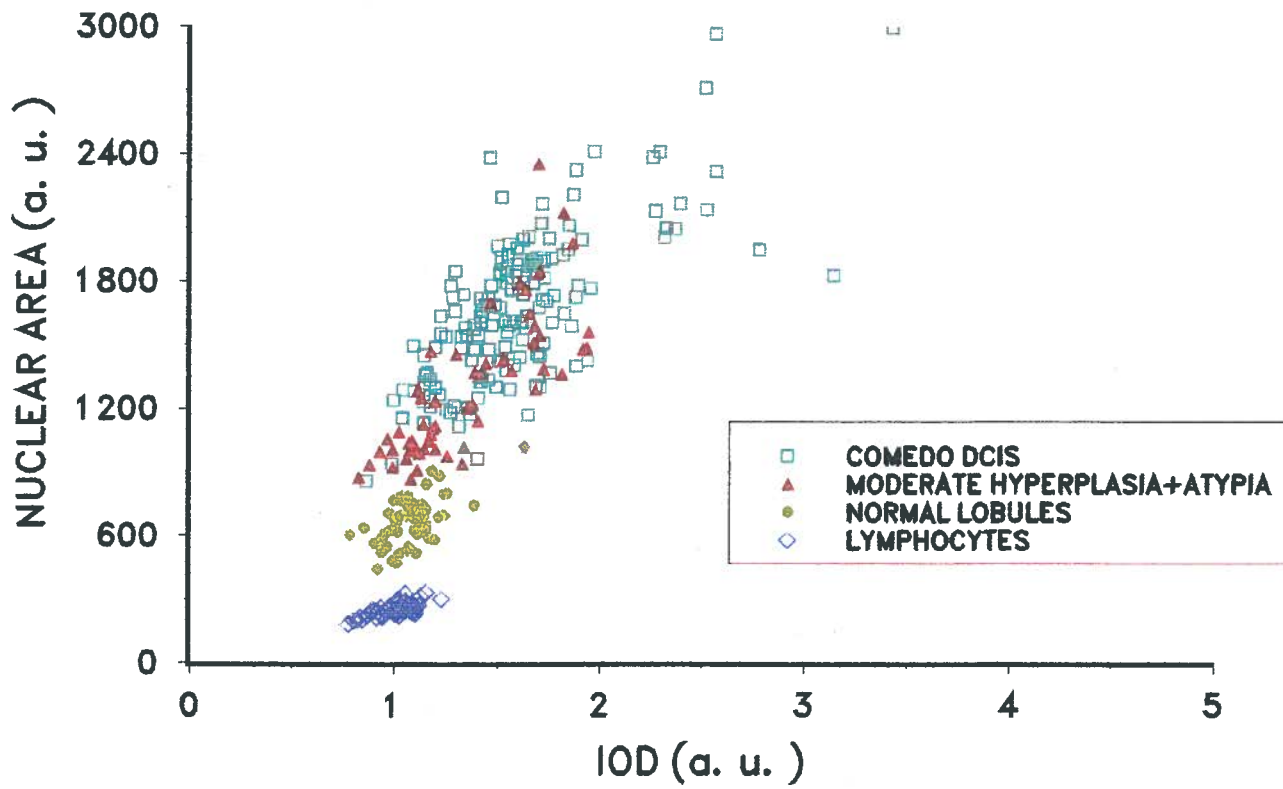


Figure 23. NUCLEAR AREA VS. IOD SCATTER PLOT OF VARIOUS HISTOLOGICAL PATTERNS PRESENT ON THE SAME SLIDE.

Table 10. DNA HISTOGRAM PARAMETERS IN SIX DIAGNOSTIC GROUPS.

<b>DIAGNOSIS OF THE ANALYZED AREA</b>	<b>NUMBER OF CASES</b>	<b>ENTROPY (STANDARD DEV.)</b>	<b>%&gt;1.25</b>	<b>%&gt;2.5</b>
<b>NORMAL GLANDS</b>	<b>20</b>	<b>0.46 (0.04)</b>	<b>14</b>	<b>0</b>
<b>NON-PROLIFERATIVE</b>	<b>8</b>	<b>0.53 (0.06)</b>	<b>35</b>	<b>0</b>
<b>PROLIFERATIVE</b>	<b>18</b>	<b>0.52 (0.05)</b>	<b>30</b>	<b>0</b>
<b>NON-COMEDO DCIS</b>	<b>60</b>	<b>0.58 (0.07)</b>	<b>40</b>	<b>3</b>
<b>COMEDO DCIS</b>	<b>21</b>	<b>0.68 (0.07)</b>	<b>62</b>	<b>3.5</b>
<b>INVASIVE CARCINOMA</b>	<b>30</b>	<b>0.63 (0.09)</b>	<b>58</b>	<b>9</b>

Table shows average values of entropy of the histogram, 1.25-exceeding rates, and 2.5-exceeding rates for the six categories of breast diseases.

seen from the lowest values in the normal group to the highest values in the invasive carcinoma group and comedo DCIS group.

In the group of benign breast diseases we detected aneuploidy in 2 patients. The first patient had a diagnosis of "moderate hyperplasia with atypia". Aneuploid peaks in this case were detected when nuclei were collected in the area with moderate hyperplasia and also in the area with only mild hyperplastic changes on the same slide. The second patient had a diagnosis of invasive carcinoma. In addition to an aneuploid peak of invasive carcinoma, similar aneuploid peaks showed up in the histograms of nuclei collected from areas with moderate, and mild hyperplastic changes. There was no DCIS present.

The values of four features (IOD, area, variation of radius, variation of optical density values in the nucleus) and two variances (variance of IOD, variance of area) are shown for six groups of diseases in Table 11. These particular features were chosen for the table because each represents a different characteristic of a nucleus: DNA content, size, shape, and chromatin texture. The two variances provide different information, which is related to the inter-nuclear variation in DNA content, size, shape, and texture. Table 11 shows that mean values of four features and their variances increase, from the lowest values in the normal group, to the highest values in the invasive carcinoma group. (The exception is comedo DCIS which always has the highest values; this may be due to a very high grade of nuclei, typical for comedo DCIS.) The standard deviations behave in the same way, increasing from normal to invasive carcinoma. The increase in standard deviation indicates a larger inter-slide variation in the group.

Table 11. THE MEAN VALUES OF THE REPRESENTATIVE FEATURES AND THEIR VARIANCES IN SIX GROUPS OF BREAST DISEASES.

FEATURES, *VARIANCES	GROUP					
	normal tissue	non-proliferative disease	proliferative disease	non-comedo DCIS	comedo DCIS	invasive carcinoma
IOD	1.08 (0.13)	1.18 (0.16)	1.14 (0.16)	1.30 (0.35)	1.62 (0.51)	1.50 (0.57)
*V IOD	0.18 (0.06)	0.25 (0.10)	0.24 (0.07)	0.34 (0.15)	0.55 (0.24)	0.45 (0.27)
area	708 (123)	867 (65)	953 (243)	1027 (332)	1635 (383)	1262 (436)
*V area	141 (34)	211 (83)	231 (92)	273 (107)	498 (192)	336 (175)
varradius	9.5 (3.6)	10.6 (3.1)	17.5 (10.3)	18.2 (12.6)	33.1 (15.0)	25.8 (13.7)
*V varradius	8.2 (2.9)	9.8 (3.0)	11.6 (3.8)	12.8 (5.5)	22.1 (7.6)	15.7 (6.9)
ODvar	0.35 (0.07)	0.39 (0.04)	0.39 (0.09)	0.39 (0.09)	0.46 (0.07)	0.43 (0.09)
*V ODvar	0.060 (0.023)	0.064 (0.016)	0.066 (0.015)	0.069 (0.028)	0.093 (0.037)	0.080 (0.029)
N° OF CASES	53	8	18	60	21	37

Mean values of the features were calculated on the slide by slide basis. The mean values of each group and the standard deviations of the means are presented.

Even though the mean values of features increase, a single feature is not sufficient to discriminate between the different groups. Therefore, combinations of two features were used to display the differences between groups on scatter plots where six points represent the mean feature values for six groups and the error bars show the standard error of the means. Figure 24 shows the increase of DNA content and nuclear size from normal tissue to invasive carcinoma, with the highest values in comedo DCIS. Non-proliferative and proliferative group are poorly distinguished by these two features. Figure 25 shows the distribution of groups by variation of radius and variance of IOD. It demonstrates how two features can be complementary in distinguishing different groups. The nuclear shape (represented by the variation of radius) of non-proliferative and normal group are similar. However, the non-proliferative group has a higher variation of nuclear DNA content on slides. The opposite situation pertains to non-proliferative and proliferative groups. They have a similar inter-nuclear variation of the DNA content, but can be distinguished by the more irregular nuclear shape of the proliferative group.

#### 4.5 HETEROGENEITY OF DUCTAL CARCINOMA *IN SITU*

The main histological types of DCIS are shown in Figures 26-29. Different histological types of DCIS are often present adjacent to each other in the same biopsy. The scatter plots of two features are shown for two such cases in Figures 30-31. The first case is an example of carcinoma *in situ* where different histological types seem to be a uniform population of cells. The second graph presents an example of more usual cases, where different types of DCIS

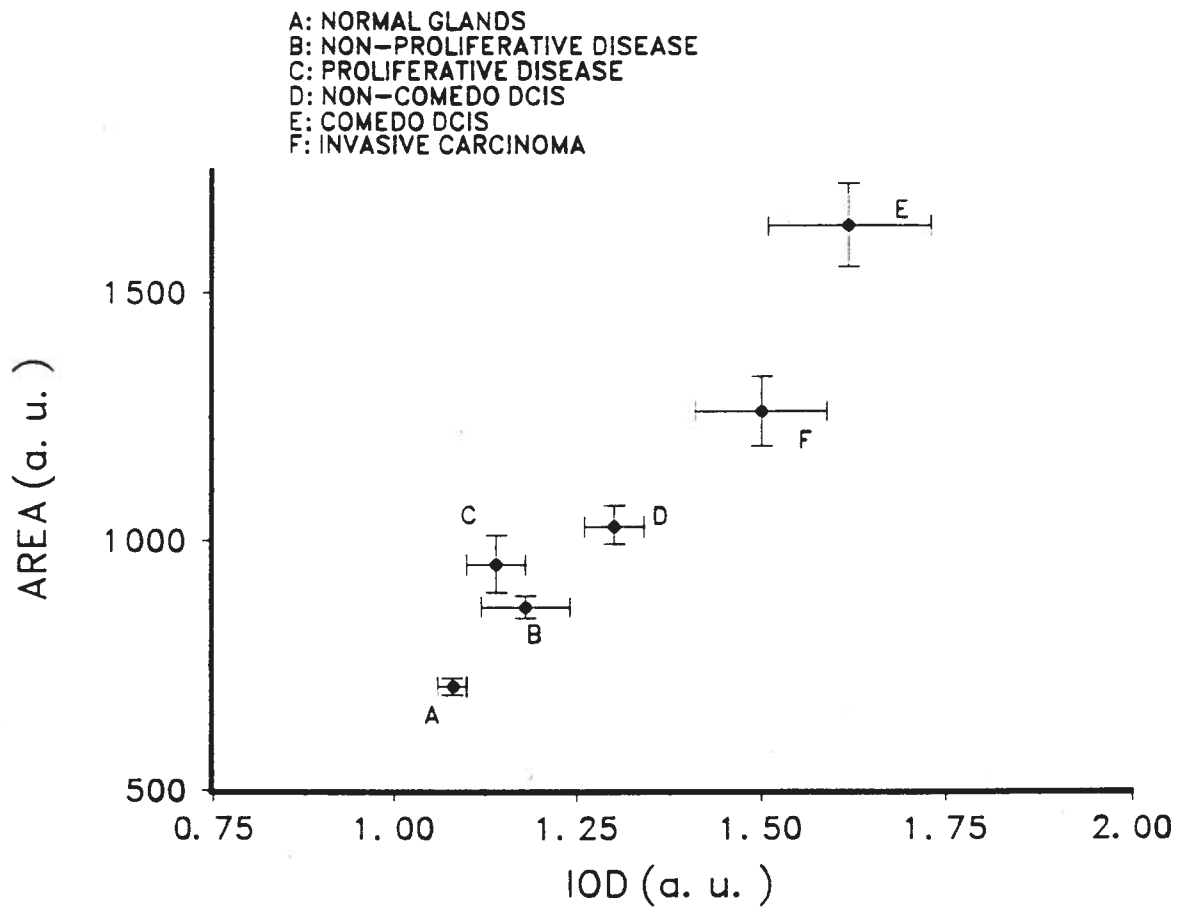


Figure 24. NUCLEAR AREA VS. IOD SCATTER PLOTS OF SIX GROUPS OF BREAST DISEASES.

There is an increase of DNA content and nuclear size from normal tissue to malignant tissue. Comedo DCIS has the highest DNA content and nuclear size.

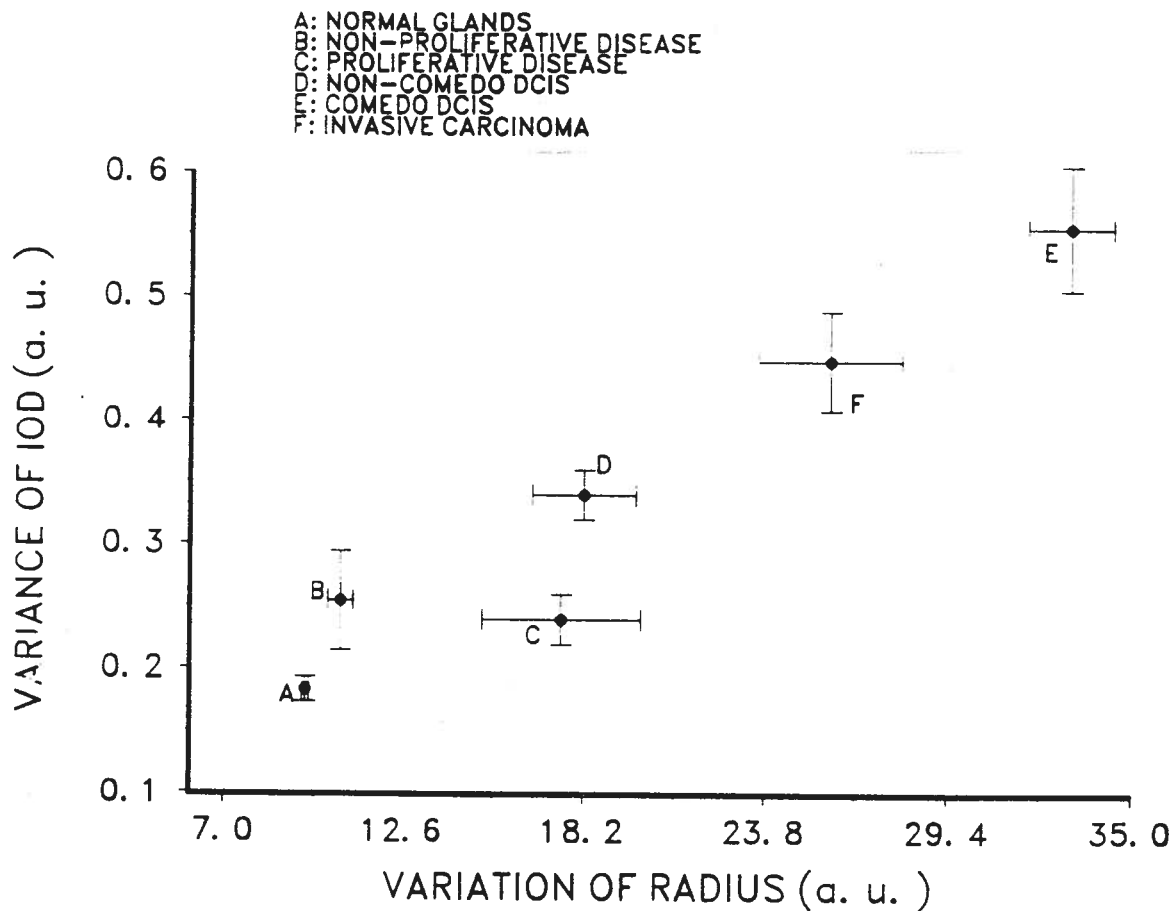


Figure 25. VARIATION OF RADIUS VS. VARIANCE OF IOD SCATTER PLOTS OF SIX GROUPS OF BREAST DISEASES.

Variation of radius increases with more irregular nuclear shape. Variance of integrated optical density is based on the internuclear variation of the DNA content. The figure demonstrates how two features can be complementary in distinguishing histopathological groups. Groups A and B are similar in the shape feature, but group B has the variation of nuclear DNA content on slides higher than A. Groups B and C have similar inter-nuclear variation of the DNA content, but can be distinguished by the more irregular nuclear shape of group C.

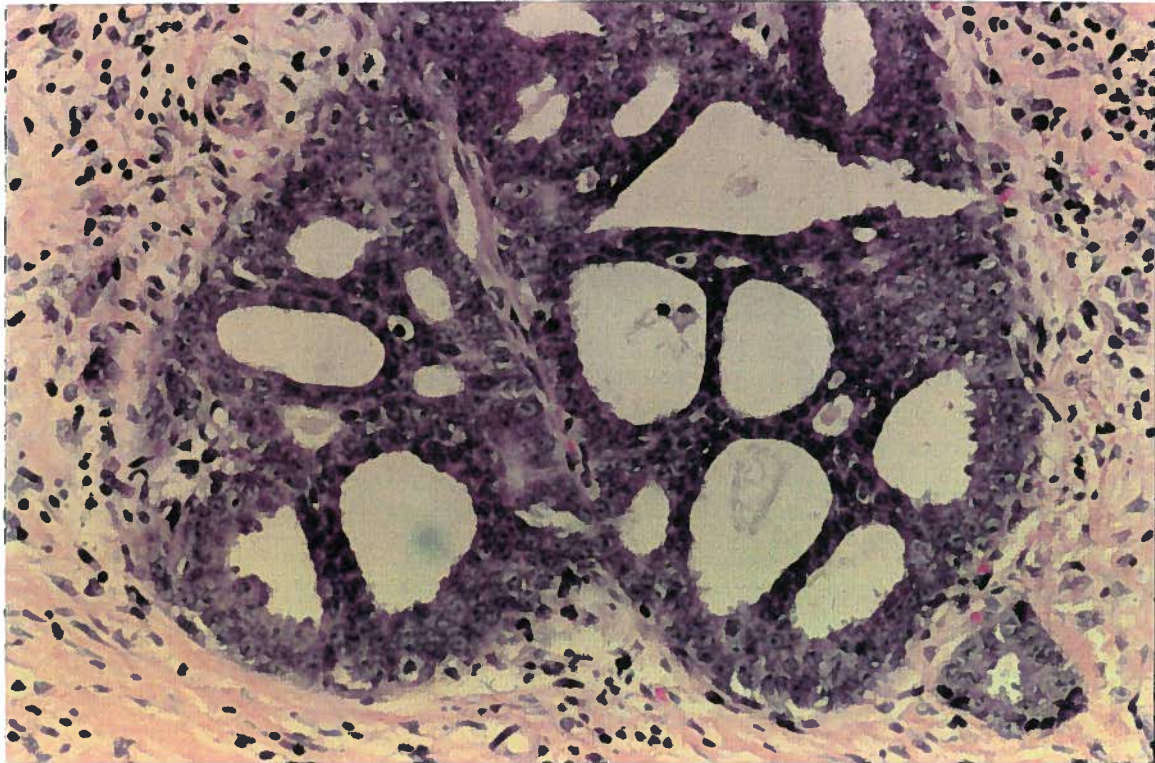


Figure 26. CRIBRIFORM DCIS.

Haematoxylin-eosin stain. Magnification on the print is approximately 172:1.

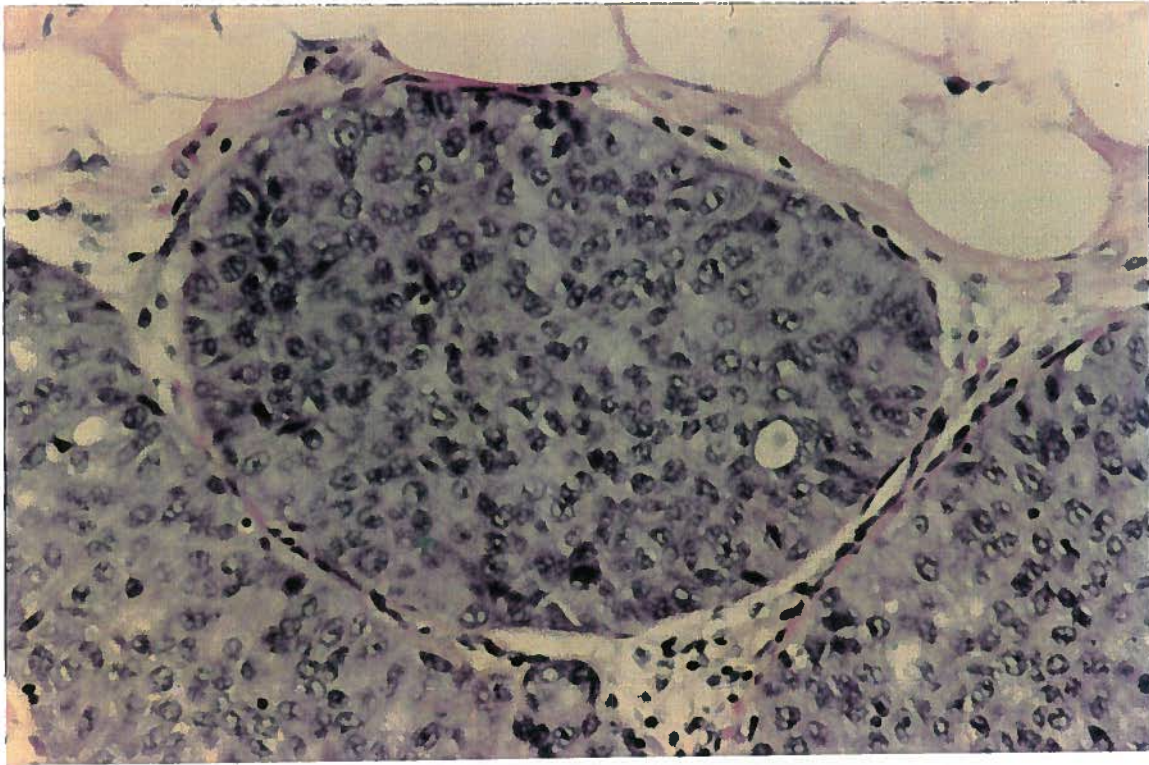


Figure 27. CONFLUENT DCIS.

Haematoxylin-eosin stain. Magnification on the print is approximately 172:1.

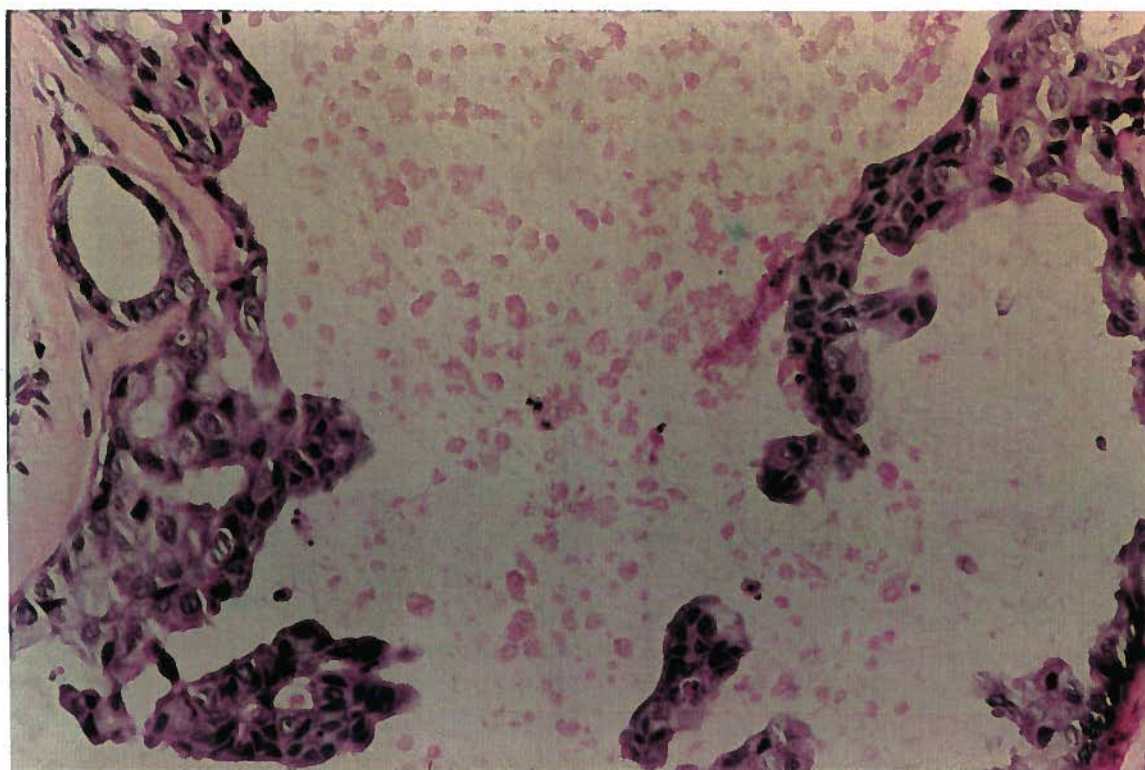


Figure 28. PAPILLARY DCIS.

Haematoxylin-eosin stain. Magnification on the print is approximately 172:1.

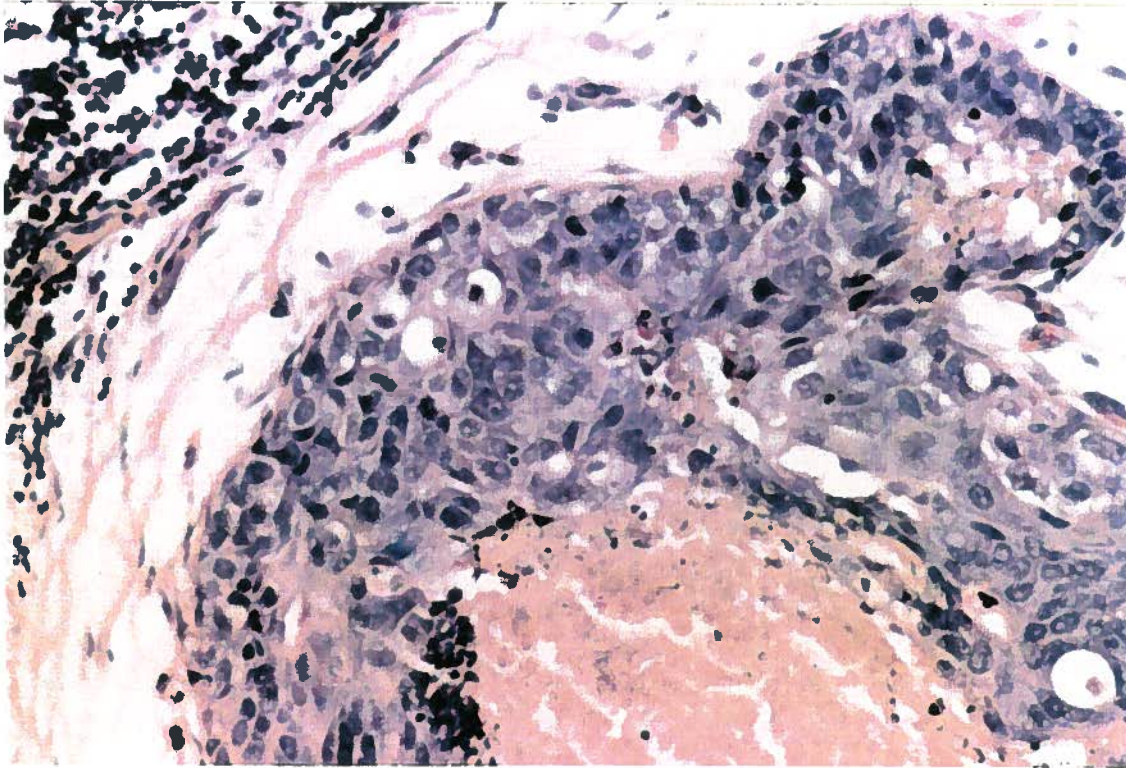


Figure 29. COMEDO DCIS.

Haematoxylin-eosin stain. Magnification on the print is approximately 172:1.

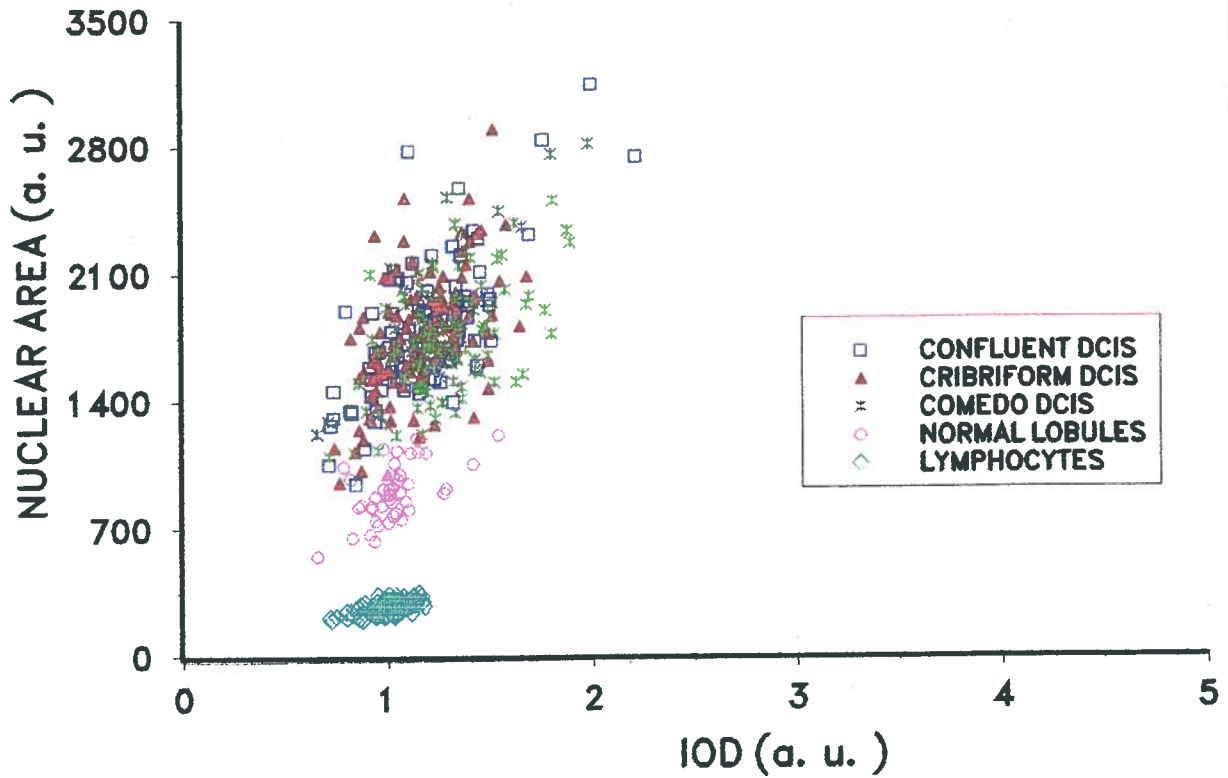


Figure 30. AREA VS. IOD SCATTER PLOTS OF VARIOUS DCIS TYPES PRESENT ON THE SAME SLIDE: CASE A.

Comedo, cribriform and confluent DCIS were present in the same tissue section. DCIS cells of different histological types had similar DNA content and nuclear size.

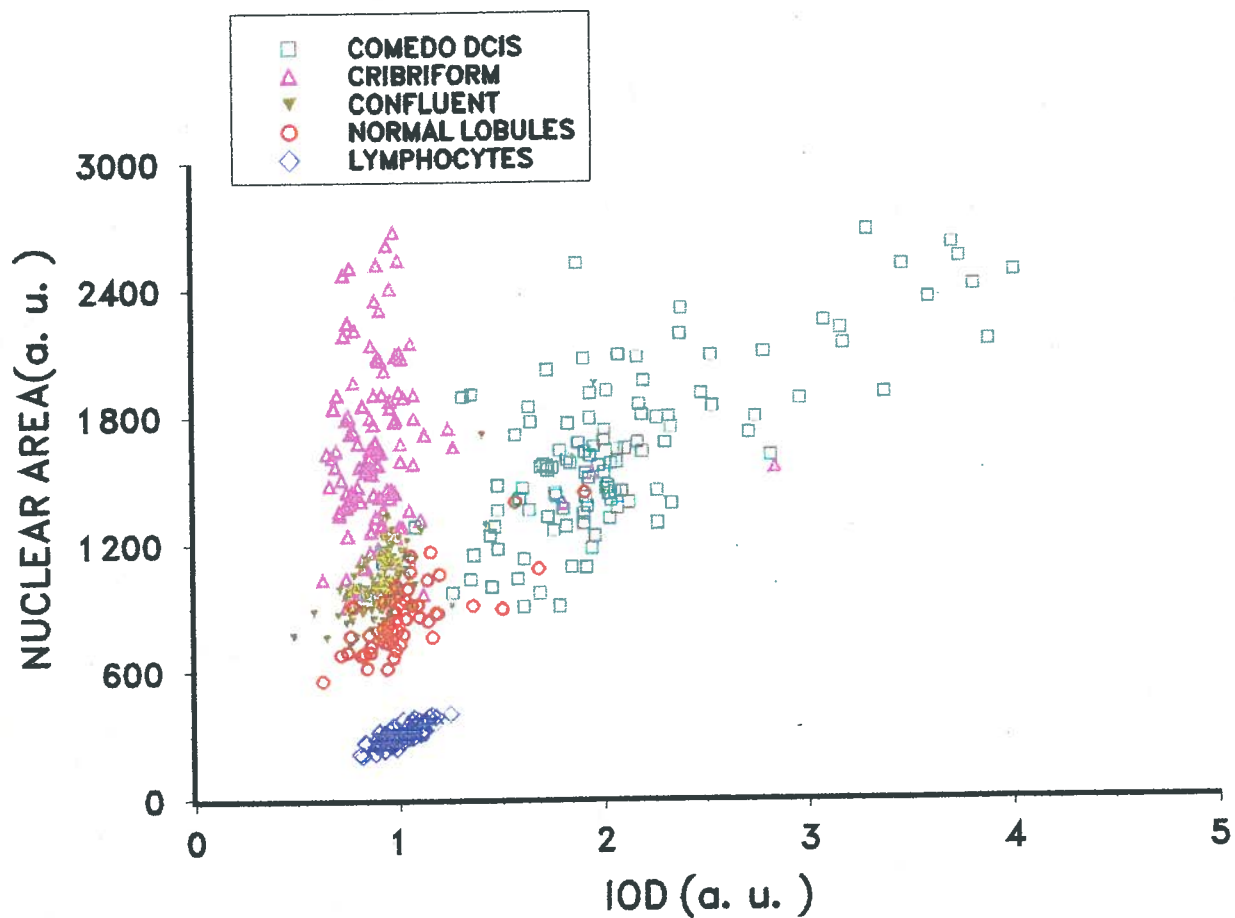


Figure 31. AREA VS. IOD SCATTER PLOTS OF VARIOUS DCIS TYPES PRESENT ON THE SAME SLIDE: CASE B.

Comedo, cribriform and confluent DCIS were present in the same tissue section. DCIS cells of different histological types differ in the DNA content and nuclear size.

seem to be composed of distinct populations of cells with different DNA content, size, and proliferation rate.

#### 4.5.A Comparison of comedo and non-comedo types

The purpose of the study was to characterize the differences between comedo and non-comedo DCIS on the basis of nuclear features. The differences in ploidy and DNA histogram parameters between comedo and non-comedo DCIS are presented in Tables 12 and 13. The comedo type has a much higher rate of aneuploidy in addition to higher IOD, average DNA index, entropy and exceeding rates.

Pictures of non-comedo and comedo nuclei are shown in Figure 32. Parametric and non-parametric T-tests were applied on the slide means and standard deviations of features to select the features that were significantly different between two groups of slides ( $p < 0.05$ ). Some of the quantitative nuclear features which were significantly different between non-comedo DCIS and comedo DCIS slides are listed in Table 14. The data indicate that comedo nuclei are larger (1, 2), have more irregular shape (3, 4) and contour (5) and higher DNA content (6). Comedo nuclei more distinctly manifest dark clumps on the bright background (11). There is an increased number of high and low density clusters (16,17). Low, medium and high density areas have more irregular shape (13,14). Gray level variation in the nucleus is larger (7), but smoother; it occurs at lower spatial frequency (12). The differences between nuclei on comedo slides are larger than on non-comedo slides. The variation of

Table 12. PLOIDY IN COMEDO AND NON-COMEDO DCIS.

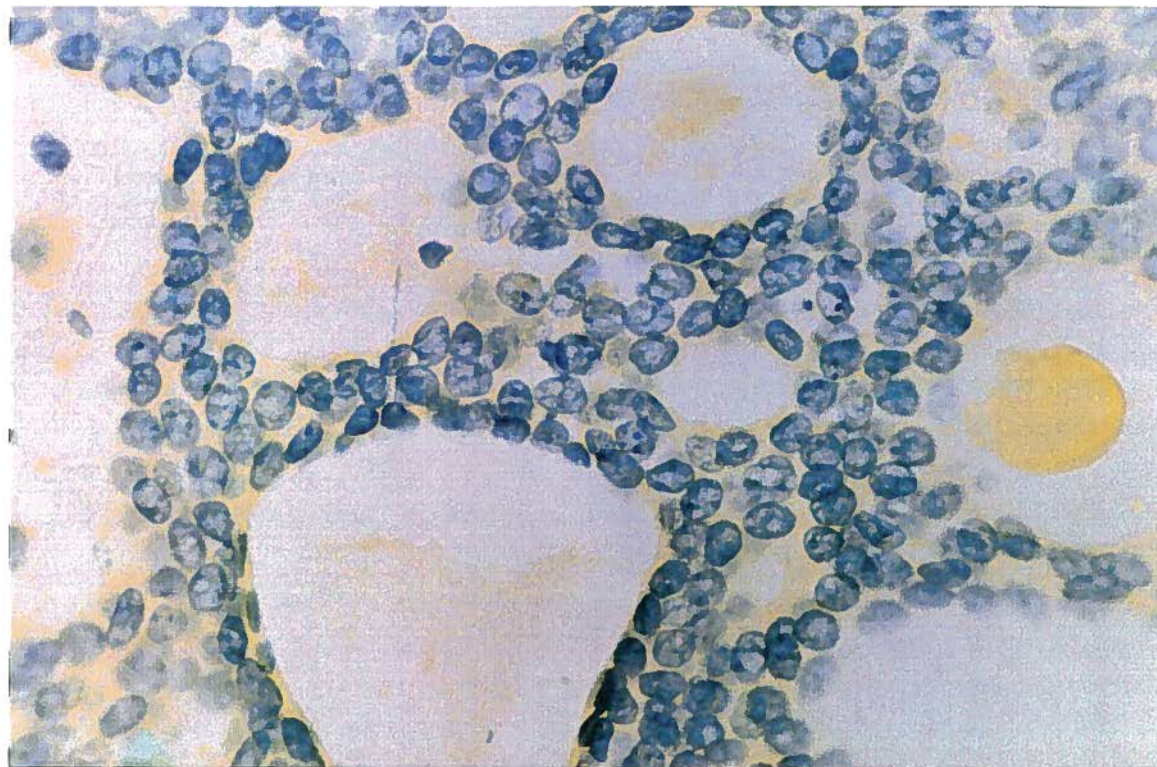
<b>TYPE</b>	<b>DIPLOID</b>	<b>ANEUPLOID</b>	<b>NUMBER OF CASES</b>
<b>NON-COMEDO</b>	<b>25 (42%)</b>	<b>34 (58%)</b>	<b>59</b>
<b>COMEDO</b>	<b>1 (5%)</b>	<b>20 (95%)</b>	<b>21</b>
<b>TOTAL</b>	<b>26 (32.5%)</b>	<b>54 (67.5%)</b>	<b>80</b>

Aneuploidy was demonstrated in 95% of comedo cases, and in 58% of non-comedo cases. Overall, 67.5% of DCIS were aneuploid.

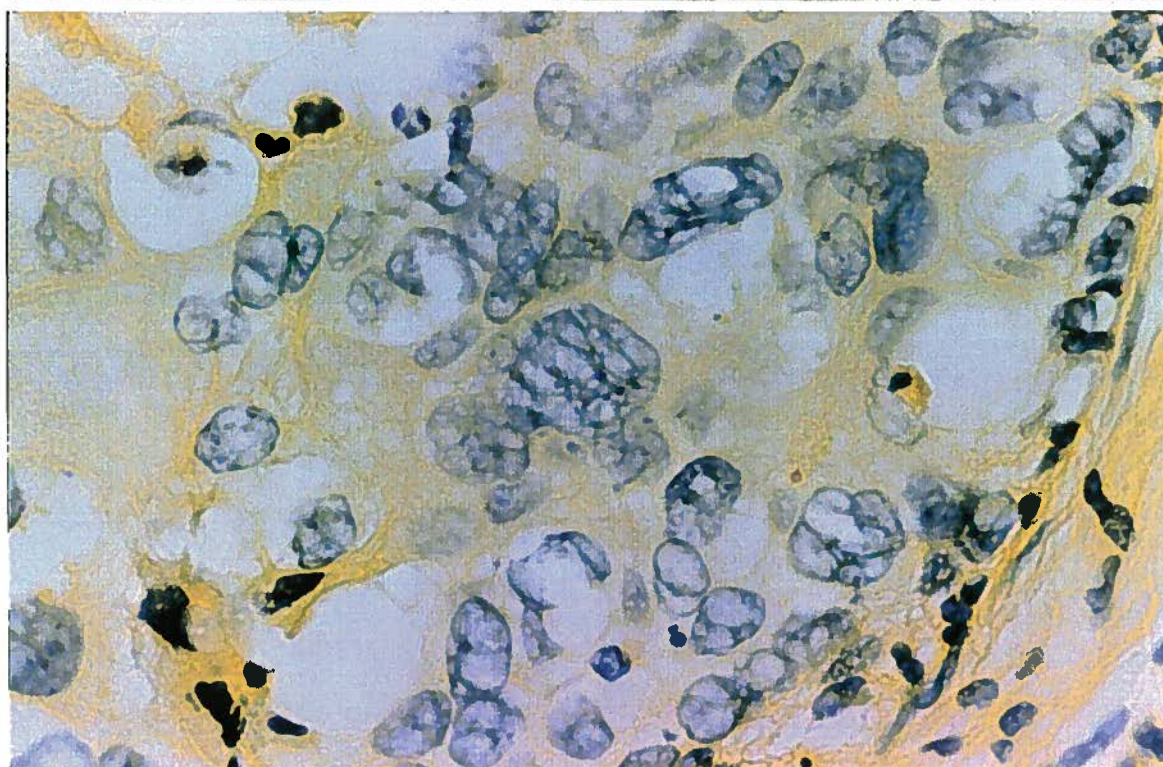
**Table 13. DNA HISTOGRAM PARAMETERS OF DIFFERENT HISTOLOGICAL TYPES OF DCIS. EACH VALUE REPRESENTS THE AVERAGE VALUE OF THE SAME HISTOLOGICAL TYPES.**

<b>HISTOLOGICAL TYPE</b>	<b>NUMBER OF CASES</b>	<b>IOD</b>	<b>DI</b>	<b>%&gt;1.25</b>	<b>%&gt;2.5</b>
<b>CRIBRIFORM</b>	<b>11</b>	<b>1.12</b>	<b>1.05</b>	<b>23</b>	<b>0</b>
<b>PAPILLARY</b>	<b>5</b>	<b>1.64</b>	<b>1.7</b>	<b>63</b>	<b>17</b>
<b>CONFLUENT/ACINAR</b>	<b>24</b>	<b>1.38</b>	<b>1.3</b>	<b>45</b>	<b>1.5</b>
<b>MIXED</b>	<b>13</b>	<b>1.30</b>	<b>1.45</b>	<b>35</b>	<b>1</b>
<b>NONSPECIFIC</b>	<b>7</b>	<b>1.15</b>	<b>1.15</b>	<b>35</b>	<b>6</b>
<b>ALL NON-COMEDO</b>	<b>60</b>	<b>1.30</b>	<b>1.38</b>	<b>40</b>	<b>2</b>
<b>ALL COMEDO</b>	<b>21</b>	<b>1.62</b>	<b>1.53</b>	<b>62</b>	<b>11</b>

Table shows the differences in histogram parameters between various histological types of DCIS. integrated optical density (IOD), DNA index (DI), and 1.25- and 2.5-exceeding rates are the lowest in cribriform type and the highest in comedo type of DCIS. Of all non-comedo DCIS the papillary type appears to be most similar to comedo DCIS.



A



B

Figure 32. MICROGRAPH OF NON-COMEDO (A) AND COMEDO (B) NUCLEI.

Thionin-SO<sub>2</sub> stain, Orange-G counterstain. Magnification on the print is approximately 430:1.

Table 14. SIGNIFICANT DIFFERENCES IN FEATURES OF NON-COMEDO AND  
COMEDO DCIS.

FEATURE	C-DCIS	NC-DCIS	p
	mean ( $\sigma$ )	mean ( $\sigma$ )	
1.AREA	1635 (383)	1030 (331)	0.000
2.MEAN RADIUS	19.9 (2.2)	16.2 (2.1)	0.000
3.VAR RADIUS	33 (15)	18 (12)	0.000
4.COMPACTNESS	6.0 (4.3)	3.4 (2.9)	0.004
5.BOUNDARY 1	44 (11)	36 (12)	0.016
6.IOD	1.6 (0.5)	1.3 (0.3)	0.003
7.OD VAR	0.46 (0.06)	0.39 (0.08)	0.000
8.OD SKEWNESS	0.76 (0.40)	0.37 (0.32)	0.000
9.OD KURTOSIS	4.0 (1.2)	3.1 (0.37)	0.000
10.VAR INTENSITY	6888 (1739)	5360 (1873)	0.002
11.SHADE	-0.63 (0.33)	-0.37 (0.24)	0.000
12.HOMOGENEITY	0.30 (0.03)	0.26 (0.02)	0.000
13.CRL	10.8 (6.9)	4.9 (4.6)	0.000
14.CRH	11.5 (4.8)	7.3 (4.4)	0.000
15.ADL	0.85 (0.1)	0.66 (0.3)	0.003
16.NH	8.2 (3.5)	4.6 (3.3)	0.000
17.NL	40.9 (16.6)	21.0 (16.7)	0.000
18.V AREA	498 (192)	273 (106)	0.000
19.V VAR R	22.1 (7.6)	12.8 (5.5)	0.000
20.V COMPACTNESS	5.6 (3.8)	2.6 (2.5)	0.002
21.V IOD	0.55 (0.24)	0.34 (0.14)	0.000
22.V TARL	0.138 (0.055)	0.098 (0.070)	0.020
23.V TERH	0.171 (0.059)	0.138 (0.072)	0.031
24.V CRH	5.95 (1.72)	3.99 (1.53)	0.000
25.V ADL	0.138 (0.098)	0.209 (0.144)	0.021
26.V NM	11.0 (2.6)	9.0 (3.0)	0.003
27.V NH	5.3 (1.7)	3.1 (1.6)	0.000
28.V HOMOGENEITY	0.043 (0.009)	0.034 (0.007)	0.000
29.V ODMAX	0.060 (0.016)	0.053 (0.015)	0.038
30.V ODVAR	0.093 (0.037)	0.069 (0.029)	0.004

Features are defined in the Methods Section (3.4). Significance was defined by the p-value of the non-parametric test ( $p < 0.05$ ).

size (18), shape (19, 20) and DNA content (21) is higher. The inter-nuclear variation of a number of texture features is also increased in comedo cases. There are larger differences among nuclei in gray level variation (28, 29, 30) and in area (22), density (23), shape (24), and number (26, 27), of low, medium or high density clusters.

In addition, a stepwise discriminant function analysis was performed on the cell by cell basis to distinguish comedo and non-comedo nuclei (9541 non-comedo nuclei vs. 2826 comedo nuclei). A combination of 10 features, which efficiently discriminated two groups of nuclei was selected: AREA, OD KURTOSIS, VAR INT, VAR OD, CRL, NM, CORRELATION, MEAN RADIUS, AVERAGE, and OD SKEWNESS. The classification did not significantly improve after forcing more features into discriminant function. The relationship between the number of the employed features and the rate of correct classification is shown in Figure 33. The discrimination between comedo and non-comedo nuclei was successful in 83% when 10 features were used. The results are shown in the jackknife classification matrix in Table 15.

#### 4.5.B Quantitative nuclear features in different histological types of non-comedo DCIS

Non-comedo DCIS were grouped according to their histological type (Table 3). Mean values and standard deviations of means were calculated for all nuclear features and their variances. In addition, DNA histogram parameters and ploidy were analyzed.

Table 16 shows differences between various histological types of DCIS,

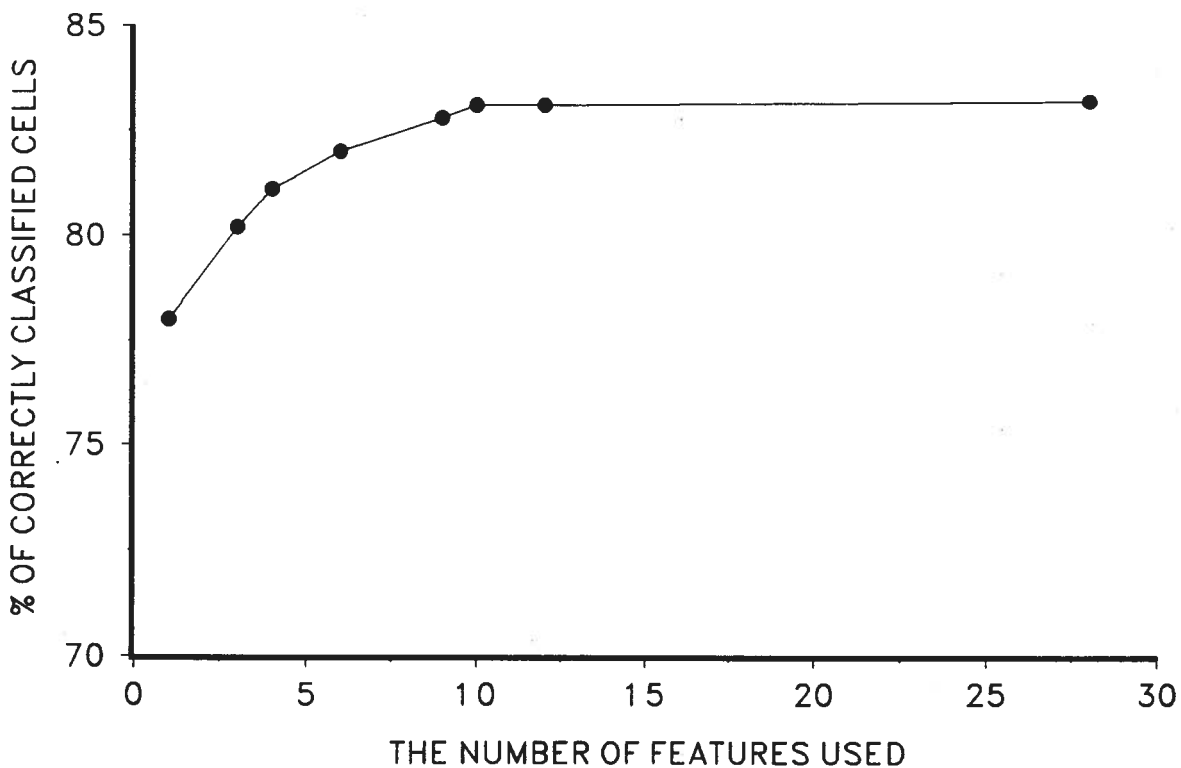


Figure 33. COMEDO VERSUS NON-COMEDO NUCLEI: THE RELATIONSHIP BETWEEN THE NUMBER OF THE EMPLOYED FEATURES AND THE RATE OF CORRECT CLASSIFICATION.

The discriminant function was performed on the cell by cell basis. A combination of 10 features was selected: AREA, OD KURTOSIS, VAR INT, VAR OD, CRL, NM, CORRELATION, MEAN RADIUS, AVERAGE, and OD SKEWNESS. The use of additional features did not significantly improve the discrimination.

**Table 15. JACKKNIFED CLASSIFICATION OF NON-COMEDO AND COMEDO  
DCIS NUCLEI.**

	CLASSIFIED GROUPS		
ACTUAL GROUPS	NON-COMEDO	COMEDO	TOTAL
NON-COMEDO	8185 (86%)	1356 (14%)	9541
COMEDO	736 (26%)	2090 (74%)	2826

Overall classification is correct in 83% (10275/12367) of nuclei.

Table 16. THE MEAN VALUES OF THE REPRESENTATIVE FEATURES, AND THEIR VARIANCES, IN DIFFERENT HISTOLOGICAL TYPES OF

DCIS

FEATURES	HISTOLOGICAL					TYPE			OF		DCIS TOTAL
	PAPILLARY	CONFLUENT/ACINAR	CRIBRIFORM	MIXED	NONSPECIFIC						
IOD	1.64 (0.59)	1.37 (0.30)	1.12 (0.17)	1.29 (0.27)	1.14 (0.51)					1.30 (0.35)	
*VIOD	0.47 (0.26)	0.35 (0.10)	0.25 (0.10)	0.35 (0.19)	0.34 (0.14)					0.34 (0.15)	
area	1106 (400)	1052 (297)	895 (240)	925 (346)	1295 (391)					1027 (332)	
*Varea	285 (81)	280 (106)	231 (89)	249 (93)	353 (149)					273 (107)	
varradius	22.3 (12.9)	17.9(12.8)	15.7 (8.0)	13.8 (12.8)	28.6 (14.2)					18.2 (12.6)	
ODvar	0.40 (0.12)	0.39 (0.06)	0.34 (0.07)	0.35 (0.09)	0.47 (0.12)					0.39 (0.09)	
N° OF CASES	5	24	11	13	7					60	

Mean feature values and standard deviations of the means are presented in the table separately for various histological types of DCIS. Mixed type refers to cases with different combinations of confluent, cribriform, and papillary type. Non-specific type refers to patterns which did not fit into any diagnostic category.

\* VIOD and Varea are feature variances.

demonstrated by the mean values, and their standard deviations, of four features and two feature variances. IOD, AREA, VAR RAD and VAR OD were chosen to represent the main feature groups (DNA content, area, shape, chromatin texture). VIOD and VAREA were chosen as the two most meaningful variances, which represent the inter-nuclear variation in the DNA content and in nuclear size on each slide. Table 16 demonstrates that differences between the types exist in the DNA content, size, shape, and chromatin distribution. The nuclear DNA content, nuclear size, the irregularity of shape and the width of the optical density distribution in the nucleus all increase, with the lowest values in cribriform type, intermediate values in mixed and confluent types, and the highest values in papillary type. The differences in these features between main histological types of DCIS are also shown in Figures 34-37. The intraslide variation of nuclear DNA content and size, shown by the two variances, is also the smallest in cribriform, and the highest in papillary type. Figure 38 shows the variance of IOD in different DCIS types. Inter-slide variation is represented by the standard deviations of the mean values. For most features, papillary type has the highest variability between cases, and cribriform group has the lowest. Non-specific type has a low nuclear DNA content, large nuclear size, large shape irregularity, and wide distribution of optical density values in the nucleus. In addition, nonspecific type has a high inter-slide variations compared to other types, which indicates that very different cases are included in this group.

Table 13 shows that the DNA histogram parameters also differ between the histological types; the average values are shown for all cases of the same histological type. A higher IOD of confluent and papillary type corresponds to a

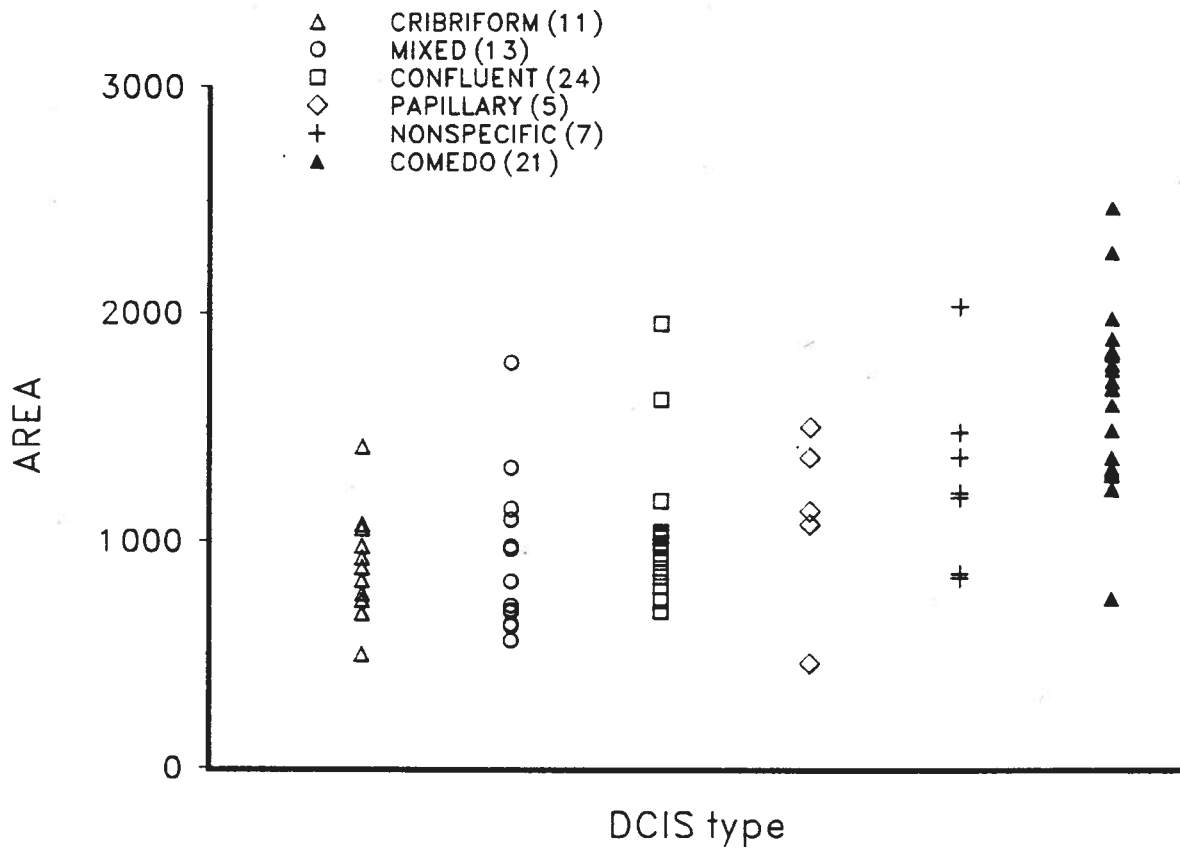


Figure 34. NUCLEAR AREA IN DIFFERENT DCIS TYPES.

Cribriform and mixed type have smaller nuclear area than other histological types of DCIS. Comedo type has the largest nuclear area.

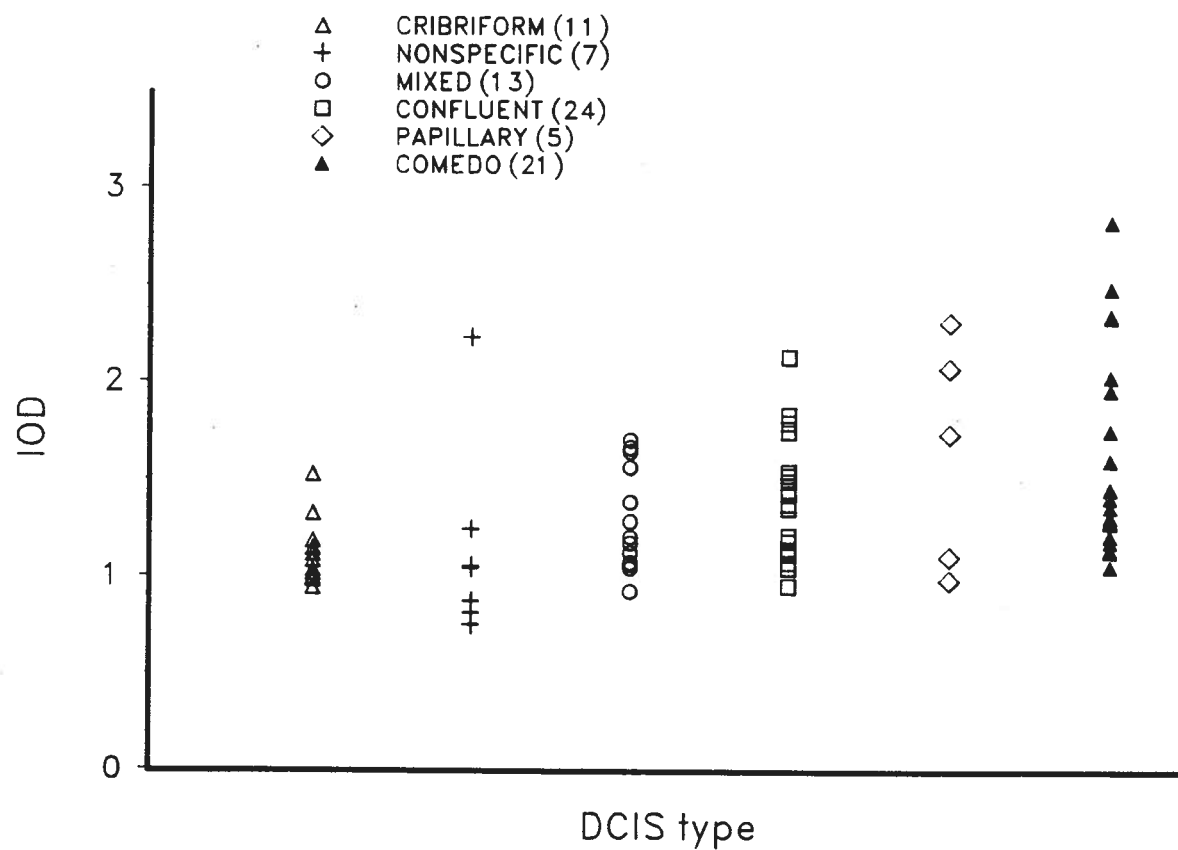


Figure 35. IOD IN DIFFERENT DCIS TYPES.

Integrated optical density is related to the nuclear DNA content. Cribriform and nonspecific type have a low DNA content. Comedo type has the highest DNA content.

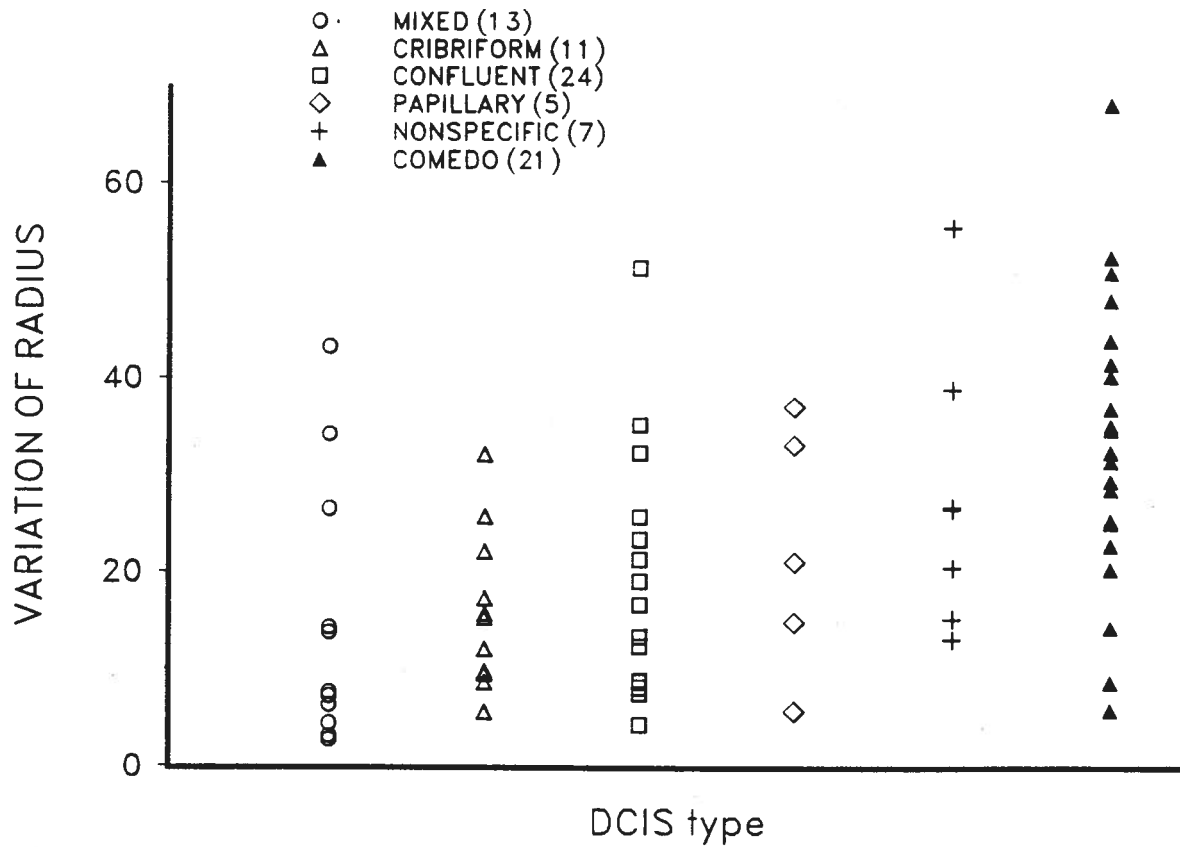


Figure 36. VARIATION OF RADIUS IN DIFFERENT DCIS TYPES.

Mixed, cribriform and confluent type have more regular nuclear shape than other types. Nuclei with the most irregular shape can be found in comedo type.

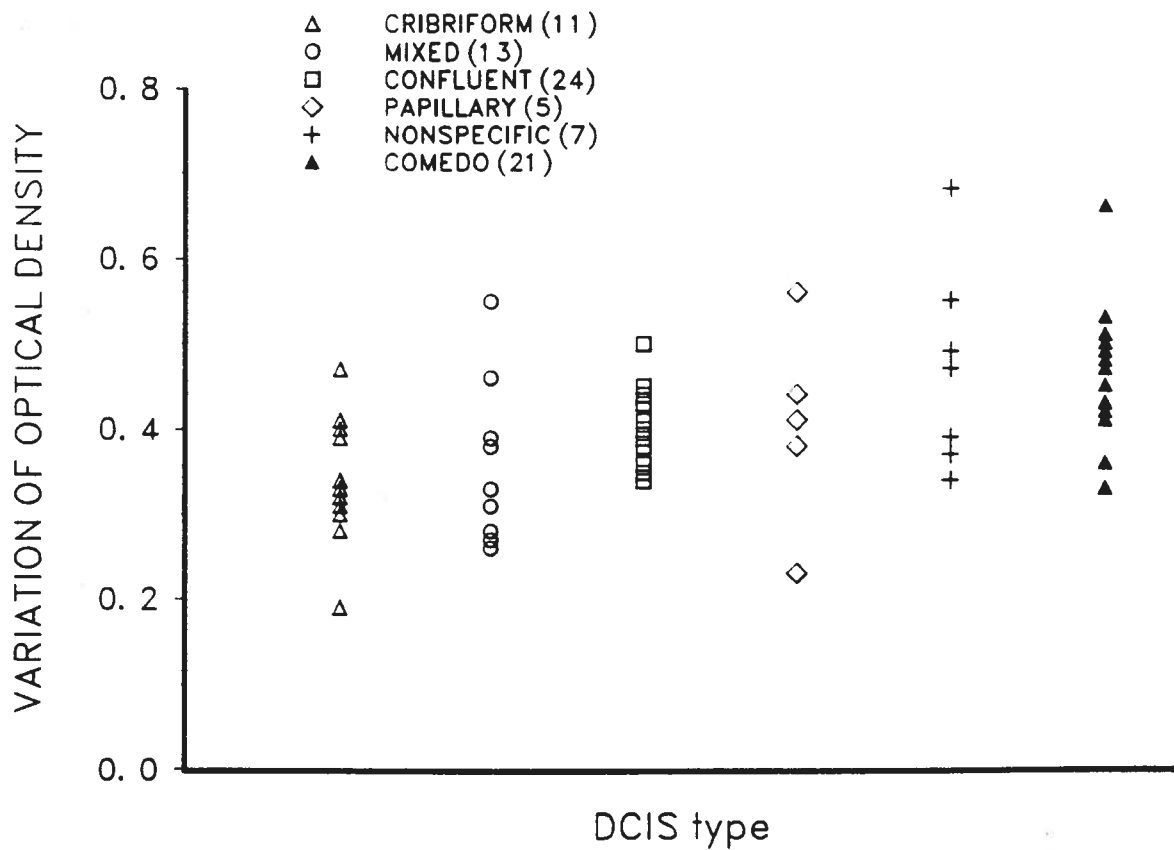


Figure 37. VARIATION OF OPTICAL DENSITY IN DIFFERENT DCIS TYPES.

Variation of optical density represents the variation in the distribution of optical density values over the pixels of a nucleus. Cribriform and mixed types have more homogeneously stained chromatin than other types.

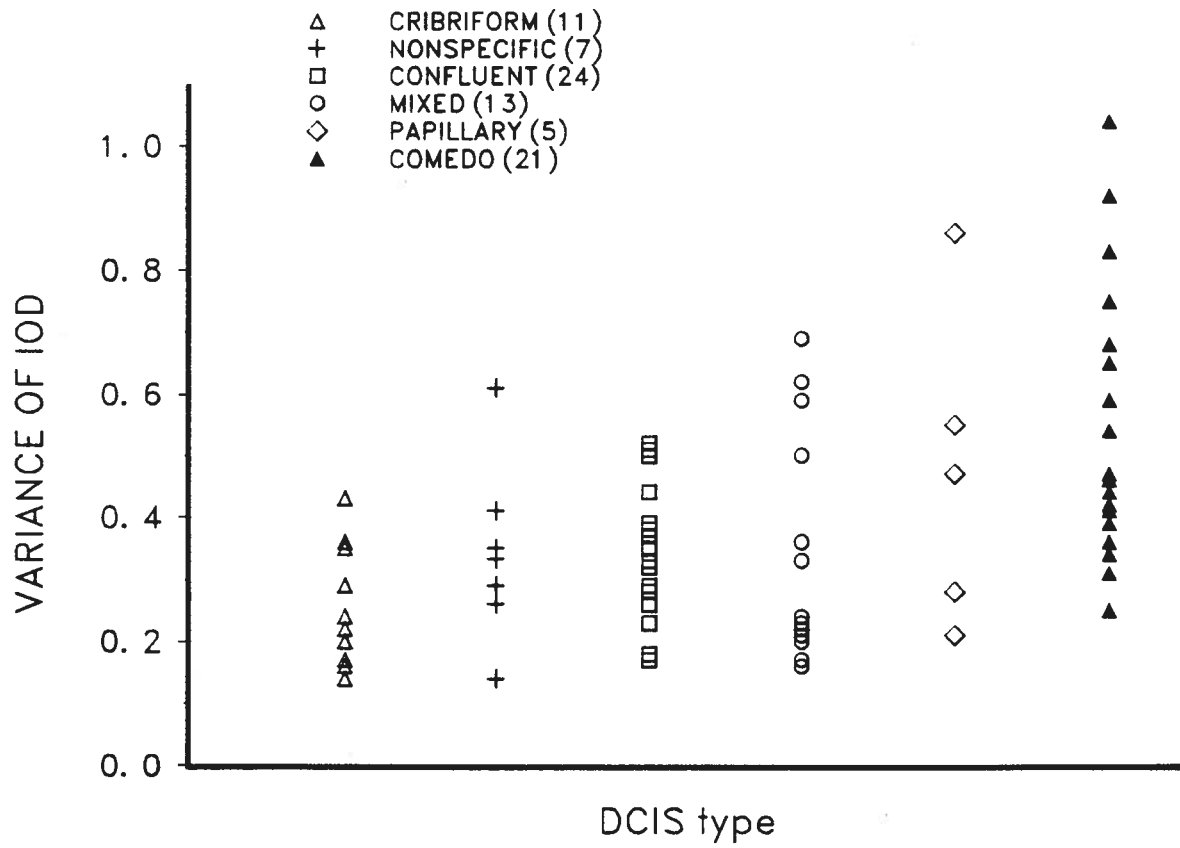


Figure 38. VARIANCE OF IOD IN DIFFERENT DCIS TYPES.

The variation of the DNA content between nuclei on each slide is the lowest for the cribriform DCIS. Comedo type has the highest internuclear variation of the DNA content.

Table 17. PLOIDY OF DIFFERENT HISTOLOGICAL TYPES OF NON-COMEDO DCIS.

<b>TYPE</b>	<b>DIPLOID</b>	<b>ANEUPLOID</b>	<b>number of cases</b>
<b>CRIBRIFORM</b>	<b>7 (64%)</b>	<b>4 (36%)</b>	<b>11</b>
<b>PAPILLARY</b>	<b>2 (40%)</b>	<b>3 (60%)</b>	<b>5</b>
<b>CONFLUENT</b>	<b>9 (37.5%)</b>	<b>15 (62.5%)</b>	<b>24</b>
<b>MIXED</b>	<b>4 (33%)</b>	<b>8 (67%)</b>	<b>12</b>
<b>NONSPECIFIC</b>	<b>3 (43%)</b>	<b>4 (57%)</b>	<b>7</b>

Cribiform type appears to have lower frequency of aneuploid cases than other types. In total, 58% (34/59) of non-comedo DCIS is aneuploid.

higher DNA index (increased DNA content in G<sub>0</sub>/G<sub>1</sub>-phase) and higher exceeding rates (increased number of either proliferating or aneuploid cells).

Table 17 presents the ploidy of different histological types of non-comedo DCIS. Cribriform type appears different from the others in the low proportion of aneuploid cases. Aneuploidy is found almost twice as often in the other histological types than in cribriform.

#### 4.6. DIFFERENCES BETWEEN PURE DCIS AND DCIS ASSOCIATED WITH INVASIVE CARCINOMA IN THE SURROUNDING TISSUE

Table 18 shows the DNA histogram parameters of different histological types of DCIS and demonstrates a comparison of plain DCIS (DCIS1) and DCIS associated with invasive breast carcinoma (DCIS2). Comedo DCIS and some of the non-comedo types (papillary, non-specific and mixed) show an increase in the average DNA index, IOD, and exceeding rates, when invasive carcinoma is present in the surrounding tissue. The confluent type shows increased IOD, but similar DI and exceeding rates, while the cribriform type exhibits slightly decreased values of histogram parameters when it is associated with invasive carcinoma.

Table 19 compares ploidy of DCIS1 and DCIS2. In non-comedo type aneuploidy rate increases from 53% in DCIS1 to 62% in DCIS2. This difference is not statistically significant. For the comedo type, the proportion of aneuploid cases is decreased in DCIS2, but this is due to a single diploid case found in this group. A further analysis of the differences between DCIS1 and DCIS2 was continued separately for comedo and non-comedo type.

**Table 18. AVERAGE VALUES OF DNA HISTOGRAM PARAMETERS OBTAINED FROM DIFFERENT HISTOLOGICAL TYPES OF DCIS (WITH OR WITHOUT ASSOCIATED INVASIVE CARCINOMA IN THE SURROUNDING TISSUE).**

HISTOLOGICAL TYPE	DCIS WITHOUT INVASIVE CARCINOMA					DCIS WITH INVASIVE CARCINOMA				
	N° of cases	IOD ( $\sigma$ )	DI	%>1.25	%>2.5	N° of cases	IOD ( $\sigma$ )	DI	%>1.25	%>2.5
cribriform	6	1.17 (0.22)	1.1	31	0	5	1.06 (0.08)	1.0	13	0
papillary	2	1.41 (0.45)	1.6	46	12	3	1.79 (0.71)	1.8	74	21
confluent/acinar	12	1.33 (0.25)	1.3	44	1.5	12	1.41 (0.34)	1.35	46	1.5
mixed	7	1.19 (0.24)	1.3	27	1	6	1.41 (0.26)	1.65	45	1
nonspecific	4	0.90 (0.12)	0.9	11	0	3	1.51 (0.63)	1.45	66	15
all noncomedo	31	1.21 (0.27)	1.35	34	1	29	1.41 (0.42)	1.4	46	3.5
all comedo	6	1.45 (0.32)	1.4	57	3	15	1.69 (0.57)	1.55	64	14

Integrated optical density (IOD), DNA index (DI), 1.25- and 2.5-exceeding rates are shown for pure ductal carcinoma *in situ* and ductal carcinoma *in situ*, which is associated with invasive carcinoma.

**Table 19. PLOIDY OF PLAIN DCIS (DCIS1) AND DCIS ASSOCIATED WITH INVASIVE CARCINOMA IN SURROUNDING BREAST TISSUE (DCIS2).**

<b>HISTOLOGICAL TYPE</b>	<b>DIPLOID</b>	<b>ANEUPLOID</b>	<b>NUMBER OF CASES</b>
<b>NON-COMEDO DCIS1</b>	<b>14 (47%)</b>	<b>16 (53%)</b>	<b>30</b>
<b>NON-COMEDO DCIS2</b>	<b>11 (38%)</b>	<b>18 (62%)</b>	<b>29</b>
<b>COMEDO DCIS1</b>	<b>0</b>	<b>6 (100%)</b>	<b>6</b>
<b>COMEDO DCIS2</b>	<b>1 (7%)</b>	<b>14 (93%)</b>	<b>15</b>

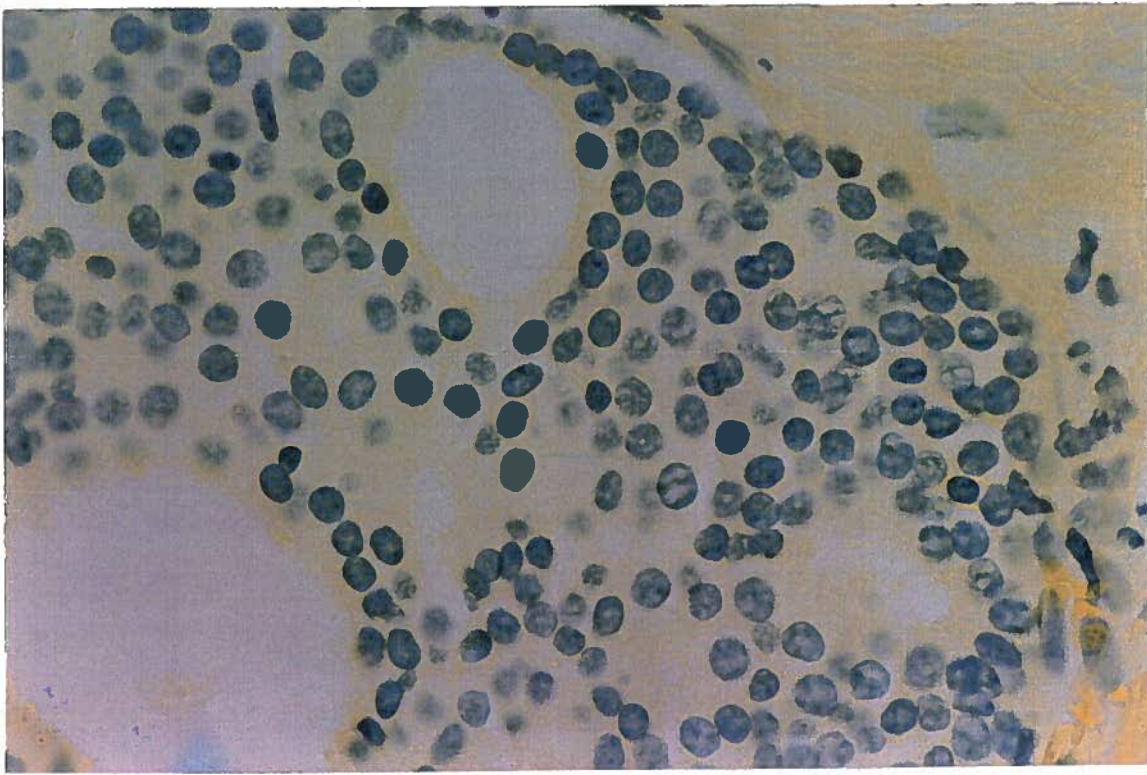
Comedo and non-comedo types are presented separately. In total, aneuploidy is found in 61% of DCIS1 (22/36) and in 72% of DCIS2 (32/44).

#### 4.6.A Non-comedo type

The purpose of the statistical analysis was: i) to demonstrate the differences in nuclear features between DCIS1 and DCIS2, and ii) to classify cases to DCIS1 or DCIS2 on the basis of discriminating nuclear features. Classification was approached in two ways. One approach was to classify cases with the discriminant function, performed on a slide by slide basis. The alternative approach was to first classify single nuclei, and then discriminate the slides on the basis of the percentage of the nuclei classified as DCIS1 or DCIS2. The number of cases and of nuclei in each group is shown in Table 3. In spite of the differences between histological types of non-comedo DCIS, various types were included, with the condition that they were equally distributed in the DCIS1 and DCIS2 group. Figure 39 shows examples of non-comedo nuclei collected from DCIS1 and DCIS2.

First parametric and non-parametric tests were applied on the means and standard deviations of features in order to select the features that were significantly different between DCIS1 and DCIS2 ( $p < 0.05$ ). Some of the features, which were shown to be significantly different by non-parametric tests or T-tests are listed in Table 20 (the p-values of non-parametric test are shown).

Table 20 shows that nuclei of DCIS with invasion in the surrounding breast tissue are rounder, less elongated (1). The fraction of nuclear area occupied with high density chromatin has more irregular shape (4). High density pixels are on average more distant from the center of the nucleus (5). There is a larger number of medium density clusters (6). The variation of gray scale



A



B

Figure 39. EXAMPLES OF DCIS1 (A) AND DCIS2 (B) NUCLEI: NON-COMEDO TYPE.

Thionin-SO<sub>2</sub> stain, Orange-G counterstain. Magnification on the print is approximately 430:1.

**Table 20. FEATURES, SIGNIFICANTLY DIFFERENT BETWEEN NON-COMEDO DCIS WITHOUT INVASION (DCIS1) AND NON-COMEDO DCIS WITH INVASIVE CANCER IN THE SURROUNDING BREAST (DCIS2).**

	<b>NC-DCIS1</b>	<b>NC-DCIS2</b>	
<b>FEATURE</b>	<b>MEAN (<math>\sigma</math>)</b>	<b>MEAN (<math>\sigma</math>)</b>	<b>p value</b>
<b>1.ELONGATION</b>	<b>1.439 (0.099)</b>	<b>1.390 (0.099)</b>	<b>0.034</b>
<b>2.CONTRAST</b>	<b>28.3 (3.8)</b>	<b>25.9 (4.4)</b>	<b>0.022</b>
<b>3.FAREA1</b>	<b>14445 (6321)</b>	<b>19383 (7148)</b>	<b>0.011</b>
<b>4.CRH</b>	<b>6.2 (4.4)</b>	<b>8.6 (4.1)</b>	<b>0.029</b>
<b>5.ADH</b>	<b>0.69 (0.13)</b>	<b>0.75 (0.09)</b>	<b>0.019</b>
<b>6.NM</b>	<b>16.9 (9.3)</b>	<b>22.5 (9.3)</b>	<b>0.022</b>
<b>7.V CRH</b>	<b>3.6 (1.5)</b>	<b>4.4 (1.5)</b>	<b>0.019</b>
<b>8.V NM</b>	<b>7.8 (2.4)</b>	<b>10.3 (3.1)</b>	<b>0.001</b>
<b>9.V FAREA1</b>	<b>5091 (2344)</b>	<b>6597 (2572)</b>	<b>0.024</b>

Features are explained in the Methods Section (3.4). Significance was defined by the p-value of the non-parametric test ( $p < 0.05$ ).

values is larger, but smoother, it occurs at a lower spatial frequency (2, 3). In samples of DCIS with associated invasion, there is an increased inter-nuclear variation of chromatin distribution, demonstrated by significantly larger variances of some texture features, such as the following variances: Irregularity of the high density area shape (7), number of medium density clusters (8), and fractal area1 (9).

The next step was discriminant function analysis on a slide by slide basis without stepwise variable selection. One feature with lowest p-value was forced to enter the discriminant analysis from each of four feature categories: Photometric features, shape features, continuous texture features and discrete texture features. The number of features was limited, since there was a small number of cases in each group. The features which entered the discriminant analysis consisted of: i) IOD (photometric feature,  $p=0.088$ ), ii) ELONGATION (shape feature,  $p=0.034$ ), iii) FRACTAL AREA 1 (continuous texture feature,  $p=0.011$ ), and iv) VNM (discrete texture feature,  $p=0.001$ ). With the stepwise discriminant function analysis the combinations of 2 and 3 features, that gave the best discrimination between non-comedo DCIS1 and non-comedo DCIS2, were selected. With only two features (VNM and ELONGATION) the classification of cases was correct in 72%. With the addition of the third feature (IOD), the classification improved to 80% correct (Table 21). The jackknife classification matrix is also shown in Table 21. Due to the number of cases in the analysis it was not appropriate to use more than three features.

The second approach to discriminate non-comedo DCIS1 and DCIS2 cases was with the use of the discriminant function formed on a cell by cell

Table 21. PURE DCIS VS. DCIS WITH ADJACENT INVASIVE CARCINOMA: NON-COMEDO TYPE.

<b>A</b>	<b>CLASSIFIED GROUPS</b>		
<b>ACTUAL GROUPS</b>	<b>DCIS1</b>	<b>DCIS2</b>	<b>TOTAL</b>
<b>DCIS1</b>	<b>28 (87%)</b>	<b>4 (13%)</b>	<b>32</b>
<b>DCIS2</b>	<b>8 (18%)</b>	<b>21 (72%)</b>	<b>29</b>

<b>B</b>	<b>CLASSIFIED GROUPS</b>		
<b>ACTUAL GROUPS</b>	<b>DCIS1</b>	<b>DCIS2</b>	<b>TOTAL</b>
<b>DCIS1</b>	<b>27 (84%)</b>	<b>5 (16%)</b>	<b>32</b>
<b>DCIS2</b>	<b>9 (31%)</b>	<b>20 (69%)</b>	<b>29</b>

Classification matrix (A) and jackknifed classification matrix (B) were obtained by the slide by slide discriminant function analysis. The analysis was performed with the use of the following three features: IOD, VNM and ELONGATION. These three features were chosen in the stepwise procedure from the set of four features which were forced to enter the analysis. Overall classification is correct in 80% (49/61) of cases. Classification obtained by the jackknife procedure is correct in 77% (47/61) of cases.

basis, followed by the classification of slides with a threshold for the proportion of DCIS1 or DCIS2 nuclei in each case. Due to the variations in the number of nuclei per case in both groups, 100 nuclei were randomly selected from each feature file to enter the analysis. In that way, every DCIS case could participate with a similar number of nuclei.

The stepwise procedure was applied on two groups of nuclei to separate non-comedo DCIS1 (3006 nuclei) and non-comedo DCIS2 (2668 nuclei). The combination of features, which was most efficient at distinguishing two groups, was selected. The relationship between number of features used and the percentage of correctly classified nuclei is shown in Figure 40. The following features were selected by a stepwise procedure: AREA, VAR INT, TARM, TERL, TERH, ADM, MHAER, C-MASS, C-MASSL, OD MAX, VAR OD, ELONGATION, ENERGY, and CONTRAST. The classification of nuclei with the discriminant function on a cell by cell basis was correct in 68% of the cases (Table 22).

Discriminant function coefficients were then applied on the original (not truncated) feature files of slides to classify single nuclei. The proportion of cells with features characteristic of DCIS2 was typically higher on the slides of DCIS2 group, than on the slides of the DCIS1 group. A threshold, which most efficiently distinguished the slides, was selected for the proportion of nuclei recognized as DCIS1 or DCIS2. Slides were then classified on the basis of this threshold. A threshold of 37% best separated DCIS1 and DCIS2 cases: Most DCIS1 cases had less than 37% of nuclei recognized as DCIS2 nuclei, and majority of DCIS2

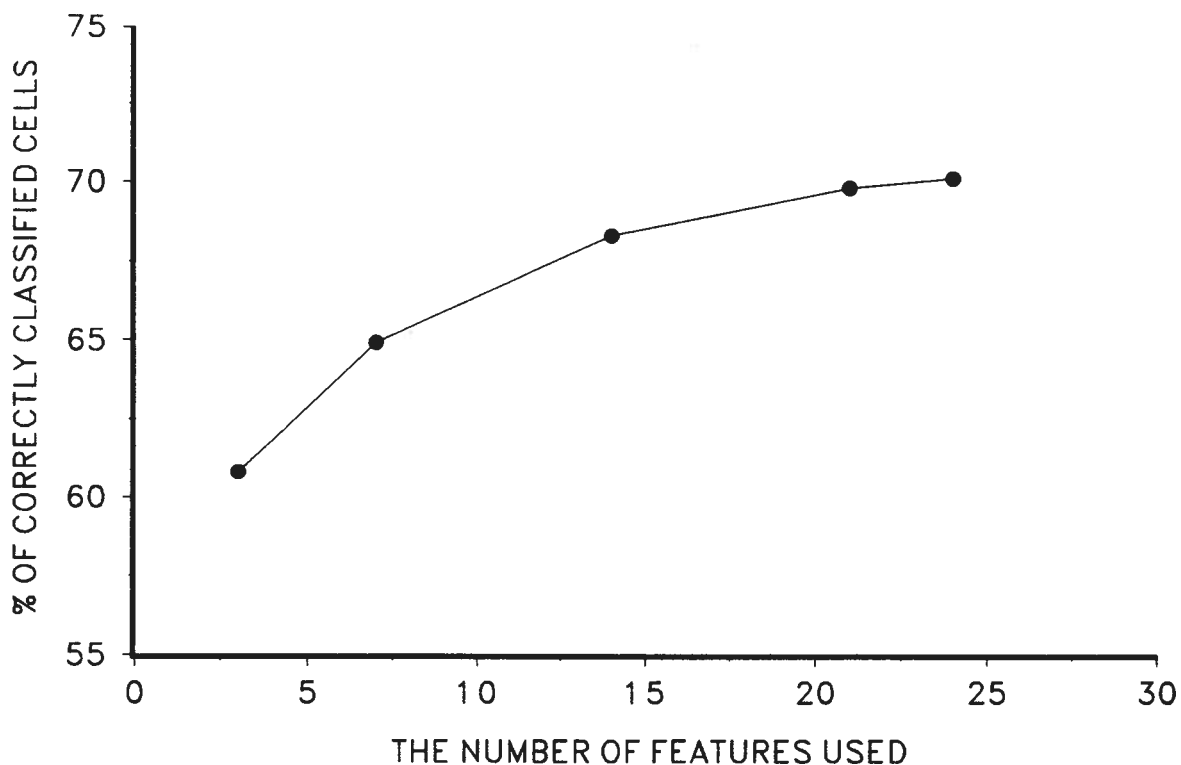


Figure 40. NON-COMEDO DCIS1 VERSUS NON-COMEDO DCIS2 NUCLEI: THE  
RELATIONSHIP BETWEEN THE NUMBER OF THE EMPLOYED FEATURES AND  
THE RATE OF CORRECT CLASSIFICATION.

The discriminant function was performed on the cell by cell basis. A combination of 14 features was selected: AREA, VAR INT, TARM, TERL, TERH, ADM, MHAER, C-MASS, C-MASSL, OD MAX, VAR OD, ELONGATION, ENERGY, and CONTRAST. The use of additional features did not significantly improve the discrimination.

Table 22. JACKKNIFED CLASSIFICATION OF NON-COMEDO DCIS1 AND NON-COMEDO DCIS2 NUCLEI.

	CLASSIFIED GROUPS		
ACTUAL GROUPS	DCIS1	DCIS2	TOTAL
DCIS1	2031 (68%)	975 (32%)	3006
DCIS2	824 (31%)	1844 (69%)	2668

Overall classification is correct in 68% (3875/5674) of nuclei.

**Table 23. DISCRIMINATION OF NON-COMEDO DCIS1 CASES AND NON-COMEDO DCIS2 CASES BASED ON THE PROPORTION OF DCIS NUCLEI ON THE SLIDES.**

ACTUAL GROUPS	CLASSIFIED GROUPS		TOTAL
	DCIS1	DCIS2	
DCIS1	21 (68%)	10 (32%)	31
DCIS2	4 (14%)	25 (86%)	29

The threshold of 37% DCIS2 nuclei was the best in distinguishing DCIS1 and DCIS2 slides. DCIS2 slides contained more than 37% of DCIS2 nuclei and DCIS1 slides contained less than 37% of DCIS2 nuclei. Overall classification is correct in 77% (46/60) of cases.

cases had more than 37% nuclei classified as DCIS2 nuclei (Figure 41). With this threshold 77% of cases (slides) were correctly classified (Table 23).

#### 4.6.B Comedo type

Comedo DCIS without associated invasive carcinoma (DCIS1) and comedo DCIS with associated invasive carcinoma in the surrounding breast (DCIS2) were analyzed. The purpose of statistical analysis was: i) to demonstrate the differences in nuclear features between comedo DCIS1 and DCIS2, and ii) to obtain a classification system on the basis of quantitative features. Examples of comedo DCIS1 and DCIS2 nuclei are shown in Figure 42.

Feature means and variances were tested by T-tests and non-parametric tests to find the differences between two groups. The differences were accepted as significant if the p value of the test was less than 0.05. Some of the features with significant differences between the two groups as shown by their p-value of non-parametric tests ( $p < 0.05$ ) are listed in Table 24.

The features listed in the Table 24 indicate that the maximum density spots are darker (1) in comedo nuclei when there is an associated invasive carcinoma in the surrounding breast tissue (DCIS2 nuclei). The samples of comedo DCIS2 have increased inter-nuclear variation of the DNA content (2). DCIS2 samples also have a larger inter-nuclear variation of various texture features, for example relative nuclear area occupied by medium density chromatin (3), relative density of medium density chromatin (4), and maximal optical density (5). The number of cases (6 vs. 15) that were analyzed was too small to run the discriminant function analysis on the slide by slide basis.

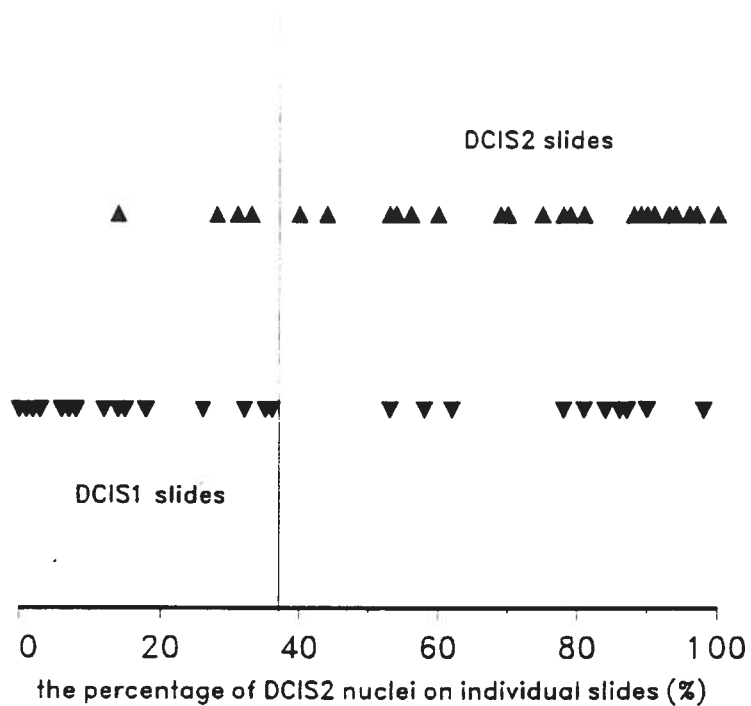
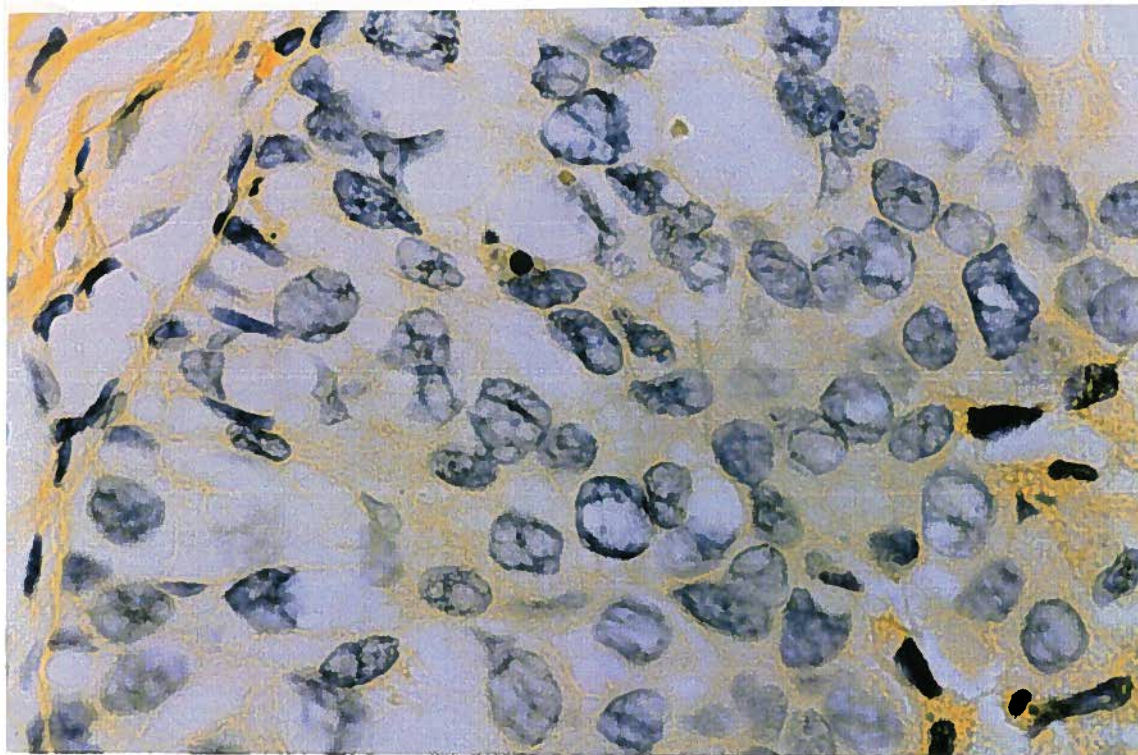
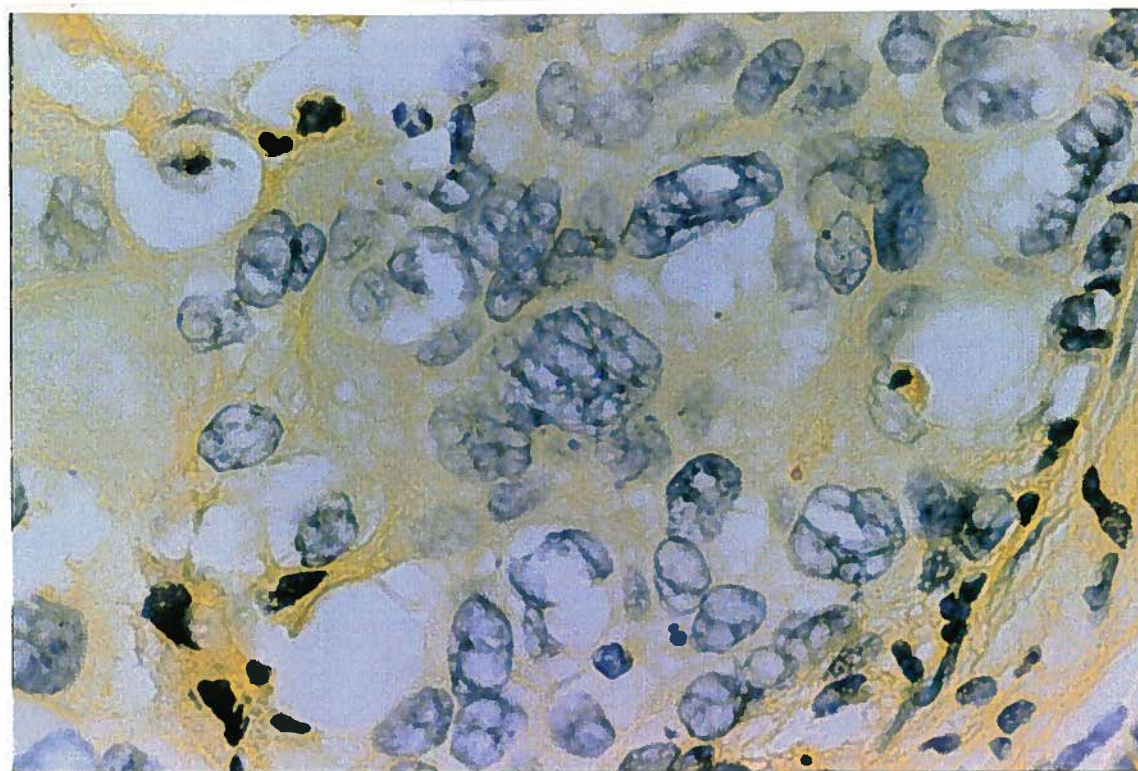


Figure 41. CLASSIFICATION OF DCIS1 (A) AND DCIS2 (B) CASES: NONCOMEDO TYPE.

A classification of cases (patients) was based on the proportion of DCIS2 nuclei on individual slides. A threshold of 37% was chosen because it separated correctly the highest number of cases.



A



B

Figure 42. EXAMPLES OF DCIS1 (A) AND DCIS2 (B) NUCLEI: COMEDO TYPE.

Thionin-SO<sub>2</sub> stain, Orange-G counterstain. Magnification on the print is approximately 172:1.

**Table 24. SIGNIFICANT DIFFERENCES IN NUCLEAR FEATURES BETWEEN COMEDO DCIS WITHOUT INVASION (DCIS1), AND COMEDO DCIS WITH ADJACENT INVASIVE CARCINOMA IN THE SURROUNDING BREAST (DCIS2).**

	<b>C-DCIS1</b>	<b>C-DCIS2</b>	
<b>FEATURE</b>	<b>mean (<math>\sigma</math>)</b>	<b>mean (<math>\sigma</math>)</b>	<b>p</b>
<b>1.OD MAX</b>	<b>0.22 (0.05)</b>	<b>0.29 (0.08)</b>	<b>0.029</b>
<b>2.V IOD</b>	<b>0.40 (0.14)</b>	<b>0.62 (0.25)</b>	<b>0.036</b>
<b>3.V TARM</b>	<b>0.09 (0.02)</b>	<b>0.13 (0.03)</b>	<b>0.029</b>
<b>4.V TERM</b>	<b>0.10 (0.02)</b>	<b>0.14 (0.04)</b>	<b>0.013</b>
<b>5.V ODMAX</b>	<b>0.048 (0.014)</b>	<b>0.065 (0.014)</b>	<b>0.024</b>
<b>6.V OD SKEW</b>	<b>0.30 (0.02)</b>	<b>0.49 (0.16)</b>	<b>0.008</b>
<b>7.V SHADE</b>	<b>0.29 (0.03)</b>	<b>0.43 (0.11)</b>	<b>0.004</b>

Features are explained in the Methods Section (3.4). Significance of the tests was defined by the p-value of the nonparametric test ( $p < 0.05$ ).

However, the analysis on the a cell by cell basis was performed to distinguish DCIS1 (693 nuclei) and DCIS2 (2133 nuclei). The relationship between the number of the employed features and the rate of correct classification is shown in Figure 43. The combination of features selected by the stepwise procedure included: VAR RAD, TARL, NL, OD MAX, VAR OD, and FRACTAL AREA 1. With the discriminant function on a cell by cell basis a correct classification of DCIS1 and DCIS2 nuclei was achieved in 82% (Table 25).

The classification of the slides with a threshold was performed in the same manner, as was described in the previous section for the analysis of non-comedo cases. The threshold of 50% was chosen for the proportion of DCIS1 and DCIS2 nuclei on the slides (Figure 44). With this threshold, all DCIS1 and DCIS2 cases of comedo type were correctly classified (Table 26).

#### 4.7 MALIGNANCY ASSOCIATED CHANGES (MAC)

Table 4 shows the number of cases and nuclei involved in this analysis. The aim of the statistical analysis was to distinguish benign breast tissues and tissues of patients with breast malignancy on the basis of measurements of nuclei from normal appearing lobules. Examples of normal nuclei from benign cases and normal nuclei from invasive carcinoma cases are shown in Figure 45. First, the discriminant function analysis was applied on normal nuclei from benign cases (normal) and on normal nuclei from invasive carcinoma cases ("MAC"). The combination of features selected by the stepwise procedure consisted of following features: TARL, TERM, ADH, MAER, OD MAX, OD SKEWNESS, HOMOGENEITY, and FRACTAL AREA 2. The relationship

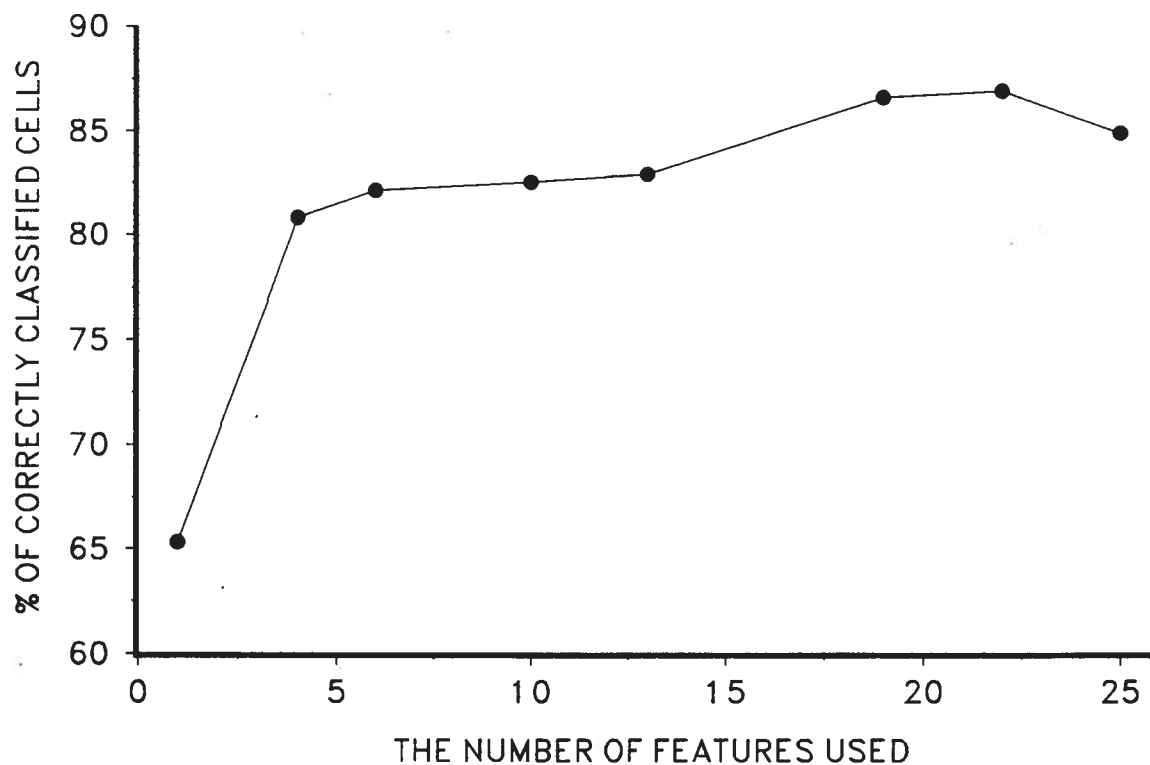


**Figure 43. COMEDO DCIS1 VERSUS COMEDO DCIS2 NUCLEI: THE RELATIONSHIP BETWEEN THE NUMBER OF THE EMPLOYED FEATURES AND THE RATE OF CORRECT CLASSIFICATION.**

The discriminant function was performed on the cell by cell basis. The combination of 6 features was selected: VAR RAD, TARL, NL, OD MAX, VAR OD, and FRACTAL AREA 1. The use of additional features did not significantly improve the discrimination.

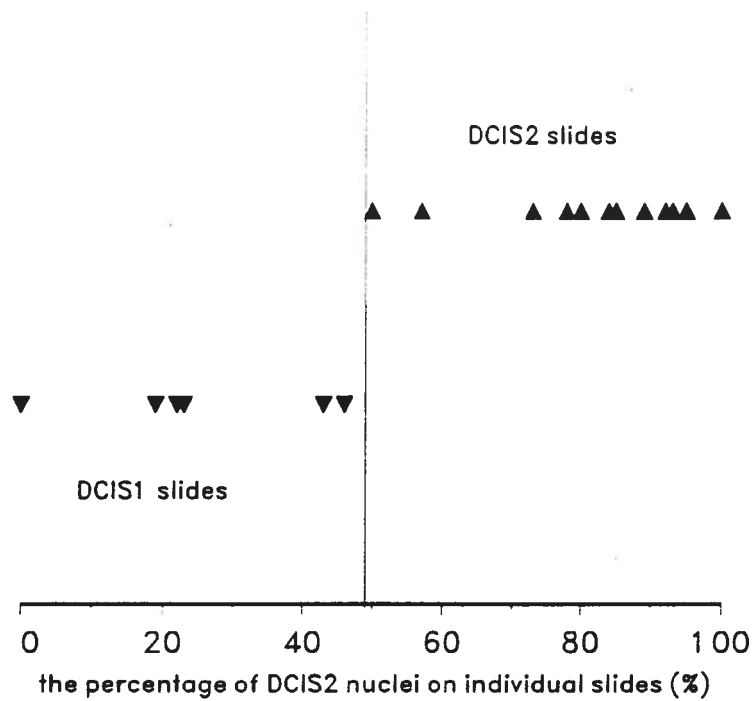


Figure 44. CLASSIFICATION OF DCIS1 (A) AND DCIS2 (B) CASES: COMEDO TYPE.

A classification of cases (patients) was based on the proportion of DCIS2 nuclei on individual slides. A threshold of 50% was chosen because it separated correctly the highest number of cases.

Table 25. JACKKNIFED CLASSIFICATION OF COMEDO DCIS1 AND COMEDO DCIS2 NUCLEI.

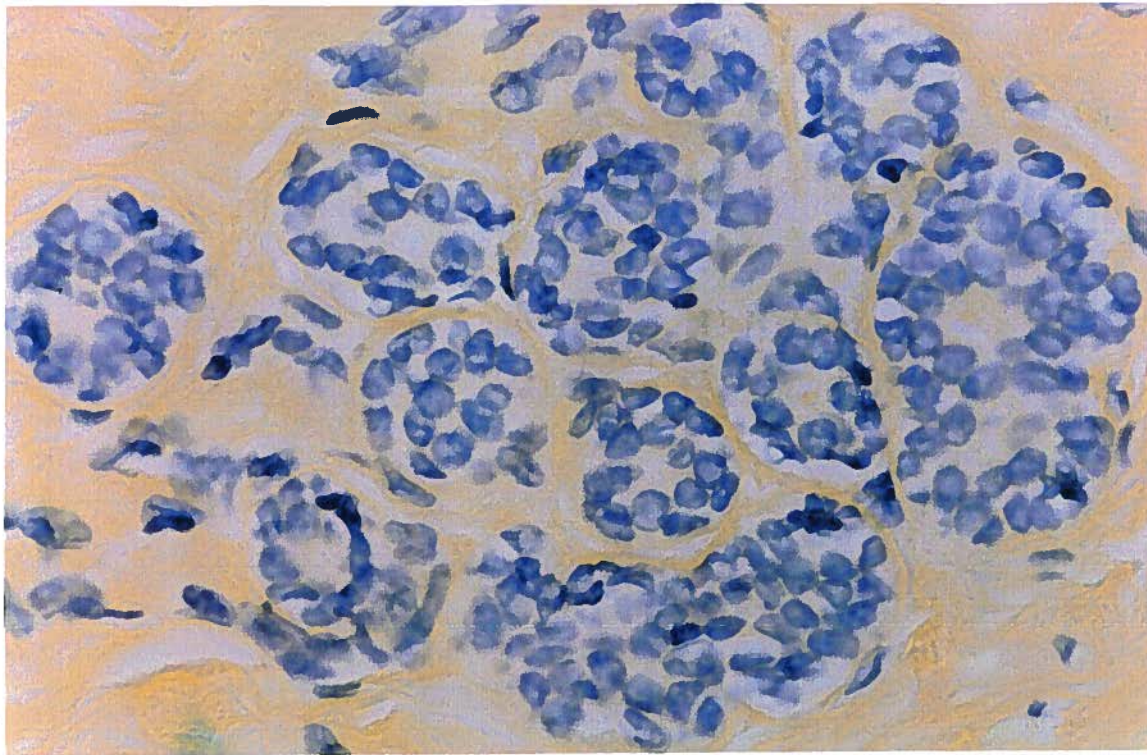
	CLASSIFIED GROUPS		
ACTUAL GROUPS	DCIS1	DCIS2	TOTAL
DCIS1	551 (80%)	142 (20%)	693
DCIS2	363 (17%)	1770 (83%)	2133

Overall classification is correct in 82% (2321/2826) of nuclei.

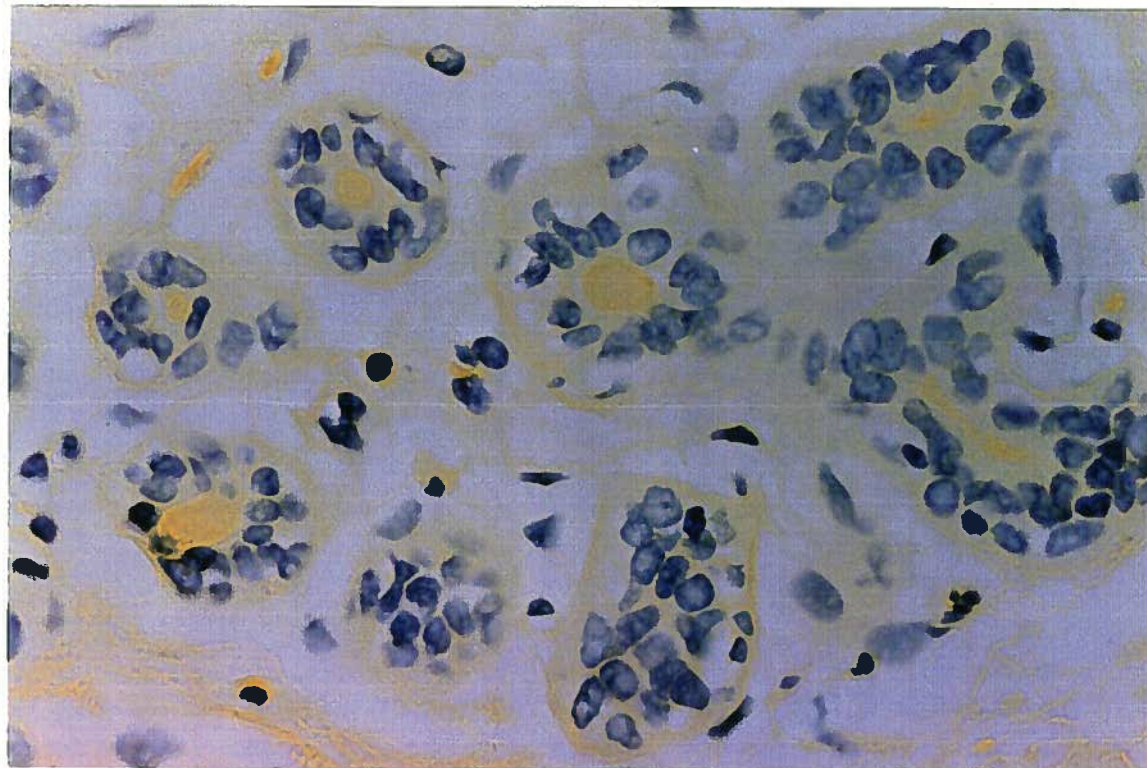
**Table 26. DISCRIMINATION OF COMEDO DCIS1 CASES AND COMEDO DCIS2 CASES WITH THE THRESHOLD FOR THE PROPORTION OF DCIS2 NUCLEI ON SLIDES.**

	CLASSIFIED GROUPS		
ACTUAL GROUPS	DCIS1	DCIS2	TOTAL
DCIS1	6 (100%)	0	6
DCIS2	0	21 (100%)	21

The threshold for the proportion of DCIS2 nuclei on the slides was 50%. Overall classification is correct in 100% (36) of cases.



A



B

Figure 45. EXAMPLES OF NORMAL NUCLEI FROM BENIGN CASES (A) AND NORMAL NUCLEI FROM INVASIVE CARCINOMA CASES (B).

Thionin-SO<sub>2</sub> stain, Orange-G counterstain. Magnification on the print is approximately 172:1.

between the number of the features used in the discriminant function and the rate of correct classification is shown in Figure 46. The classification of nuclei with the discriminant function was correct in 76% of cases (Table 27).

The above discriminant function was applied on the nuclei of individual cases to recognize the proportion of "MAC" nuclei on each slide. Most carcinoma cases had higher frequency of "MAC" nuclei than benign cases. The threshold of 34% "MAC" nuclei was selected. Cases with more than 34% of "MAC" nuclei were classified as carcinoma cases and cases with less than 34% of "MAC" nuclei were classified as benign. With this threshold 91% of carcinoma cases and 80% of benign cases were correctly classified (Table 28). Overall, the classification of slides was correct in 86% (37/43). This discriminant function was tested on normal nuclei collected from the cases with carcinoma *in situ*. The proportion of "MAC" nuclei was higher than 34% in seven of the eleven cases.

The second aim was to distinguish normal nuclei from the same 20 benign cases and normal nuclei from 34 malignant cases. Eleven DCIS cases (577 normal nuclei) were added to previously described invasive carcinoma cases. Following features were selected by the stepwise procedure: AREA, TARL, TARH, MAER, OD MAX, VAR OD, and OD SKEWNESS. The results of this approach are shown in Table 29. As described before, the discriminant function was applied on the nuclei of individual cases, and the threshold was selected, which most efficiently separated benign and malignant cases (Figure 47). With 34% of "MAC" nuclei as a threshold, 82% malignant and 80% of benign cases were correctly recognized (Table 30). Overall, the classification obtained with the discriminant function was accurate in 81% of cases (44/54).

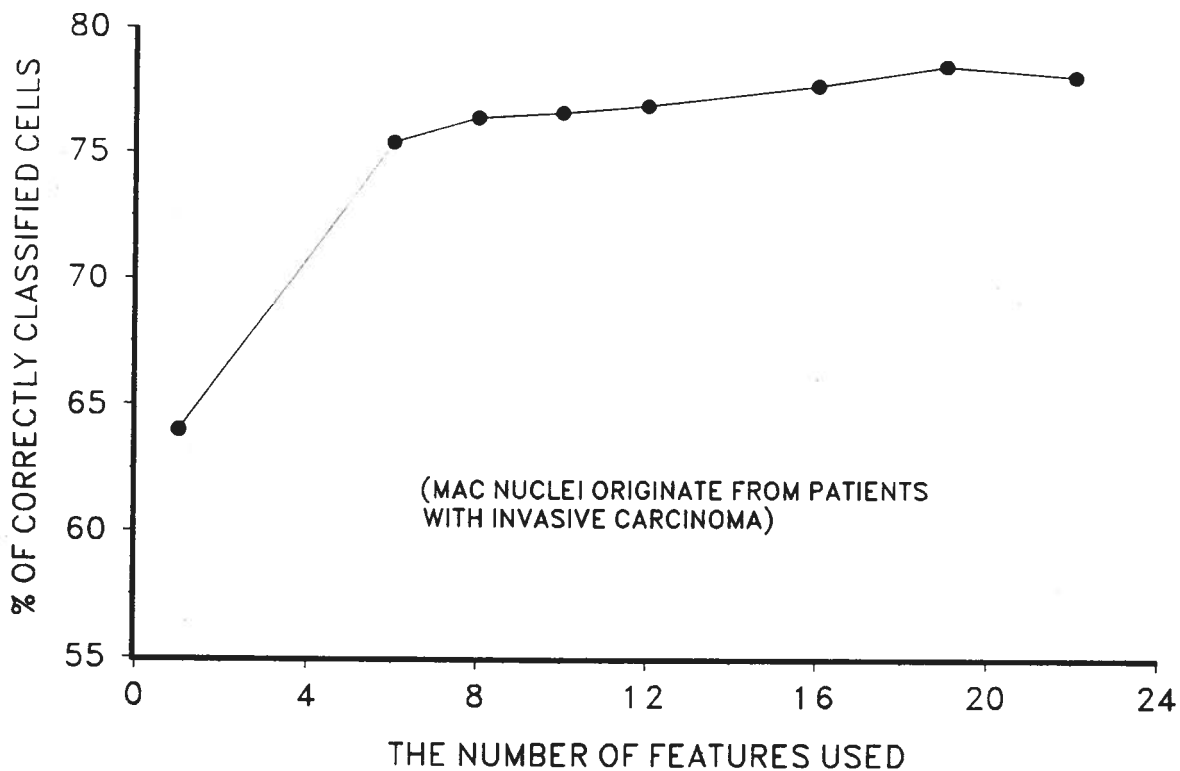


Figure 46. NORMAL VERSUS "MAC" NUCLEI: THE RELATIONSHIP BETWEEN THE NUMBER OF THE EMPLOYED FEATURES AND THE RATE OF CORRECT CLASSIFICATION.

The discriminant function was performed on the cell by cell basis. The combination of 8 features was selected: TARL, TERM, ADH, MAER, OD MAX, OD SKEWNESS, HOMOGENEITY, and FRACTAL AREA 2. The use of additional features did not significantly improve the discrimination.

Table 27. JACKKNIFED CLASSIFICATION OF NUCLEI TO NORMAL NUCLEI AND  
"MAC" NUCLEI (A).

	CLASSIFIED GROUPS		
ACTUAL GROUPS	NORMAL	MAC	TOTAL
NORMAL	1532 (79%)	399 (13%)	1931
MAC	338 (18%)	850 (72%)	1188

Images of the nuclei were collected from normal appearing lobules of benign cases (the first group) and from normal appearing lobules of invasive carcinoma cases (the second group, "MAC"). Overall classification based on nuclear features is correct in 76% (2382/3119) of nuclei.

**Table 28. CLASSIFICATION OF BENIGN CASES AND INVASIVE CARCINOMA CASES  
ACCORDING TO THE PROPORTION OF "MAC" NUCLEI.**

	CLASSIFIED GROUPS		
ACTUAL GROUPS	BENIGN	MALIGNANT	TOTAL
BENIGN	16 (80%)	4 (20%)	20
MALIGNANT	2 (9%)	21 (91%)	23

Threshold of 34% MAC nuclei on the slide is used to distinguish benign and malignant cases. Majority of malignant cases have more than one third of nuclei characteristic of MAC. Majority of benign cases have less than of nuclei typical of MAC. Classification is correct in 86% (37/43) of cases.

**Table 29. JACKKNIFED CLASSIFICATION OF NUCLEI TO NORMAL NUCLEI AND "MAC" POSITIVE NUCLEI (B).**

	CLASSIFIED GROUPS		
ACTUAL GROUPS	NORMAL	MAC	TOTAL
NORMAL	1538 (80%)	393 (20%)	1931
MAC	551 (31%)	1214 (69%)	1765

Images of the nuclei were collected from normal appearing lobules of benign cases (one group) and from normal appearing lobules of malignant cases (second group). In the second group DCIS cases are included in addition to invasive carcinoma cases. Overall classification based on nuclear features is correct in 74% (2752/3696) of nuclei.

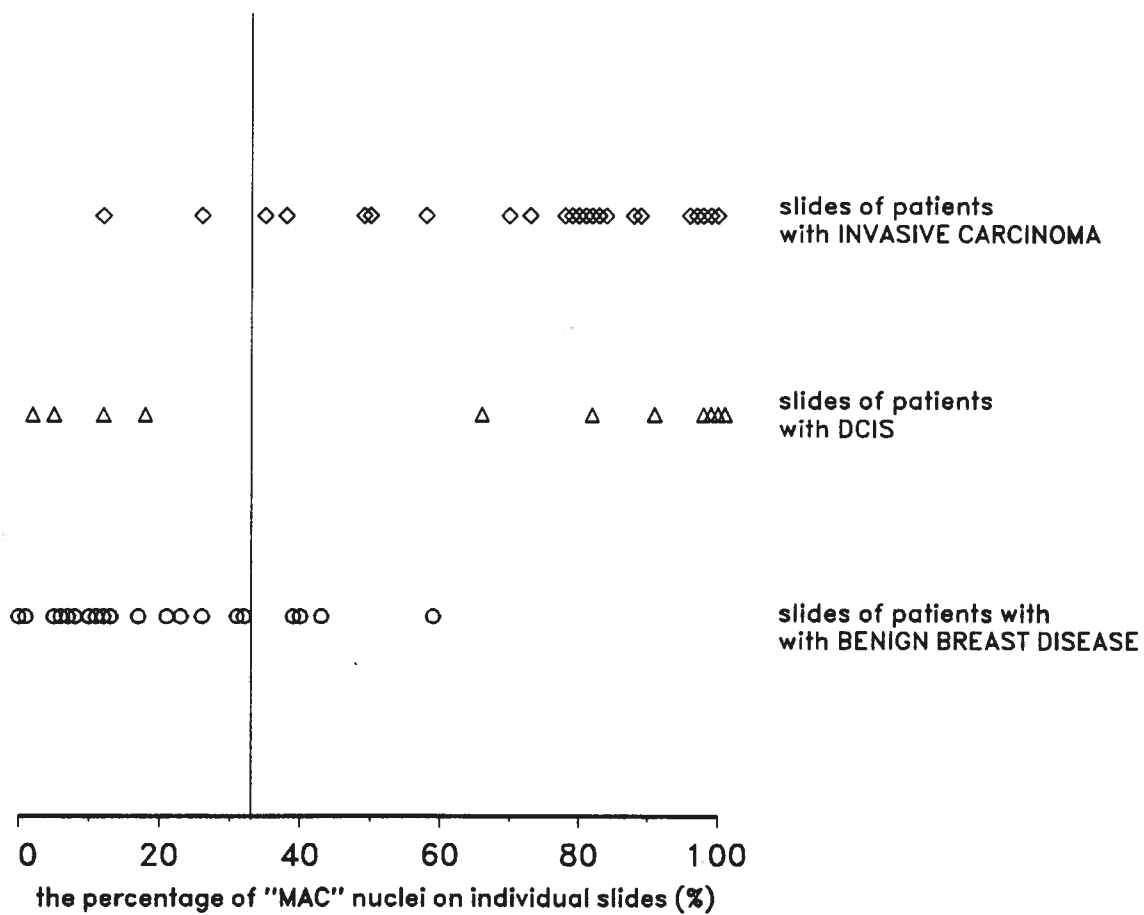


Figure 47. CLASSIFICATION OF MALIGNANT AND BENIGN CASES.

The classification was based on the proportion of MAC nuclei on individual slides.

Table 30. CLASSIFICATION OF BENIGN AND MALIGNANT (*IN SITU* AND INVASIVE CARCINOMA) CASES ACCORDING TO THE PROPORTION OF "MAC" NUCLEI.

ACTUAL GROUPS	CLASSIFIED GROUPS		TOTAL
	BENIGN	MALIGNANT	
BENIGN	16 (80%)	4 (20%)	20
DCIS	4 (36%)	7 (63%)	11
INVASIVE CANCER	2 (9%)	21 (91%)	23

Carcinoma *in situ* is included in this analysis. Threshold of 34% is used to distinguish benign and malignant cases. Majority of malignant cases have more than one third of nuclei characteristic of MAC. Majority of benign cases have less than of nuclei typical of MAC. The proportion of "MAC" nuclei is higher in invasive carcinoma than in carcinoma *in situ*. Classification is correct in 81% (44/54) of cases.

## 5. DISCUSSION

The following studies were performed in this thesis: i) DNA measurements on tissue sections were evaluated in comparison with other cytometry techniques, ii) the relationship between quantitative nuclear features and histopathological classification was examined, iii) different histological DCIS types were characterized on the basis of nuclear features, iv) differences in nuclear morphology between pure ductal carcinoma *in situ* (DCIS1) and ductal carcinoma *in situ* with synchronous invasive carcinoma (DCIS2) were defined, and v) changes of nuclear morphology of epithelial cells from normal appearing tissue adjacent to invasive carcinoma (MAC) were analyzed.

### 5.1 COMPARISON OF DIFFERENT CYTOMETRY TECHNIQUES

Tissue sections are important for morphometric studies such as the analysis of architectural pattern of tissues, as well as nuclear morphology and chromatin texture describing the DNA distribution in the nuclei. Tissue sections are generally not recommended to be used for the DNA ploidy measurements due to possible errors based on the sectioned and overlapped nuclei. However, image cytometry (IC) on tissue sections has an advantage of preserved architecture and selective sampling of nuclei. This is particularly important for the analysis of specimens with small areas of diseased tissue or with a variety of histological patterns present in the same region, such as premalignant changes or *in situ* tumors. With IC measurements on breast tissue sections it is possible to analyze a single small duct filled with malignant cells, which is very useful in

the analysis of small, early tumors. The preserved architecture in sections also allows precise selection of the nuclei of interest where a variety of tissue patterns are present in the same region. This is very important for the analysis of small malignant or premalignant breast lesions which can not be performed by FC. These were the reasons for choosing the measurements on sections as the most appropriate for this study.

One of the aims in this thesis was to evaluate the reliability of tissue section measurements in detecting an aneuploid cell population. For that purpose we compared the DNA content measurements of IC performed on tissue sections to the DNA content obtained with other cytometry techniques. First IC of tissue sections and FC were compared on 51 tissue blocks with invasive carcinoma. Secondly, IC measurements performed on tissue sections were compared to measurements of corresponding smears and cytopins in seven cases of invasive breast carcinoma.

Archival breast specimens were used in the study. There are several disadvantages of DNA ploidy analysis of deparaffinized tissues. It has been demonstrated that formalin fixation alters the staining pattern of nuclei for intercalating dyes or for dyes using the Feulgen procedure (Becker 1990). The same study showed the influence of the various chromatin states on the fluorescence intensity obtained by the Propidium iodide staining of formaldehyde fixed cells. Such variations of staining may be the cause of bimodal or pseudoaneuploid peaks. It has also been found that the disaggregation procedure produces a high staining variability (Schimmelpenning 1990). The embedded tissue measurements show larger coefficients of variation of the peaks than the measurements performed on fresh tissue. Another consequence

of the staining variability is that external standards can not be applied, so that in FC and in IC measurements, the peak of internal diploid cells (tumor, stromal, inflammatory, normal parenchymal) should be used as the diploid reference value. IC measurements on tissue sections have a unique advantage of preserved architecture which allows more specific diagnosis of different cell types and the use of visualized internal control cells.

IC of tissue sections in this study showed a relatively narrow DNA distribution in the diploid cases. There were no problems with the interpretation of diploid histograms. However, in some of the aneuploid cases the IOD distribution obtained with IC of tissue sections was indeed very wide, and the peak was difficult to select. In part, this was caused by increased irregularity of shape and size in aneuploid nuclei. As a consequence a higher proportion of incomplete or overlapped nuclei was included in the measurements. Also, the wide distribution in some IC histograms characteristically accompanied aneuploid peaks and was probably a reflection of tumor heterogeneity.

#### 5.1.A Flow cytometry and image cytometry of tissue sections

IC agreed with FC in ploidy in nearly 80% of cases. IC results corresponded strongly to FC aneuploid cases (nearly 90%). However, almost one half of FC diploid cases were found to be aneuploid by IC.

FC alone detected aneuploid DNA content in five tumors. Three of these cases had a diploid IC histogram and a FC histogram with DI values just slightly above the artificially set limit of 1.1. They were therefore classified as aneuploid by FC. Near-diploid cases of histograms derived from paraffin embedded tissue

have been questioned previously (Joensuu 1990, Fernö 1992, Fosså 1992). The other possibility is that IC has failed to detect these peridiploid peaks. In the remaining cases with the discordant ploidy outcome, clear differences in DI were evident. IC evidently failed to detect aneuploidy in two and FC in six cases. These results suggested that no method was superior in detecting the aneuploidy. However, IC seemed to be more efficient if FC peridiploid cases were not considered. Because all the cells were representative in the IC histograms this method possibly had a better chance to detect an abnormality.

DI of cases where both methods agreed on ploidy showed a poor correlation. The disagreements could be explained by the heterogeneity of tumors and differences in sampling, cut and overlapped nuclei in IC on tissue sections, differential staining of disaggregated nuclei for FC, and subjective interpretation of the histograms.

The cases with additional DCIS are examples of complex situations which are often present in breast cancer specimens. It is known that an extensive DCIS in the specimen with invasive ductal cancer is associated with a high risk of residual intraductal tumor in the remaining breast tissue. Moreover, extensive DCIS predicts the recurrence of infiltrating ductal cancer after breast-conserving therapy (Holland 1990). This suggests that the ploidy of DCIS in invasive breast cancer specimens might have a prognostic value. Unfortunately in DNA cytometric studies these situations usually do not receive much attention and the prognostic implications of DNA content of DCIS in invasive cancer specimens are not yet established. Measurements on tissue sections could be useful for such studies.

Overall, the results of this study show that, contrary to the present belief, IC performance on tissue sections is not inferior to FC in DNA ploidy measurements on archival breast cancer tissue. IC can not determine the DI value as accurately as FC, but on the other hand it appears to be more capable of detecting aneuploidy. Also, with the measurements on tissue sections it is possible to analyze affected tissue confined to a very small area and to select specific nuclei of interest when a variety of disease patterns are present in the same region. In addition, IC can provide more extensive information on nuclear morphology and structure. Nuclear grade seems to be one of the most reliable predictors of the outcome in node-negative breast cancer. With image cytometry measurements it is possible to determine nuclear grade in an objective way with the use of a variety of nuclear features which reflect the distribution of the chromatin and the nuclear shape and size as well as the DNA amount (Larsimont 1989). Therefore, IC of tissue sections appears to be a suitable complementary method to FC in studying the prognosis of breast cancer.

#### 5.1.B Comparison of different image cytometry techniques

In seven cases of invasive breast carcinoma three IC techniques were used to measure the nuclear DNA content. Archival smears of fine needle aspirate and corresponding tissue blocks from subsequent biopsies were available for each patient. Tissue sections and cytopspins with disaggregated nuclei were prepared from tissue blocks. IC measurements were then performed in an automated way on smears and cytopspins, and manually on tissue sections.

All three techniques detected an aneuploid peak in 3 cases. The cytopsin measurement failed to show an aneuploid peak in one case. The smear also failed in another case. The measurements on tissue sections disagreed with the other two methods in one case, where an additional peak was detected. Reasons for the failure to detect an aneuploid peak could be in tumor heterogeneity and differences in sampling. IC of tissue sections actually performed the best in the detection of aneuploidy as it did not miss any of the aneuploid cases. Moreover, in the case where tissue section measurement disagreed with the other two techniques by detecting an aneuploid peak, this peak might have been the result of the selective sampling of a small population of aneuploid cells which were diluted by other cells in the smear and cytopsin.

The DNA histogram parameters were determined for all 21 histograms. Agreement between three techniques on the position of the aneuploid peaks occurred only in two cases. The discrepancies in the DNA index in other cases may be the consequence of tumor heterogeneity. Other possible reasons for the discrepancies are: i) the damage to nuclei caused by the disaggregation procedure for cytopsin, ii) a differential staining due to the different fixation of smears, or iii) a wide distribution of values in the histograms of tissue sections due to cut and overlapped nuclei. The exceeding rates and entropies of the histograms differed completely for different techniques because of the different sampling procedures involved. Generally, values were the highest in histograms of tissue sections where only carcinoma cells were analyzed.

It is clear that the measurements on tissue sections have many disadvantages, such as the relatively small number of cells that can be analyzed in an acceptable time period (2-3 hours per sample for 200 diagnostic cells and

50 control cells), wide distribution of values in the DNA histograms, and low accuracy in the position of the peaks. However, the results of the present study showed that the IC measurements of tissue sections are at least as valuable in the detection of aneuploidy as the automated measurements performed on smears or cytospins.

## 5.2 THE CORRELATION BETWEEN QUANTITATIVE NUCLEAR FEATURES AND ADVANCING MORPHOLOGICAL CHANGES

In the search for new important prognostic characteristics it is important to develop an objective and reproducible analysis of breast premalignant changes and carcinoma *in situ*. One approach to developing an objective classification is the use of IC measurements of nuclear features. IC features express morphologic nuclear characteristics in a quantitative way.

The use of various nuclear features for diagnostic or prognostic purposes may offer superior results compared to the DNA content alone. The value of using multiple nuclear features (ploidy, texture and morphometric features) in the grading of invasive breast carcinoma has been recognized in many studies (Stenkvist 1978, Baak 1985, Umbricht 1989, Larsimont 1989, Dawson 1991, Komitowski 1990, Theissig 1991). Quantitative nuclear features reflect the morphological changes which are visualized by the pathologist for the purpose of grading the nuclear atypia, but have the advantage of being more sensitive, more objective and more reproducible.

It is thought that in the process of malignant transformation the breast tissue undergoes a sequence of multiple genetic alterations. It has been

postulated that these molecular events are associated with morphological alterations. One of the aims of this study was to investigate the relationship between quantitative nuclear features and morphological changes of breast tissue which are used by pathologists for diagnostic purposes.

Various breast diseases were analyzed by IC measurements being performed on tissue sections. The analyzed cases were then grouped to six major groups: Normal tissue, non-proliferative disease, proliferative disease, non-comedo DCIS, comedo DCIS and invasive carcinoma. Differences in quantitative nuclear features relating to size, shape, nuclear DNA content and texture were demonstrated between major groups of breast diseases. The differences indicated that it may be possible to use quantitative features for diagnostic purposes as an adjunct to the visual analysis of tissue morphology. However, this must be further studied on narrower categories of breast diseases. Also, for the purpose of the classification of breast diseases on the basis of nuclear features the inter-observer disagreements in diagnosis should be taken into account.

The present study showed that changes in nuclear features correlated with the increasing histopathological abnormality. These results were in agreement with other studies where a similar increase in the irregularity of nuclear features was found on tissues other than breast (Bibbo 1989, Petein 1991, Mulder 1992, Salmon 1992). Similar observations were made in a morphometric study of Pienta et al. (Pienta 1991). In their study, size and some shape parameters were measured on normal tissue, carcinoma *in situ*, lymph node negative, lymph node positive, and metastatic breast cancer. Nuclear area

and the intraslide variation of mean nuclear area increased with more severe histologic changes.

In the present study, non-proliferative disease, proliferative disease, DCIS, and invasive carcinoma showed increasing degrees of nuclear alterations compared to the normal tissue. Increasing abnormalities in the nuclear DNA content and chromatin distribution as well as in nuclear size and shape were demonstrated. The occasional findings of aneuploidy in lesions, such as simple hyperplasia, indicated substantial genetic changes and illustrated the premalignant nature of these diseases. Aneuploidy of non malignant tissue suggested higher progressive potential compared to similar tissues with diploid DNA content.

In addition to the increase in the mean values of the features, the intraslide and interslide variability showed a similar increase. The lowest interslide and intraslide variations of shape, size, texture, and DNA content, were found in the normal group. The variations became larger in non-proliferative and proliferative disease, showed further increase in non-comedo DCIS, and were the highest in the invasive carcinoma and comedo DCIS groups.

The deviation of quantitative nuclear features increased in parallel with the severity of the diagnosis and could be indicative of progression. The progressive alteration of nuclear features indicates, that nuclear characteristics of breast diseases, represented by a combination of quantitative, objectively analyzed features, could be important for the prognosis of benign breast disease, as well as DCIS.

### 5.3 HETEROGENEITY OF DUCTAL CARCINOMA *IN SITU*

It is known that DCIS is a heterogeneous group of tumors, with varying morphology and with different clinical presentation. Moreover, the progressive potential and natural history of DCIS cover a wide range of possibilities.

The association between aneuploidy of carcinoma *in situ* and its progression to invasive carcinoma was previously demonstrated on cervical tissue (Bibbo 1989). It has been suggested that aneuploidy may be associated with more aggressive nature of carcinoma *in situ* in the breast (DCIS). In the present study the ploidy pattern and DNA histogram parameters of various types of DCIS were analyzed. DNA histogram parameters included IOD, DNA index, 1.25 exceeding rate and 2.5 exceeding rate.

Aneuploidy was found in 67% of all DCIS cases. This was in agreement with previous studies (Crissman 1990, Schimmelpenning 1992, Fisher 1992, Pallis 1992). Differences were characterized in the incidence of aneuploidy between comedo and non-comedo types and also between different non-comedo types. The high values of histogram parameters and a high proportion of aneuploid cases in certain histological types could be linked to a more aggressive nature of these tumors.

An example is comedo DCIS. The aggressive nature of this DCIS type is well known. Comedo DCIS is a high grade lesion, which is more often associated with microinvasion, and has a high capacity to recur or to progress to invasive cancer (Lagios 1989, Patchefsky 1989, Schwartz 1992). On the contrary, the cribriform type is regarded as an entity with a relatively low progressive potential, which is often estrogen receptor positive, and has a low

proliferation rate, low incidence of microinvasion, low frequency of aneuploidy, and infrequent overexpression of c-erbB-2 oncogene (Meyer 1986, Patchefsky 1989, Locker 1990, Crissman 1990, Schimmelpenning 1992, Bur 1992).

In the present study comedo type showed the highest aneuploidy rate (95%), and the highest values of the DNA histogram parameters of all DCIS. Cribriform type had the lowest values of DNA histogram parameters, and the lowest proportion of aneuploid cases (36%). Other histological types were between cribriform and comedo type, with the aneuploidy frequencies of 60-67%. Also, confluent, mixed, and papillary types had intermediate values of histogram parameters. These results indicated that aneuploidy and high values of DNA histogram parameters were associated with certain types of DCIS which are believed to have higher progressive potential. Moreover, they suggested the importance of aneuploidy in the prognosis of individual DCIS cases.

One of the aims of the present study was to characterize the diversity of DCIS histological types on the basis of their quantitative nuclear features. Histological types of non-comedo DCIS are usually identified on the basis of their pattern of growth and differences in the architecture rather than on the basis of their nuclear morphology. In the present study differences in nuclear features between major histological types of DCIS were demonstrated. In addition to the nuclear DNA content, other nuclear characteristics, such as shape, size and chromatin texture, showed the same tendency when different histological types were compared. The cribriform type had feature values most similar to the features of normal tissue. Feature values showed an increase in the confluent and mixed types and were even higher in the papillary type of DCIS. Comedo DCIS had the largest nuclei, most irregular nuclear shape and

the distribution of chromatin which was least similar to the normal cells. The intraslide variation of nuclear size and of nuclear DNA content (represented by variances of area and IOD) increased in the same order.

These results were in agreement with the increase in aneuploidy rate and in DNA histogram parameters, as described. The repeated increase in the irregularity of nuclear size, shape, and chromatin texture was observed in the same order of histological types: i) cribriform, ii) mixed and confluent, iii) papillary, and iv) comedo. The results paralleled previously described differences in progressive potential related to the specific histological types of DCIS. The increased nuclear DNA content and the irregularity of nuclear morphology were both associated with more aggressive histological types of DCIS. Furthermore, these results indicated that quantitative analysis of nuclear size, shape and chromatin texture could have a prognostic value in individual DCIS cases.

#### 5.4 DIFFERENCES BETWEEN PURE CARCINOMA IN SITU AND CARCINOMA IN SITU ASSOCIATED WITH INVASIVE BREAST CARCINOMA IN THE SURROUNDING TISSUE

The differences in ploidy of DCIS without associated invasive cancer (DCIS1) and DCIS with invasive cancer in the surrounding breast (DCIS2) have been studied previously. Two different groups reported discordant results (Carpenter 1987B, Fisher 1992). This is an important subject related to the invasive potential of DCIS. If it were true that there is a higher proportion of aneuploid cases of DCIS associated with invasive breast carcinoma in the

adjacent tissue, this would favor the association of aneuploidy with a higher progressive potential of DCIS. Our results showed an overall increase in aneuploidy from 53% in DCIS1 to 62% in DCIS2 for the non-comedo type. All comedo cases except one were aneuploid regardless of the presence or absence of invasive carcinoma in the adjacent tissue.

The morphological differences between DCIS1 and DCIS2 nuclei have not been yet described in the literature. In the present study their existence was confirmed for the first time. We confirmed that nuclei of DCIS1 and nuclei of DCIS2 have differences in morphology, mostly in the chromatin distribution, which can be detected by quantitative analysis of nuclear features. Furthermore, we showed that DCIS1 and DCIS2 cases could be discriminated with a classification system based on quantitative nuclear features. This was shown both for comedo and non-comedo type of DCIS.

#### *Non-comedo type*

For non-comedo DCIS, the characteristic changes associated with the presence of invasive cancer in the neighboring tissue were: i) higher degree of roundness, and ii) changes in the chromatin texture. Another characteristic of non-comedo DCIS2 nuclei was an increased inter-nuclear variation of some texture features, which corresponds to the increased variability in the chromatin distribution in the sample. With the discriminant function analysis on slide by slide basis we obtained a classification system for non-comedo DCIS based solely on the nuclear features. The non-comedo DCIS cases with or without invasive cancer were correctly recognized in 80% of cases. Another approach to discriminate cases with and without associated invasive cancer was used where the discriminant function was formed on a cell by cell basis. The

discriminant function was then applied to the nuclei of each slide to determine the proportion of DCIS1 and DCIS2 nuclei on the individual slides. Finally the slides could be distinguished by setting a threshold for the proportion of nuclei on each slide which were recognized by the discriminant function as DCIS1 or DCIS2. The best separating threshold was 37%: Most DCIS1 slides contained less than 37% DCIS2 nuclei and most DCIS2 slides had more than 37% DCIS2 nuclei. The classification of cases with the use of this approach was correct in 77% of the sample cases. This represented a good agreement with the slide by slide based classification above.

#### Comedo type

The comparison of comedo DCIS1 and DCIS2 cases also showed differences in nuclear features. DCIS2 cases had higher maximal optical density values, increased variation of various texture features and increased variation in the nuclear DNA content. It is interesting that the increased variation of nuclear content was shown to be an important indicator of bad prognosis in invasive breast carcinoma (Stenkvist 1982). The discriminant function analysis was performed on a cell by cell basis and then comedo cases were classified on the basis of the frequency of DCIS1 or DCIS2 nuclei which were present on individual slides. The classification of comedo cases was successful in all cases (100%).

These results are not unexpected. The aggressive nature of comedo DCIS is well known. The aggressive nature of comedo DCIS is well known. This type of DCIS is most often aneuploid (Locker 1990, Schimmelpenning 1992, Killeen 1991, Pallis 1992). Compared to non-comedo DCIS, comedo type much more often exhibits an increased expression of c-erbB-2 oncogene, which has

been associated with a bad prognosis in invasive breast carcinoma (van de Vijver 1988, Bartkova 1990). Immunostaining of estrogen receptors is more often negative in comedo type than in other, better differentiated DCIS types (Bur 1992). The expression of mutant p53 protein, which has been associated with genetic instability and tumor progression, is also much more often present in comedo type than in non-comedo types (Poller 1993). Comedo tumors have a higher growth rate than other types of DCIS (Meyer 1986). The expression of nm23, a metastasis suppressor gene, is commonly negative in a proportion of cells in comedo DCIS while all cells show positive staining in other histological types of DCIS (Royds 1993). Microinvasion is very commonly found in association with comedo type DCIS (Patchefsky 1989) and is often multifocal. This is less frequently seen in the non-comedo types. It has been previously demonstrated that comedo DCIS has a higher capacity to recur or to progress to invasive cancer than other types of DCIS (Lagios 1989, Schwartz 1992). Altogether, comedo DCIS seem to be a uniform group of fast growing highly progressive tumors.

It is possible to speculate that non-comedo DCIS found in invasive specimens is more heterogeneous in its progressive potential than comedo DCIS. Some foci of non-comedo DCIS may have the tendency to progress to invasive carcinoma, while others may still be at much lower stages in the process of progression to invasive carcinoma. In such non-comedo cases the nuclear features related to the invasive potential may not be expressed uniformly throughout the tumor being present only in a proportion of the DCIS ducts.

In conclusion, the reason for the morphological differences between DCIS1 and DCIS2 nuclei is not clear. Specific changes in nuclear morphology

characteristic of DCIS associated with invasive carcinoma in the surrounding breast indicate that quantitative nuclear features may be predictive of the subsequent behavior of DCIS tumors. These findings are of interest in view of their clinical relevance and it is very important to confirm them in further studies on larger groups of patients.

## 5.5 MALIGNANCY ASSOCIATED CHANGES

One of the most important aims of this thesis was to demonstrate the existence of slight morphological changes in normal appearing breast tissue adjacent to breast carcinoma. These changes were previously described in other tissues as malignancy associated changes (MAC).

Only nuclei from normal appearing lobules were analyzed for two groups of cases. In one group the cases originated from malignant biopsies. In the second group the cases originated from benign biopsies with minimal proliferative changes. Normal nuclei from the two groups were then separated on the basis of their feature values to "true normal" nuclei and to "MAC" nuclei. The majority of the discriminating features selected by the stepwise procedure in the discriminant function analysis were texture features, such as nuclear area occupied with low density chromatin, the distance of high density chromatin from the center of the nucleus, maximum of nuclear optical density, fractal textures, homogeneity of chromatin distribution, and skewness of the optical density distribution.

With the classification system based on the proportion of "MAC" nuclei on each slide it was possible to discriminate between malignant and benign cases.

The proportion of "MAC" nuclei was usually more than a third of all nuclei on the slides originating from malignant biopsies. On the contrary, "MAC" nuclei rarely represented more than one third of all nuclei on the slides obtained from benign biopsies. With the use of this threshold 91% of malignant cases and 80% of benign cases could be correctly recognized. Overall, with the classification based on IC measurements of normal nuclei it was possible to accurately distinguish benign and malignant cases in 86%. The differences in nuclear features characteristic of MAC could be used as a marker suggestive of occult malignancy in the breast when only benign changes are found in the biopsy. However, the importance of this finding is not in the diagnosis of malignancy in the breast tissue because this is very simple in the majority of cases where carcinoma is present in the biopsy. Much more significant is the fact that the chromatin distribution of apparently normal tissues can provide this information.

Changes in morphology of normal nuclei collected from malignant biopsies may reflect the effect of the invasive cancer cells on the neighboring tissue. Another possible answer is that the differences in nuclear features represent a field effect of hypothetical carcinogens. The frequently found multicentricity of breast carcinoma supports the theory of field carcinogenesis in breast tissue (Anastassiades 1993, Ashikari 1977, Rosen 1980, Lagios 1982, Silverstein 1987, Patchefsky 1989). MAC are therefore suggestive of a higher risk of developing malignancy: A benign biopsy with a high frequency of "MAC" nuclei would be suspicious for a high progressive potential of benign changes.

It is also possible that MAC are associated with the recurrence after the local removal of carcinoma *in situ* or invasive carcinoma. This suggests that the analysis of normal tissue may be important in the management of patients with *in*

*situ* or invasive carcinoma of the breast. However, this is only a speculation which must be examined in further studies by the analysis of such cases.

## 6. SUMMARY

The aim of this study was to obtain prognostic information, based on the nuclear morphology and nuclear DNA content, for benign breast disease and ductal carcinoma *in situ* (DCIS). Image cytometry measurements performed on tissue sections were used to accomplish the objectives of this thesis.

The adequacy of the DNA measurements performed on tissue sections was confirmed in comparison with other cytometric techniques. It was shown that the nuclear DNA content measurements of tissue sections are as reliable in the detection of aneuploidy as nuclear DNA measurements performed by flow cytometry or automated image cytometry techniques using smears or cytopins.

Progressive changes in quantitative nuclear features were identified from measurements on different breast diseases; features changed in parallel with the increasing risk of these diseases for the subsequent development of invasive carcinoma. These results suggested that nuclear measurements were meaningful for studying prognosis of breast diseases.

Next, the differences in nuclear morphology and DNA content, were characterized between different histological types of DCIS. The nuclear DNA content, size, irregularity of shape and chromatin texture increased from the lowest values in cribriform type to the highest values in comedo type DCIS. Aneuploidy was demonstrated in about 60% of non-comedo DCIS and in 95% of comedo DCIS.

An important objective was to characterize differences between pure DCIS and DCIS associated with invasion in surrounding tissue and to distinguish these two types of DCIS on the basis of quantitative nuclear features. This was

accomplished by the detection of nuclear features of DCIS, which were indicative of the presence of invasive carcinoma in the surrounding breast tissue. The classification system based on nuclear features was used to discriminate between cases with pure DCIS and cases with DCIS which had invasive cancer in the surrounding tissue. The classification was correct in 80% of non-comedo cases and in 100% of comedo cases.

Finally, the existence of malignancy associated changes (MAC) in breast tissue was demonstrated. Marker features, characteristic of MAC, were detected in epithelial nuclei from normal appearing lobules in breasts which were resected for carcinoma. The frequency of "MAC" nuclei was low in benign tissue, increased in tissue with DCIS and was the highest in tissues with invasive carcinoma. Based solely on the measurements of nuclei in normal appearing lobules it was possible to discriminate between patients with benign breast disease and patients with invasive carcinoma in more than 85% of cases.

In conclusion, this work has shown that nuclear measurements obtained by image cytometry of tissue sections provide information which could be useful for diagnosis and prognosis in benign breast diseases or ductal carcinoma *in situ* (DCIS). Nuclear features could be applied as a tool to make the diagnosis of benign breast diseases more objective. Malignancy associated changes (MAC) in breast tissue could be employed as a marker for an occult malignancy in the breast and possibly as a marker of increased risk for the subsequent development of malignancy. Nuclear features of DCIS, indicative of the presence of invasive carcinoma in the adjacent breast tissue, could be applied as a marker for the invasive disease in the surrounding breast in cases where only DCIS is found in the biopsy. These marker features may be related to

differences in invasive potential between pure DCIS and DCIS associated with invasive carcinoma and may be predictive of the subsequent behavior of DCIS tumors.

Because of the clinical relevance of these findings it is very important to confirm the results in future studies on larger number of patients and to expand the findings: i) with the analysis of MAC in patients with benign breast disease who subsequently developed malignancy in their breast, ii) with the analysis of patients with DCIS which were misdiagnosed or treated only by local excision and had the recurrence with invasive carcinoma. If confirmed this method could become an important aid in the treatment planning of patients with benign breast disease and DCIS.

## 7. REFERENCES

1. Alpers CE and Wellings SR. The prevalence of carcinoma *in situ* in normal and cancer-associated breasts. *Hum Pathol* 1985;16:796-807.
2. Anastassiades O, Iakovou E, Stavridou N, Gogas J, Karameris A. Multicentricity in breast cancer. A study of 366 cases. *Am J Clin Pathol* 1993;99:238-243.
3. Anderson TJ, Lamb J, Donnan P, Alexander FE, Huggins A, Muir BB, Kirkpatrick AE, Chetty U, Hepburn W, Smith A, Prescott RJ, Forrest P. Comparative pathology of breast cancer in a randomized trial of screening. *Br J Cancer* 1991;64:108-113.
4. Annual report, British Columbia Cancer Agency, 1990/1991.
5. Arnesson LG, Smeds S, Fagerberg G, Grönroft O. Follow-up of two treatment modalities for ductal cancer *in situ* of the breast. *Br J Surg* 1989;76:672-675.
6. Ashikari R, Huvos AG, Snyder RE. Prospective study of non-infiltrating carcinoma of the breast. *Cancer* 1977;39:435-439.
7. Atkin NB. The clinical usefulness of determining ploidy patterns in human tumors as measured by slide -based Feulgen microspectrophotometry. *Analyt Quant Cytol Histol* 1991;13:75-79.
8. Auer G, Caspersson T, Wallgren A. DNA content and survival in mammary carcinoma. *Analyt Quant Cytol* 1980;3:161-165.
9. Auer G, Eriksson E, Azavedo E, Caspersson T, Wallgren A. Prognostic significance of nuclear DNA content in mammary adenocarcinomas in humans. *Cancer Research* 1984;44:394-396.
10. Auer G., Askensten U., Ahrens O. Cytophotometry. *Human Pathology* 1989;20:518-527.

11. Baak J.P., Dop van H. et al.: The value of morphometry to classic prognosticators in breast cancer. *Cancer* 1985;56:374-382.
12. Baldetorp B, Fernö M, Fallenius A, Fallenius-Vecchi G, Idvall I, Olsson H, Sigurdsson H, Åkerman M, Killander D. Image cytometric DNA analysis in human breast cancer analysis may add prognostic information in diploid cases with low S-phase fraction by flow cytometry. *Cytometry* 1992;13:577-585.
13. Bartkova J, Barnes DM, Millis RR, Gullick WJ. Immunohistochemical demonstration of c-erbB-2 protein in mammary ductal carcinoma *in situ*. *Hum Pathol* 1990;21:1164-1167.
14. Bauer HCF, Kreichbergs A, Tribukeit B. DNA microspectrophotometry of bone sarcomas in tissue sections as compared to imprint and flow DNA analysis. *Cytometry* 1986;7:544-550.
15. Bauer TW, Tubbs RR, Edinger MG, Suit PF, Gephardt GN, Levin HS. A prospective comparison of DNA quantitation by image and flow cytometry. *Am J Clin Pathol* 1990;93:322-326.
16. Becker RL, Mikel UV. Interrelation of formalin fixation, chromatin compactness and DNA values as measured by flow and image cytometry. *Analyt Quant Cytol* 1990;12:333-341.
17. Beerman H, Bonsing BA, van de Vijver MJ, Hermans J, Kluin PM, Caspers RJ, van de Velde CJH, Cornelisse CJ. DNA ploidy of primary breast cancer and local recurrence after breast-conserving therapy. *Br J Cancer* 1991;64:139-143.
18. Berryman I, Sterret GF, Papadimitriou JM. Feulgen DNA cytomorphometry in histologic sections of mammary neoplasms. *Analyt Quant Cytol* 1984;6(1):19-23.
19. Bibbo M, Bartels PH, Galera-Davidson H, Dytch HE, Wied GL. Markers for malignancy in the nuclear texture of histologically normal tissues from patients with thyroid tumors. *Analyt Quant Cytol Histol* 1986;8:167-175.

20. Bibbo M, Montag AG, Lerma-Puertas E, Dytch HE, Leelakusolvong S, Bartels PH. Karyometric marker features in tissue adjacent to invasive cervical carcinomas. *Analyt Quant Cytol Histol* 1989;11:281-285.
21. Bibbo M, Dytch EH, Alenghat E, Bartels PH, Wied GL. Dna ploidy profiles as prognostic indicators in CIN lesions. *Am J Clin Pathol* 1989;92:261-265.
22. Bibbo M, Michelassi F, Bartels PH, Dytch H, Bania C, Lerma E, Montag AG. Karyometric marker features in normal-appearing glands adjacent to human colonic adenocarcinoma. *Cancer Res* 1990;50:147-151.
23. Black MM, Barclay THC, Cutler SJ, Hankey BF, Asire AJ. Association of atypical characteristics of benign breast lesions with subsequent risk of breast cancer. *Cancer* 1972;29:338-343.
24. BMDP Statistical Software Manual, Vol. 2. Dixon WJ ed., University of California press, Berkeley, CA, 1988.
25. Böcking A, Chatelain R, Biesterfeld S, Noll E, Biesterfeld D, Wohltmann D, Goecke C. DNA grading of malignancy in breast cancer. Prognostic validity, reproducibility and comparison with other classifications. *Analyt Quant Cytol* 1989;11:73-79.
26. Böcking A, Chatelain R, Homge M, Daniel R, Gillissen A, Wohltmann D. Representativity and reproducibility of DNA malignancy grading in different carcinomas. *Analyt Quant Cytol* 1989;11:81-86.
27. Bornstein BA, Recht A, Connolly JL, Schnitt SJ, Cady B, Koufman C, Love S, Osteen RT, Harris JR. Results of treating ductal carcinoma *in situ* of the breast with conservative surgery and radiation therapy. *Cancer* 1991;67:7-13.
28. Bose KK, Curley S, Smith WJ, Allison DC. Differences in the flow and absorption cytometric DNA distributions of mouse hepatocytes and tumor cells. *Cytometry* 1989;10:388-393.

29. Bur ME, Zimarowski MJ, Schnitt SJ, Baker S, Lew R. Estrogen receptor immunohistochemistry in carcinoma *in situ* of the breast. *Cancer* 1992;69:1174-1181.
30. Carpenter R, Cooke T, Matthews J, Dowle C, Burn K, Locker A, Blamey R. Does flow cytometry accurately determine tumour ploidy? *Br J Surg* 1988;75:1263, Abstract.
31. Carpenter R, Matthews J, Gibbs N, Thomas B, Boulter P, Cooke T. Prognostic value of cellular DNA content in the management of ductal carcinoma *in situ* of the female breast. *Br J Cancer* 1987A;56:859-880, Abstract.
32. Carpenter R, Gibbs M, Matthews J, Cooke T. Importance of cellular DNA content in pre-malignant breast disease and pre-invasive carcinoma of the female breast. *Br J Surg* 1987B;74:905-906.
33. Carpenter R, Boulter PS, Cooke T, Gibbs NM. Management of screen detected ductal carcinoma *in situ* of the female breast. *Br J Surg* 1989;76:564-567.
34. Carter D, Smith RRL. Carcinoma *in situ* of the breast. *Cancer* 1977;40:1189-1193.
35. Clark GM, Dressler LG, Owens MA, Pounds G, Oldaker T, McGuire WL. Prediction of relapse or survival in patients with node-negative breast cancer by DNA flow cytometry. *N Engl J Med* 1989;320:627-633.
36. Cope C, Rowe D, Delbridge L, Philips J, Friedlander M. Comparison of image analysis and flow cytometric determination of cellular DNA content. *J Clin Pathol* 1991;44:147-151.
37. Cornelisse CJ, de Koning HR, Moolenaar AJ, van de Velde CJ, Ploem JS. Image and flow cytometric analysis of DNA content in breast cancer. Relation to estrogen content and lymph node involvement. *Analyt Quant Cytol* 1984;6:9-18.

38. Cornelisse CJ, Van Driel-Kulker AM. DNA image cytometry on machine selected breast cancer cells and a comparison between flow cytometry and scanning cytophotometry. *Cytometry* 1985;6:471-477.
39. Cornelisse CJ, van de Velde CJH, Caspers RJC, Moolenaar AJ, Hermans J. DNA ploidy and survival in breast cancer patients. *Cytometry* 1987;8:225-234.
40. Crissman A, Visscher DW, Kubus J. Image cytophotometric DNA analysis of atypical hyperplasias and intraductal carcinomas of the breast. *Arch Pathol Lab Med* 1990;114:1249-1253.
41. Dawson AE, Austin RE, Weinberg DS. Nuclear grading of breast carcinoma by image analysis. *Am J Clin Pathol* 1991;95:4-11.
42. De Potter CR, Praet MM, Slavin RE, Verbeeck P, Roels HJ. Feulgen DNA content and mitotic activity in proliferative breast disease. A comparison with ductal carcinoma *in situ*. *Histopathology* 1987;11:1307-1319.
43. Dressler LG, Seamer LC, Owens MA, Clark GM, McGuire WL. DNA flow cytometry and prognostic factors in 1331 frozen breast cancer specimens. *Cancer* 1988;61:420-427.
44. Dupont WD, Page DL. Risk factors for breast cancer in women with proliferative breast diseases. *N Engl J Med* 1985;312:146-151.
45. Dupont WD, Parl FF, Hartmann WH, Brinton LA, Winfield AC, Worrel JA, Schuyler PA, Plummer WD. Breast cancer risk associated with proliferative breast disease and atypical hyperplasia. *Cancer* 1993;71:1258-1265.
46. Elledge RM, McGuire WL, Osborne CK. Prognostic factors in breast cancer. *Seminars in Oncology* 1992;19:244-253.
47. Ellis IO, Dilks B, Gilmour AS, Locker AP, Elston CW, Blamey RW. Comparison of static and flow cytometry in the estimation of breast cancer nuclear DNA content. *Analyt Cell Pathol* 1989;1:49, Abstract.

48. Elsheikh TM, Silverman JF, McCool JW, Riley RS. Comparative DNA analysis of solid tumors by flow cytometric and image analyses of touch imprints and flow cell suspensions. *Am J Clin Pathol* 1992;98:296-304.
49. Ewers SB, Långström E, Baldetorp B, Killander D. Flow-cytometric DNA analysis in primary breast carcinomas and clinicopathological correlations. *Cytometry* 1984;5:408-419.
50. Falkmer UG, Hagmar T, Auer G. Efficacy of combined image and flow cytometric DNA assessments in human breast cancer: a methodological study based on a routine histopathological material of 2024 excised tumour specimens. *Analyt Cell Pathol* 1990;2:297-312.
51. Fallenius AG, Askensten UG, Skoog LK, Auer GU. The reliability of microspectrophotometric and flow cytometric nuclear DNA measurements in adenocarcinomas of the breast. *Cytometry* 1987;8:260-266.
52. Fallenius AG, Auer GU, Carstensten JM. Prognostic significance of DNA measurements in 409 consecutive breast cancer patients. *Cancer* 1988;62:331-341.
53. Feinberg AP, Coffey DS. The concept of DNA rearrangement in carcinogenesis and development of tumor cell heterogeneity. In: *Tumor cell heterogeneity*. Owens AH et al, Eds., Academic Press, New York, 1982; pp. 469-494.
54. Fernö M, Baldetorp B, Ewers SB, Idvall I, Olsson H, Sigurdsson H, Killander D. One or multiple samplings for flow cytometric DNA analyses in breast cancer - prognostic implications? *Cytometry* 1992;13:241-249.
55. Fisher B, Gunduz N, Constantino J, Fischer ER, Redmond C, Mamounas EP, Siderits R. DNA flow cytometric analysis of primary operable breast cancer. Relation of ploidy and S-phase fraction to outcome of patients in NSABP B-04. *Cancer* 1991;68:1465-1475.

56. Fisher ER, Sass R, Fisher B, Wickerham L, Paik SM, Collaborating NSABP investigators. Pathologic findings from the national surgical adjuvant breast project (Protocol 6) I. Intraductal carcinoma (DCIS). *Cancer* 1986;57:197-208.
57. Fisher ER, Siderits R. Value of cytometric analysis for distinction of intraductal carcinoma of the breast. *Breast Cancer Res Treat* 1992;21:155-164.
58. Finch RR. A classification of nuclear aberrations in relation to malignancy associated changes (MAC). *Acta Cytol* 1971;15:553-558.
59. Fosså SD, Berner A, Waehre H, Heiden T, Holm Juul ME, van den Ouden D, Pettersen EO, Wang N, Tribukait B. DNA ploidy in cell nuclei from paraffin-embedded material - comparison of results from two laboratories. *Cytometry* 1992;13:395-403.
60. Fuhr JE, Frye A, Kattine AA, van Meter S. Flow cytometric determination of breast tumor heterogeneity. *Cancer* 1991;67:1401-1405.
61. Garner DM, MacAulay C, Harrison A, Korbelik J, Maticic J, Anderson GH, Palcic B. Automated cervical screening system: ACCESS-1400. Presented at: Automated cervical cancer screening. Second Annual International Symposium. Atlanta, Georgia, 1992.
62. Ghali VS, Liao S, Teplitz C, Prudente R. A comparative study of DNA ploidy in 115 fresh-frozen breast carcinomas by image analysis versus flow cytometry. *Cancer* 1992;70:2668-2672.
63. Gump FE, Jicha DL, Ozello L. Ductal carcinoma *in situ* (DCIS): A revised concept. *Surgery* 1987;102:790-794.
64. Hanselaar AGJM, Vooijs GP, Van't Hof-Grootenboer AE, Pahlplatz MMM. Cytophotometric analysis of cervical intraepithelial neoplasia grade III, with and without synchronous invasive squamous cell carcinoma. *Cytometry* 1990;11:901-906.

65. Hanselaar AGJM, Vooijs GP, Mayall BH, Pahlplatz MMM, Van't Hof-Grootenboer AE. DNA changes in progressive cervical intraepithelial neoplasia. *Analyt Cell Pathol* 1992;4:315-324.
66. Haroske G, Bergander S, König R, Meyer W. Application of malignancy - associated changes of the cervical epithelium in a hierarchic classification concept. *Analyt Cell Pathol* 1990;2:189-198.
67. Haroske G, Kunze KD, Theissig F. Prognostic significance of image cytometry DNA parameters in tissue sections from breast and gastric cancers. *Analyt Cell Pathol* 1991;3:11-24.
68. Harris J.R.: Clinical management of ductal carcinoma *in situ*. In: Breast diseases. Harris J.R. et al, Eds., J.B. Lippincott, Philadelphia, 1991; pp. 233-238.
69. Hedley DW, Friedlander ML, Taylor IW, Rugg CA, Musgrove EA. Method for analysis of cellular DNA content of paraffin-embedded pathological material using flow cytometry. *J Histochem Cytochem* 1983;31:1333-1335.
70. Holland R, Hendriks JHCL, Verbeek ALM, Mravunac M, Schuurmans Stekhoven JH. Extent, distribution, and mammographic/histological correlations of breast carcinoma *in situ*. *Lancet* 1990 A;335:519-522.
71. Holland R, Connolly JL, Gelman R, Mravunac M, Hendriks JHCL, Verbeek ALM, Schnitt SJ, Silver B, Boyages J, Harris JR. The presence of an extensive intraductal component following a limited excision correlates with prominent residual disease in the remainder of the breast. *J Clin Oncol* 1990 B;8:113-118.
72. Hutchinson ML, Isenstein LM, Martin JJ, Zahniser DJ. Measurement of subvisual changes in cervical squamous metaplastic cells for detecting abnormality. *Analyt Quant Cytol Histol* 1992;14:330-334.
73. Izuo M, Okagaki T, Richart R, Lattes R. Nuclear DNA content in hyperplastic lesions of cystic disease of the breast with special reference to malignant alteration. *Cancer* 1971;28:620-627.

74. Jaggi B, Poon SSS, Mac Aulay C, Palcic B. Imaging system for morphometric assesment of conventionally and fluorescently stained cells. *Cytometry* 1988;9:566-572.
75. Jaggi B, Poon SSS, Pontifex B, Fengler J, Palcic B. Evaluation of a quantitative microscope for image cytometry. In : *Advances in analytical cellular pathology*, Elsevier Science Publishers B.V., 1990.
76. Jaggi B, Poon S, Pontifex B, Fengler J, Marquis J, Palcic B. A quantitative microscope for image cytometry. *SPIE* 1991;1448:89-97.
77. Jensen RA, Page DL, Dupont WD, Rogers LW. Invasive breast cancer risk in women with sclerosing adenosis. *Cancer* 1989;64:1977-1983.
78. Joensuu H, Kallioniemi OP. Different opinions on classification of DNA histograms produced from paraffin-embedded tissue. *Cytometry* 1989;10:711-717.
79. Joensuu H, Alanen KA, Klemi PJ, Aine R. Evidence for false aneuploid peaks in flow cytometric analysis of paraffin-embedded tissue. *Cytometry* 1990;11:431-437.
80. Joensuu H, Toikkanen S, Klemi PJ. Histological features, DNA content and prognosis of breast carcinoma found incidentally or in screening. *Br J Cancer* 1991;64:588-592.
81. Kallioniemi OP, Blanco G, Alavaikko M, Hietanen T, Mattila J, Lauslahti K. Tumor DNA ploidy as an independent prognostic factor in breast cancer. *Br J Cancer* 1987;56:637-642.
82. Killen J, Namiki H. DNA analysis of ductal carcinoma *in situ* of the breast. A comparison with histologic features. *Cancer* 1991;68:2602-2607.
83. King EB, Chew KL, Duarte L, Hom JD, Mayall BH, Miller TR, Petrakis NL. Image cytometric classification of premalignant breast disease in fine needle aspirates. *Cancer* 1988;62:114-124.

84. Kinne DW, Petrek JA, Osborne MP, Fracchia AA, DePalo AA, Rosen PP. Breast carcinoma *in situ*. Arch Surg 1989;124:33-36.
85. Komitowski D, Janson C. Quantitative features of chromatin structure in the prognosis of breast cancer. Cancer 1990;65:2725-2730.
86. Koss LG, Stewart FW, Foote FW, Jordan MJ, Bader GM, Day E. Some histologic aspects of behaviour of epidermoid carcinoma *in situ* and related lesions of the uterine cervix: A long-term prospective study. Cancer 1963;12:1160-1211.
87. Koss LG. The Papanicolau test for cervical cancer detection. A triumph and a tragedy. JAMA 1989;261:737-743.
88. Kreicbergs A, Cewrien G, Tribukait B, Zetterberg A. Comparative single cell and flow DNA analysis of bone sarcoma. Anal Quant Cytol 1981;3:121-127.
89. Lagios MD, Westdahl PR, Margolin FR, Rose MR. Duct carcinoma *in situ*: Relationship of extent of noninvasive disease to the frequency of occult invasion, multicentricity, lymph node metastases, and short-term treatment failures. Cancer 1982;50:1309-1314.
90. Lagios MD, Margolin FR, Westdahl PR, Rose MR. Mammographically detected duct carcinoma *in situ*. Frequency of local recurrence following tylectomy and prognostic effect of nuclear grade on local recurrence. Cancer 1989;63:618-624.
91. Larsimont D, Kiss R, D'Olne D, De Launoit Y, Mattheiem W, Paridaens R, Pasteels JL, Gompel C. Correlation between nuclear cytomorphometric parameters and estrogen receptor levels in breast cancer. Cancer 1989B;63:2162-2168.
92. Larsimont D, Kiss R, D'Olne D, De Launoit Y, Mattheiem W, Paridaens R, Pasteels JL, Verhest A. Relationship between computerized morphonuclear image analysis and histopathologic grading of breast cancer. Analyt Quant Cytol 1989A;11:433-439.

93. Lerma-Puertas E, Galera-Davidson H, Bartels PH, Kim DH, Dytch HE, Bibbo M. Karyometric marker features in fine needle aspirates of follicular adenoma of the thyroid. *Analyt Quant Cytol Histol* 1989;12:223-228.
94. Locker AP, Horrocks C, Gilmour AS, Ellis IO, Dowle CS, Elston CW, Blamey RW. Flow cytometric and histological analysis of ductal carcinoma *in situ* of the breast. *Br J Surg* 1990;77:564-567.
95. London SJ, Connolly JL, Schnitt SJ, Colditz GA. A prospective study of benign breast disease and the risk of breast cancer. *JAMA* 1992;267:941-944.
96. Mac Aulay C. Development, implementation and evaluation of segmentation algorithms for the automatic classification of cervical cells. Ph.D.thesis, Physics, University of British Columbia, Canada, 1989.
97. McGuire WL, Tandon AK, Allred DC, Chamness GC, Clark GM. How to use prognostic factors in axillary node-negative breast cancer patients. *J Nat Cancer Inst* 1990;82:1006-1015.
98. McKinna JA, Davey JB, Walsh GA, A'Hern RP, Curling G, Frankland H, Viggers J. The early diagnosis of breast cancer - a twenty-year experience at the royal marsden hospital. *Eur J Cancer* 1992;4:911-916.
99. Meyer JS. Cell kinetics of histologic variants of *in situ* breast carcinoma. *Breast Cancer Res Treat* 1986;7:171-180.
100. Mikel UV, Becker RL. A comparative study of quantitative stains for DNA in image cytometry. *Analyt Quant Cytol Histol* 1991;13:253-260.
101. Montag AG, Bartels PH, Lerma -Puertas E, Dytch HE, Leelakusolvong S, Bibbo M. Karyometric Marker features in tissue adjacent to *in situ* cervical carcinomas. *Analyt Quant Cytol Histol* 1989;11:275-280.

102. Montag AG, Bartels PH, Dytch HE, Lerma-Puertas E, Michelassi F, Bibbo M. Karyometric features in nuclei near colonic adenocarcinoma. Statistical analysis. *Analyt Quant Cytol Pathol* 1991;13:159-167.
103. Mulder JWR, Offerhaus GJA, de Feyter EP, Floyd JJ, Kern SE, Vogelstein B, Hamilton SR. The relationship of quantitative nuclear morphology to molecular genetic alterations in the adenoma-carcinoma sequence of the large bowel. *Am J Path* 1992;141:797-804.
104. Ngoi SS, Staiano-Coico L, Godwin TA, Wong RJ, DeCosse JJ. Abnormal DNA ploidy and proliferative patterns in superficial colonic epithelium adjacent to colorectal cancer. *Cancer* 1990;66:953-959.
105. Nieburgs HE, Goldberg AF, Bertini B, Silagi J, Pacheco B, Reisman H. Malignancy associated changes (MAC) in blood and bone marrow cells of patients with malignant tumors. *Acta Cytol* 1967;11:415-423.
106. Nieburgs HE. Recent progress in the interpretation of malignancy associated changes (MAC). *Acta Cytol* 1968;12:445-453.
107. Nielsen M, Thomsen JL, Primdahl S, Dyreborg U, Andersen JA. Breast cancer and atypia among young and middle aged women: A study of 110 medicolegal autopsies. *Br J Cancer* 1987;56:814-819.
108. Norris HJ, Bahr GF, Mikel UV. A comparative morphometric and cytophotometric study of intraductal hyperplasia and intraductal carcinoma of the breast. *Analyt quant Cytol Histol* 1988;10:1-9.
109. Nowell PC. Chromosomal and molecular clues to tumor progression. *Seminars in Oncology* 1989;16:116-127.
110. Opfermann M, Brugal G, Vassilakos P. Cytometry of breast carcinoma: significance of ploidy balance and proliferation index. *Cytometry* 1987;8:217-224.

111. Oud PS, Hendrik JBJ, Huysmans ACLM, Pahlplatz MMM, Hermkens HG, Tas J, James J, Vooijs GP. The use of light green and orange II as quantitative protein stains and their combination with the Feulgen method for the simultaneous determination of protein and DNA. *Histochem* 1984;80:49-57.
112. Page DL, Anderson TJ. *Diagnostic histopathology of the breast*. Edinburgh: Churchill Livingstone, 1987; pp. 120-192.
113. Page DL, Dupont WD, Rogers LW, Landerberger M. Intraductal carcinoma of the breast: Follow-up after biopsy only. *Cancer* 1982;49:751-758.
114. Page DL, Dupont WD, Rogers LW, Rados MS. Atypical hyperplastic lesions of the female breast. *Cancer* 1985;55:2698-2708.
115. Page DL. Cancer risk assessment in benign breast biopsies. *Hum Path* 1986;17:871-874.
116. Palcic B, Jaggi B, MacAulay C. The importance of image quality for computing texture features in biomedical specimens. *SPIE* 1990;1205:155-162.
117. Palli D, del Turco MR, Simoncini R, Bianchi S. Benign breast disease and breast cancer: a case control study in a cohort in Italy. *Br J Cancer* 1991;47:703-706.
118. Pallis L, Skoog L, Falkmer U, Wilking N, Rutquist LE, Auer G, Cedermark B. The DNA profile of breast cancer *in situ*. *Eur J Surg Oncol* 1992;18:108-111.
119. Patchefsky AS, Schwartz GF, Finkelstein SD, Prestipino A, Sohn SE, Singer JS, Feig SA. Heterogeneity of intraductal carcinoma of the breast. *Cancer* 1989;63:731-741.

120. Petein M, Michel P, van Velthoven R, Pasteels JL, Brawer MK, Davis JR, Nagle RB, Kiss R. Morphonuclear relationship between prostatic intraepithelial neoplasia and cancers as assessed by digital cell image analysis. *Am J Clin Pathol* 1991;96:628-634.
121. Pienta KJ, Partin AW, Coffey DS. Cancer as a disease of DNA organization and dynamic cell structure. *Cancer Res* 1989;49:2525-2532.
122. Pienta KJ, Coffey DS. Correlation of nuclear morphometry with progression of breast cancer. *Cancer* 1991;68:2012-2016.
123. Poller DN, Roberts EC, Bell JA, Elston CW, Blamey RW, Ellis IO. p53 protein expression in mammary ductal carcinoma *in situ*: Relationship to immunochemical expression of estrogen receptor and c-erbB-2 protein. *Hum Pathol* 1993;24:463-468.
124. Price P, Sinnet HD, Gusterson B, Walsh G, A'Hern RP, McKinna JA. Duct carcinoma *in situ*: predictors of local recurrence and progression in patients treated by surgery alone. *Br J Cancer* 1990;61:869-872.
125. Raju U, Zarbo RJ, Kubus J, Schultz DS. The histologic spectrum of apocrine breast proliferations: A comparative study of morphology and DNA content by image analysis. *Hum Pathol* 1993;24:173-181.
126. Rodenburg CJ, Ploem-Zaaijer JJ, Cornelisse CJ, Mesker WE, Hermans J, Heintz PAM, Ploem JS, Fleuren GJ. Use of DNA image cytometry in addition to flow cytometry for the study of patients with advanced ovarian cancer. *Cancer Research* 1987;47:3938-3941.
127. Roos G, Arnerlöv C, Emdin S. Retrospective DNA analysis of T3/T4 breast carcinoma using cytomorphometry and flow cytometry: A comparative study with prognostic evaluation. *Anal Quant Cytol* 1988;10:189-193.
128. Rosai J. Borderline epithelial lesion of the breast. *Am J Surg Pathol* 1991;15:209-221.

129. Rosen PP, Braun DW, Kinne DE. Clinical significance of pre-invasive breast carcinoma. *Cancer* 1980;46:919-925.
130. Royds JA, Stephenson TJ, Rees RC, Shorthouse AJ, Silcocks PB. Nm23 protein expression in ductal *in situ* and invasive human breast carcinoma. *J Natl Cancer Inst* 1993;85:727-731.
131. Salmon I, Kiss R, Franc B, Gasperin P, Heimann R, Pasteels JL, Verhest A. Comparison of morphonuclear features in normal, benign and neoplastic thyroid tissue by digital cell image analysis. *Analyt Quant Cytol Histol* 1992;14:
132. Schimmelpenning H, Falkmer UG, Hamper K, Seifert G, Auer GU. Variations in Feulgen stainability of epithelial parenchymal cells extracted from paraffin-embedded salivary gland specimens. *Cytometry* 1990;11:475-480.
133. Schimmelpenning H, Eriksson ET, Pallis L, Skoog L, Cedermark B, Auer G. Immunohistochemical c-erbB-2 protooncogene expression and nuclear DNA content in human mammary carcinoma *in situ*. *Am J Clin Pathol* 1992;97(Suppl 1):S48-S52.
134. Schnitt SJ, Silen W, Sadowsky NL, Connolly JL, Harris JR. Ductal carcinoma *in situ* (intraductal carcinoma) of the breast. *N Engl J Med* 1988;318:898-903.
135. Schnitt S.J.: Pathology of *in situ* carcinoma. In: Breast diseases. Harris J.R. et al, Eds., J.B. Lippincott, Philadelphia, 1991; pp. 229-232.
136. Schnitt SJ, Connolly JL, Tavassoli FA, Fechner RE, Kempson RL, Gelman R, Page DL. Interobserver reproducibility in the diagnosis of ductal proliferative breast lesions using standardized criteria. *Am J Surg Pathol* 1992;16:1133-1143.
137. Schwartz GF, Finkel GC, Garcia JC, Patchefsky AS. Subclinical ductal carcinoma *in situ* of the breast. *Cancer* 1992;70:2468-2474.

138. Silverstein MJ, Rosser RJ, Gierson ED, Waisman JR, Gamagami P, Hoffman RS, Fingerhut AG, Lewinsky BS, Colburn W, Handel N. Axillary lymph node dissection for intraduct breast carcinoma - is it indicated? *Cancer* 1987;59:1819-1824.
139. Stacey-Clear A, McCarthy KA, HallDA, Pile-Spellman E, White G, Hulka C, Whitman GJ, Mahoney E, Kopans DB. Breast cancer survival among women under age 50: is mammography detrimental? *Lancet* 1992;340:991-994.
140. Stenkivist B, Westman-Naeser S, Holmquist J, Nordin B, Bengtsson E, Vegelius J, Eriksson O, Fox CH. Computerized nuclear morphology as an objective method for characterizing human cancer cell populations. *Cancer Res* 1978;38:4688-4697.
141. Stenkivist B, Bengtsson E, Dahlqvist B, Eklund G, Eriksson O, Jarkrans T, Nordin B. Predicting breast cancer recurrence. *Cancer* 1982;50:2884-2893.
142. Stenkivist B, Strande G. Entropy as an algorithm for the statistical description of DNA cytometric data obtained by image analysis microscopy. *Analyt Cell Path* 1990;2:59-165.
143. Swank PR, Greenberg DS, Hunter NR, Spjut HJ, Estrada R, Trahan EB, Montalvo J. Identification of features of metaplastic cells in sputum for the detection of squamous-cell carcinoma of the lung. *Diagn Cytopathol* 1989;5:98-103.
144. Tavassoli FA, Norris HJ. A comparison of the results of long-term follow-up for atypical intraductal hyperplasia and intraductal hyperplasia of the breast. *Cancer* 1990;65:518-529.
145. Teplitz RL, Butler BB, Tesluk H, Min BH, Russel LA, Jensen HM, Hill LR. Quantitative DNA patterns in human preneoplastic breast lesions. *Analyt Quant Cytol* 1990;12:98-102.

146. Tezcan A, Garner D, Lam P, Korbelik J, Palcic B. An investigation of the three nuclear stains: Thionin, gallocyanin, and hematoxylin, for automated quantitative image cytometry of specimens from uterine cervix. *Cytometry* 1994, submitted.
147. Theissig F, Dimmer V, Haroske G, Kunze KD, Meyer W. Use of nuclear image cytometry, histopathological grading and DNA cytometry to make breast cancer prognosis more objective. *Analyt Cell Pathol* 1991;3:351-360.
148. Troncosco P, Dytch HE, Bibbo M, Wied GL, Dawson PJ. The significance of DNA measurements in a histologically defined subset of infiltrating ductal carcinomas of the breast with the long-term follow-up. *Analyt Quant Cytol* 1989;11(3):166-172.
149. Umbricht C, Oberholzer M, Gschwind R, Christen H, Torhorst J. Prognostic significance (relapse, non-relapse) of nuclear shape parameters in lymph node negative breast cancer. *Analyt Cell Path* 1989;1:11-23.
150. Uyterlinde AM, Schipper NW, Baak JPA, Peterse H, Matze E. Limited prognostic value of cellular DNA content to classical and morphometrical parameters in invasive ductal breast cancer. *Am J Clin Pathol* 1988;89:301-307.
151. Uyterlinde AM, Smeulders AWM, Baak JPA. Reproducibility and comparison of quantitative DNA histogram features obtained with a scanning microdensitometer and a flow cytometer in breast cancers. *Analyt Quant Cytol* 1989;11(5):353-360.
152. Van der Linden JC, Lindeman J, Baak JPA, Meijer CJLM, Herman CJ. The multivariate prognostic index and nuclear DNA content are independent prognostic factors in primary breast cancer patients. *Cytometry* 1989;10:56-61.
153. Van de Vijver MJ, Peterse JL, Mooi WJ, Wisman P, Lomans J, Dilesio O, Nusse R. Neu protein overexpression in breast cancer. Association with comedo-type ductal carcinoma *in situ* and limited prognostic value in stage II breast cancer. *N Engl J Med* 1988;319:1239-1245.

154. Van Oppen Toth B, Meisels A, St-Pierre S. Malignancy associated changes in sputum: A correlated study of 315 patients. *Acta Cytol* 1975;19:573-576.
155. Von Rosen A, Rutquist LE, Carstensten J, Fallenius A, Skoog L. Prognostic value of nuclear DNA content in breast cancer in relation to tumor size, nodal status, and estrogen receptor content. *Breast Cancer Res Treat* 1989;13:23-32.
156. Visscher DW, Sarkar FH, Crissman JD. Correlation of DNA ploidy with c-erbB-2 expression in preinvasive and invasive breast tumors. *Analyt Quant Cytol Histol* 1991;13:418-424.
157. Wang N, Stenkvisit BG, Tribukait B. Morphometry of the normal and malignant prostate in relation to DNA ploidy. *Analyt Quant Cytol Histol* 1992;14:210-216.
158. Weber JE. Applications of multivariate analysis in diagnostic cytology. *Analyt Quant Cytol Histol* 1988;10:54-72.
159. Weber JE. Applications of statistical analysis in diagnostic histopathology and cytopathology. *Analyt Quant Cytol Histol* 1988;10:73-86.
160. Wellings SR, Jensen HM, Marcum RG. An atlas of subgross pathology of the human breast with special reference to possible precancerous lesions. *JNCI* 1975;55:231-273.
161. Wied GL, Bibbo M, Pishotta FT, Bartels PH. Intermediate cell markers for malignancy. Consistency of expression. *Analyt Quant Cytol* 1984;6:243-246.
162. Wied GL, Bartels PH, Bibbo M, Dytch HE. Image Analysis in quantitative Cytopathology and Histopathology. *Hum Path* 1989;20:549-570.

163. Wilbur DC, Zakowski MF, Kosciol CM, Sojda DF, Pastuszak WT. DNA ploidy in breast lesions. A comparative study using two commercial image analysis systems and flow cytometry. *Analyt Quant Cytol* 1990;12(1):28-32. 43.
164. Zahniser DJ, Wong KL, Brenner JF, Ball HG, Garcia GL, Hutchinson ML. Contextual analysis and intermediate cell markers enhance high-resolution cell image analysis for automated cervical smear diagnosis. *Cytometry* 1991;12:10-14.
165. Zbieranowski I, LeRiche JC, Palcic B, Gascoyne R, Connors J. Determination of DNA ploidy in archival tissue from non-Hodgkin's lymphoma using flow and image cytometry. *Analyt Cell Pathol* 1992;4:303-313.